NTNU

Norwegian University of
Science and Technology

Cytotoxic and inflammatory responses in IL-1 deficient cells exposed to carbon nanotubes

Torunn Rønningen

Biotechnology

Submission date: May 2011

Supervisor: Aage Haugen, IBT

Co-supervisor: Shan Zienolddiny, STAMI

Norwegian University of Science and Technology
Department of Biotechnology

Acknowledgements

This thesis was performed at the National Institute of Occupational Health (NIOH) as a part of the Masters degree in Biotechnology at the Norwegian University of Science and Technology from September 2010 – May 2011. Supervisors were Professor, Dr. Philos Aage Haugen and Dr. Philos Shan Zienolddiny.

I would like to thank Aage Haugen for the opportunity to perform my Master's thesis at NIOH. I would also like to thank Shan Zienolddiny for very good guidance, and enthusiasm through the work with the Master's thesis. A special thank goes to Nina Landvik for help both in the lab and with theoretical questions, thank you for always being friendly and helpful.

I am also grateful to Tove Andreassen and Kristine Haugen for tutoring in the lab. Thank you for your guidance, patience and helpfulness. I want to thank Yke Arnoldussen and Vidar Skaug for good help with theoretical questions. I would also like to thank scientist Asbjørn Skogstad for performing the characterization of the nanoparticles.

I want to thank the rest of the Toxicological Section at NIOH for pleasant lunches and for making me feel welcome.

To the other students at the 5th floor - thank you for good conversations, cooperation and laughs. A special thank goes to Lone Nilsen and Audun Bersaas for pleasant company during long evenings at the lab, and through the writing period.

Last, but not least, I am very grateful to my family who support and believe in me.

Finally, I wish to thank Kristian Grøv for support and positivity, and for always encouraging me to do my best.

Oslo, 16.05.11

Torunn Rønningen

Abstract

Nanotechnology is an emerging industry manufacturing engineered nanomaterials used in industry, general consumer products and medicine. Nanomaterials are made of nanoparticles which have at least one dimension less than 100 nm. The toxicological properties of nanoparticles are under increasing concern because of their nano size and unique physico-chemical properties. Carbon nanotubes (CNT) are a group of nanomaterials that are under extensive toxicological investigations due to their fiber-like structure and structural similarity with asbestos. Inhalation of fiber-like compounds such as asbestos has been shown to lead to several adverse health effects including fibrosis and cancer. Similar to asbestos, CNTs, in particular multi-walled CNTs (MWCNT), have been shown to induce biological responses such as oxidative stress, inflammation, DNA damage and cell death. However the effects have been observed to differ between different CNTs. It is also hypothesized that genetic factors may modulate the cellular responses following exposure to CNTs, especially genes involved in inflammation. *IL-1* is such a gene, encoding an important pro-inflammatory cytokine.

To investigate the effect of *Il1* on the cellular responses following exposure to CNTs, an *Il1* model system including a wild-type *Il1* cell line and an *Il1a/b* $^{(-/-)}$ knock-out cell line were used. Two MWCNTs, one produced in Norway (MWCNT-NO) and one produced in Japan (MWCNT-JP) were investigated for cytotoxicity (WST-8 assay), apoptotic cell death (Hoechst/PI) and alterations in gene expression (qRT-PCR). The effects were then compared with cells exposed to Crocidolite asbestos and hydrogen peroxide.

The results showed a dose and time dependent increase in toxicity for both MWCNT-NO and MWCNT-JP. MWCNT-JP was shown to be the most toxic at low doses and also induced a higher level of gene expression. MWCNT-NO, however, showed similar patterns to Crocidolite asbestos both concerning toxicity and gene expression after 24 hours in the *Il1a/b* KO cell line. A common property of MWCNT-NO and MWCNT-JP was the ability to induce expression of the *Ptgs2* (*COX-2*) gene, an effect which was not seen for Crocidolite or H_2O_2. *Il1* seemed to influence the biological response following MWCNT exposure, with increased toxicity in the knock-out cell line following MWCNT-JP exposure, and differential gene expression of *Tnfa* and *Il6* between cell lines following MWCNT-NO exposure. Neither of the MWCNTs induced apoptotic cell death in the cell lines used. The reasons for the differences between particles in toxicity and inflammatory potential may be due to the higher length of the MWCNT-JP or different production method used, but several other factors may also be involved including differences in contaminations, surface charge and aggregation /agglomeration state.

In summary, our results show that MWCNTs from two different producers affect cellular responses differentially. The changes in toxicity and gene expression following exposure varied between the tested MWCNTs, as well as between cell lines with different genetic background.

Abbreviations

AP-1	Activating protein-1
BSA	Bovine Serum albumin
cDNA	Complimentary DNA
COX-2	Cyclooxygenase 2
CNT	Carbon nanotube
CVD	Chemical vapor deposition
DM	Dispersion media
DMSO	Dimethylsufoxide
DPPC	1,2- dipalmitoyl-sn-glycero-3-phosphocholine
EGFR	Epidermal growth factor receptor
FBS	Fetal bovine serum
HARN	High aspect-ratio nanoparticles
H_2O_2	Hydrogen peroxide
IκB	Inhibitory protein kappa B
IL-1	Interleukin 1
IL-1R	Interleukin 1 receptor
IL-6	Interleukin 6
KO	Knock-out
LAF	Laminar air flow
MAPK	Mitogen-activated protein kinase
3-MCA	3-methylcholanthrene
MCP-1	Monocyte chemotactic protein-1
MWCNT	Multi walled carbon nanotube
MWCNT-JP	Multi-walled carbon nanotube produced in Japan
MWCNT-NO	Multi-walled carbon nanotube produced in Norway
NF-κB	Nuclear factor kappa B
NP	Nanoparticle
NSAID	Non-steroidal anti-inflammatory drugs
PBS	Phosphate buffered saline
PCR	Polymerase chain reaction
PTGS2/COX-2	Prostaglandin-endoperoxide synthase 2/Cyclooxygenase 2
qRT-PCR	Quantitative reverse transcriptase PCR
RNS	Reactive nitrogen species
ROS	Reactive oxygen species
SD	Standard deviation
SE	Standard error
SEM	Scanning electron microscopy
SWCNT	Single walled carbon nanotube
TNF-α	Tumor necrosis factor alpha
TNFR	Tumor necrosis factor receptor
TLR	Toll-like receptor
TP53	Tumor protein 53
WT	Wild-type

Contents

1. Introduction

1.1 Nanotechnology and nanomaterials

Nanotechnology is an emerging industry manufacturing engineered nanomaterials with many applications especially within industry, medicine and general consumer products [1]. Nanomaterials are made from nanoparticles, where a nanoparticle (NP) is defined as a particle with at least one of the dimension at the nano scale (1 – 100 nm). NPs often have different properties compared to the material on the macro scale e.g. different color, transition from metal to liquid form, electrical insulators become conductive etc [2].

The physico-chemical properties of nanoparticles are unique and include large surface area compared to the size of the particle, increased catalytic activity and reactivity. Different NPs include metal nanoparticles, metal oxide nanoparticles and carbon based nanoparticles [1]. An overview of some of the different nanomaterials, their properties, and possible applications, is listed in Table 1.1.

Table 1.1 Some examples of different nanomaterials, their properties and applications.

Nanomaterial	Properties	Application
Ag	Anti microbial	Disinfectant in swimming pools, clothes etc.
TiO_2	Attenuation of UV-B radiation, photocatalytic activity	Sunscreen, cosmetics, pharmaceuticals etc
ZnO	High catalytical activity in oxidation and photochemical reactions	Paint, cosmetics, drug carriers
Al_2O_3	Inhibits corrosion and chemical attack	Metallic paints, cosmetics, medical devices
Fullerenes	Antioxidant properties, better conductivity	Organic solar cells, polymers, electronics, antioxidants
Carbon nanotubes	High mechanical strength, electrical conductivity, catalytical properties.	Electronics, optics, biomedical carriers

1.2 Carbon nanotubes

Carbon nanotubes (CNTs) are tubes made from graphene sheets, first described by Iijima in 1991[3]. CNTs with one simple wall are called single-walled carbon nanotubes (SWCNT), while CNTs with two or more layers (up to 50 layers) are called multi-walled carbon nanotubes (MWCNT). The MWCNTs are especially useful because they allow chemical modifications of the outer layer, e.g. functionalization or coating with proteins, polymers or metals to improve dispersion or to obtain specific functions [4]. MWCNTs normally have a diameter of 1.4 – 100 nm and have a high length compared to their diameter, usually several µm. The length/diameter ratio is very high and they are classified as high aspect-ratio nanoparticles (HARN) [5].

CNTs have unique properties such as high mechanical strength, high electrical conductivity, high chemical stability, large surface area and unique optical properties, which make them useful in many technological and biomedical applications. Examples of applications are in electronics, polymer composites, thermoplastics, coatings and adhesives. CNTs are also

promising for use in medical application, as contrast fluid, or for targeted drug or gene delivery [4, 6].

CNTs are mainly synthesized by three methods; by arc discharge, laser ablation or chemical vapor deposition (CVD). The arc discharge and the laser ablation methods produce CNTs from graphitic carbon, while CVD uses gaseous hydrocarbons as precursor (CO, methane, ethylene etc.). In all these methods, energy is applied to a carbon source, to produce carbon fragments which will form CNTs. They all involve thermal vaporization of carbon and metal catalysts. Metal catalysts used in the manufacturing process can deposit in the tubes, causing contaminations. Generally, SWCNTs contain larger amounts of metals than MWCNTs, this is caused by the need for large amounts of catalysts in the synthesis of SWCNT. Carbon nanotubes are normally purified after production by acid treatment which reduces the degree of metal contaminations [7, 8].

1.3 Biological effects of exposure to nanoparticles

The unique physico-chemical properties of nanoparticles which are promising for use in industry and medicine are also what possibly make them more toxic compared to the materials on a macro scale. The small size, large surface area and high reactivity are important factors for causing possible toxic effects. The toxic effect of particles is mainly thought to be mediated by an oxidative mechanism through generation of reactive oxygen/nitrogen species (ROS/RNS). Oxidative stress leads to local tissue damage and inflammation. Chronic exposure to nanomaterials can cause chronic inflammation leading to an increased risk for the development of airway diseases, cardiovascular diseases, fibrosis or cancer [2].

In mammalian systems, the main exposure route to nanoparticles is through the respiratory system, but exposure through gastrointestinal tract and skin may also occur. Nanoparticles can deposit into all parts of the respiratory tract, the nasal, tracheobronchial and alveolar regions. There are concerns about exposure in the nasal region, leading to deposition into the brain. Normally, deposited particles in the alveoli are removed by the action of alveolar macrophages. Because of their small size, nanoparticles are hypothesized to be able to cross biological barriers. They are hypothesized to be able to enter circulation, leading to exposure of tissues, which are normally not directly exposed to particles [1, 7].

Nanoparticles are in the same size range as biomolecules in the cells, including DNA, RNA and proteins. It has been shown that nanoparticles are readily internalized into the cell and are even capable of entering the nucleus which may cause interaction and damage to DNA. Transport of CNTs into the cell is hypothesized to occur via several mechanisms including active transport through endocytosis/phagocytosis, or passively, though so-called nanopenetration of the plasma membrane as illustrated in Figure 1.1. Inside the cell, CNTs can interact with cellular structures like mitochondria or DNA, causing adverse effects [9, 10].

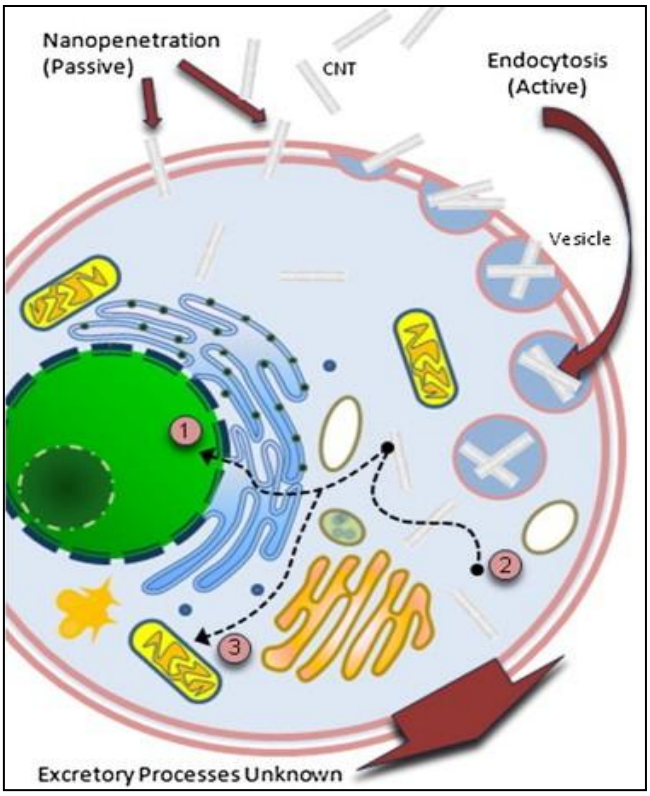

Figure 1.1 Hypothesized mechanisms for the cellular uptake of carbon nanotubes. Particles are taken up into the cells mainly via receptor mediated endocytosis or nanopenetration of the plasma membrane. Inside the cell, CNTs may interact with several targets, including 1: DNA, if the particles are able to cross the nuclear membrane, 2: compounds present in the cytosol, like proteins, lipids and RNA, 3: cellular organelles like mitochondria. From Firme and Bandaru [10].

Nanoparticles are thought to cause adverse effects by affecting cellular processes like inflammation, oxidative stress, DNA maintenance, cell proliferation and cell death and may be mutagenic due to direct interactions with DNA. Figure 1.2 shows an overview of important mechanisms involved in the cellular effects of exposure to nanoparticles.

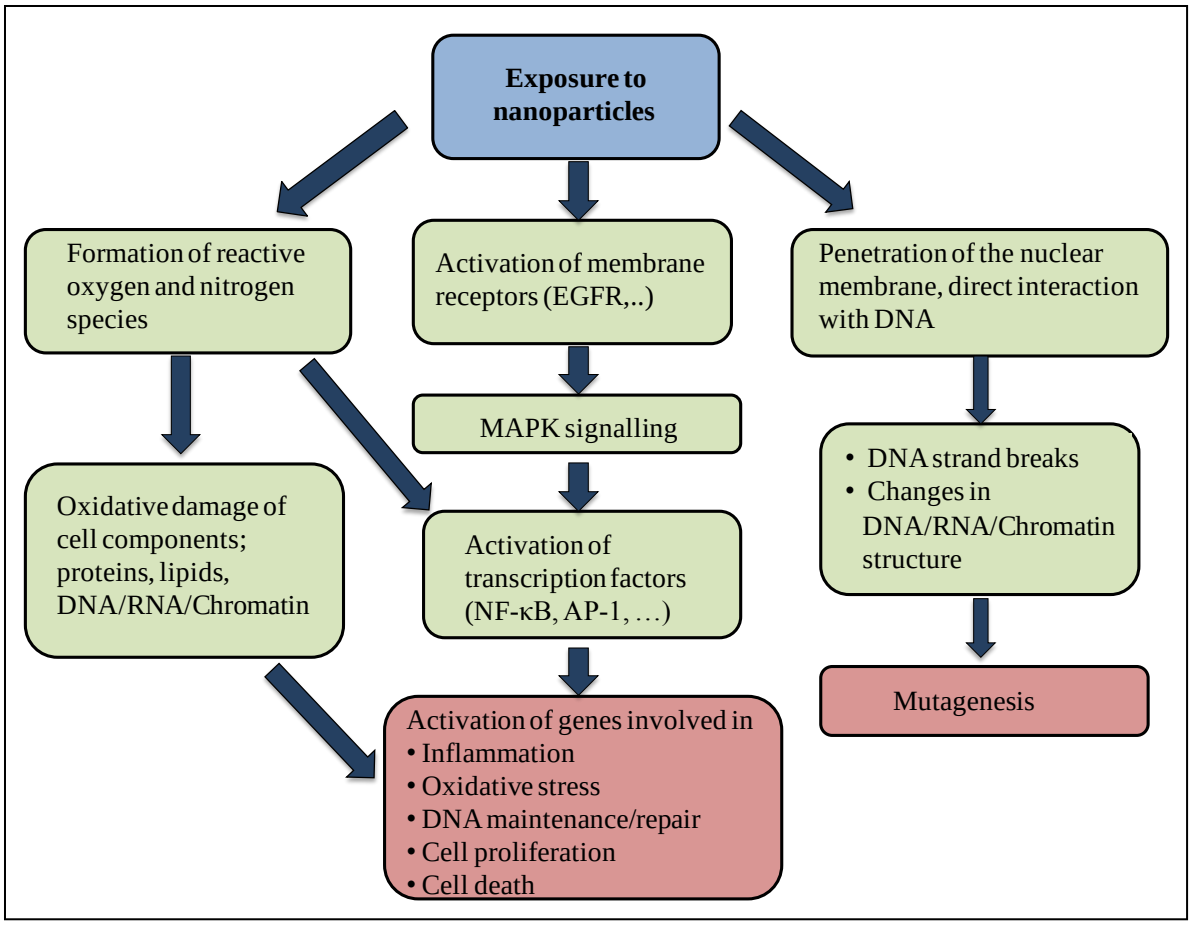

Figure 1.2: Hypothesized cellular effects of exposure to nanoparticles, modified from Mühlfeld et al. [11]

1.3.1 Asbestos-like cellular effects of MWCNTs

A fiber is defined as a material with a length that is over three times larger than the diameter (WHO), with asbestos fibers as a typical example. Asbestos is a silicate mineral with long fiber-like structures, and was previously a much used building material due to its physical properties. Asbestos comes in several forms including Chrysotile, Crocidolite and Amosite. Several adverse effects have been linked to the exposure of asbestos, including the development of lung fibrosis, lung cancer and mesothelioma, often up to 20 -30 years after exposure. The development of malignant mesothelioma is a condition considered to be highly specific for asbestos exposure. Asbestos is thought to induce mesothelioma by translocation of fibers from the lung to the pleura causing inflammatory and oxidative damage to the lung as well as mesothelial cells [12, 13].

Due to their similarity in shape and biopersistence, CNTs are hypothesized to be carcinogenic through the many of the same mechanisms as asbestos. Long CNTs are thought to induce the process of frustrated phagocytosis in the lungs, which is typical for the pathogenicity of asbestos. The process of frustrated phagocytosis is schematically illustrated in Figure 1.3. This process is thought to apply to so-called long CNTs with a length > 15 µm, which are not tangled or agglomerated. When entering the deep regions of the lung, particles are recognized by immune cells, and macrophages attempt to engulf the particles. When the particles are too long compared to the cell, the macrophages are not able to engulf the particles. This causes

the macrophages to maintain a chronic release of ROS and inflammatory mediators, causing inflammation. Like asbestos, carbon nanotubes can be biopersistent because of their graphitic, hydrophobic surface. CNTs can also contain metal contaminations which can cause additional oxidative damage through the Haber-Weiss reaction [5, 13].

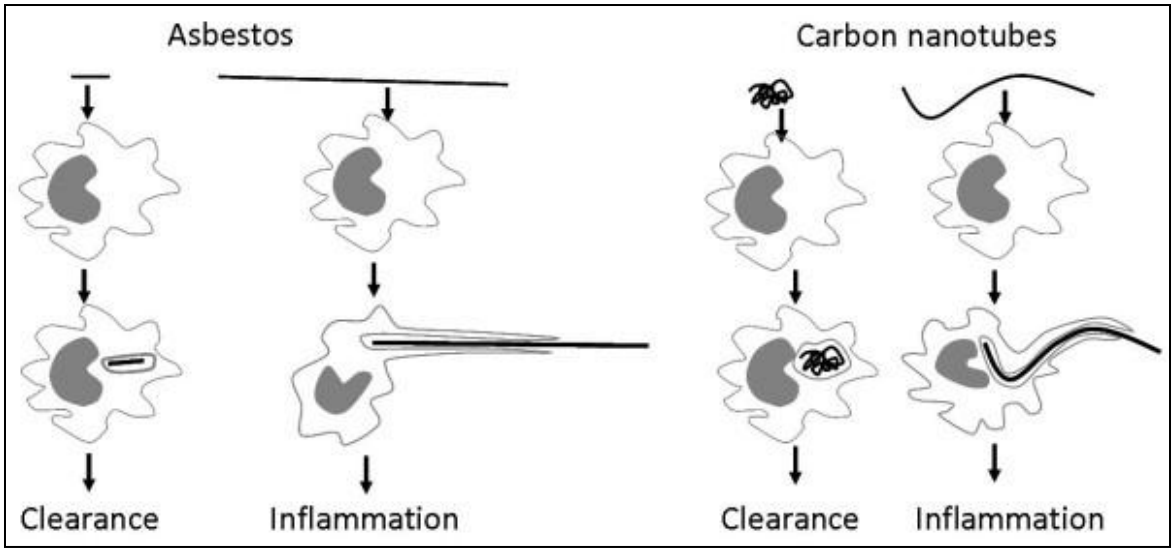

Figure 1.3: Illustration of the process of frustrated phagocytosis, and its relation to the shape of carbon nanotubes. Short asbestos fibers or tangled/aggregated CNTs are able to be engulfed by macrophages, causing clearance of the particles. Long, straight untangled CNTs or asbestos fibers are not able to be taken up by the macrophages, causing so-called frustrated phagocytosis and inflammatory responses. From Donaldson et al. [5].

In a study performed by Poland et al, the mesothelial lining of the body cavity of mice was exposed to asbestos fibers and MWCNT of different length. The results showed a length-dependent, asbestos-like effect of MWCNTs. The long and untangled MWCNTs induced inflammation and caused formation of granulomas, the same responses compared to exposure to long asbestos fibers. Shorter or tangled particles did not show a similar response. However, it has not been shown whether the particles are able to translocate from the lung to the mesothelial lining in the form of long untangled fibers. The actual exposure of the mesothelial lining to these fibers is unknown. The agglomeration state and deposition of the particles within the lung seems to be an important parameter determining whether translocation takes place or not [13, 14].

Exposure to asbestos *in vitro* has been shown to induce expression of transcription factors NF-κB and AP-1, release of cytokines/chemokines and apoptosis [15]. Similar findings have been found after exposure to MWCNTs [16]. Similar to asbestos, the toxicity of MWCNTs has shown to be size dependent, with long MWCNT being the most toxic, inducing DNA damage and inflammation [17]. Asbestos has also been shown to be mutagenic *in vivo*, inducing specific mutations after exposure in rats. These mutations specifically include G →T transversions which are related to the formation of 8-OHdG, a DNA adduct which is caused by oxidative DNA damage [18]. A similar mutagenic effect may also be hypothesized for CNTs. CNTs have shown genotoxic potential in several *in vitro* studies, including studies on the human lung epithelial cell line BEAS-2B [19, 20].

1.3.2 Parameters affecting toxicity of carbon nanotubes

Carbon nanotubes are a heterogeneous group of materials, with differences in structure, amount of impurities and physico-chemical properties. The toxicity between different carbon nanotubes seems to differ greatly. The main physico-chemical properties which are relevant in relation to the toxicity of CNTs are size, shape, agglomeration/aggregation state and surface properties of the particles. Surface properties include surface area, charge, reactivity, chemistry, in addition to solubility and crystallinity. These are properties that depend on the method of production, and the dispersion of the particles [21].

The size and shape of the CNTs have been shown to be crucial for toxicity. Longer CNTs are assumed to be more toxic because of the high aspect-ratio. The shape of the tubes also has an effect because it influences the ability to enter the deep regions of the lungs. Straight fibers are considered more toxic than tangled ones with similar length [5, 14]. The effect of size and shape on inflammatory responses and DNA damage has been shown in a recent study by Yamashita et al. In this study, DNA damage was studied using the Comet assay in human lung cancer cell lines, and inflammation was measured by intraperitoneal injection of mice followed by measuring the number of infiltrating cells after 24 hours. Long MWCNTs with high diameter were shown to result in the highest degree of DNA damage and inflammation, compared to CNTs that were shorter or had a smaller diameter [17].

Carbon nanotubes tend to aggregate or agglomerate in solution because of strong hydrophobic interactions between the particles. The aggregation/agglomeration state will affect the hydrodynamic diameter of the particles, influencing their deposition in the respiratory system, which greatly affect their biological effect [21]. When inhaled in aggregates/agglomerates, particles will often not appear as single fibers, which may affect the toxicity. SWCNTs generally seem to aggregate more than MWCNTs because of strong van der Waals forces.

Biopersistence is an important aspect of carbon nanotube-induced toxicity. The graphitic, hydrophobic nature of the CNTs, make them biopersistent, possibly causing a longer exposure period in the lung, and greater damage. The degree of hydrophobicity will differ between different carbon nanotubes and with different surface modifications. Pure CNTs with low levels of defects will be very biopersistent, consistent with the strong hydrophobic graphene material [6].

1.4 Oxidative stress responses

The toxicity of nanoparticles and CNTs in particular is thought to be mediated to a large degree by their ability to influence the cellular production of ROS/RNS.

1.4.1. Generation of ROS/RNS

A schematic overview of the formation of intracellular ROS/RNS is shown in Figure 1.3. Under normal conditions, the cells' various antioxidant defenses (catalase, glutathione peroxidase system, etc) neutralize the ROS/RNS rapidly. When the amount of ROS/RNS overrides the antioxidant defense systems, the cell is called to be in a state of oxidative stress [22].

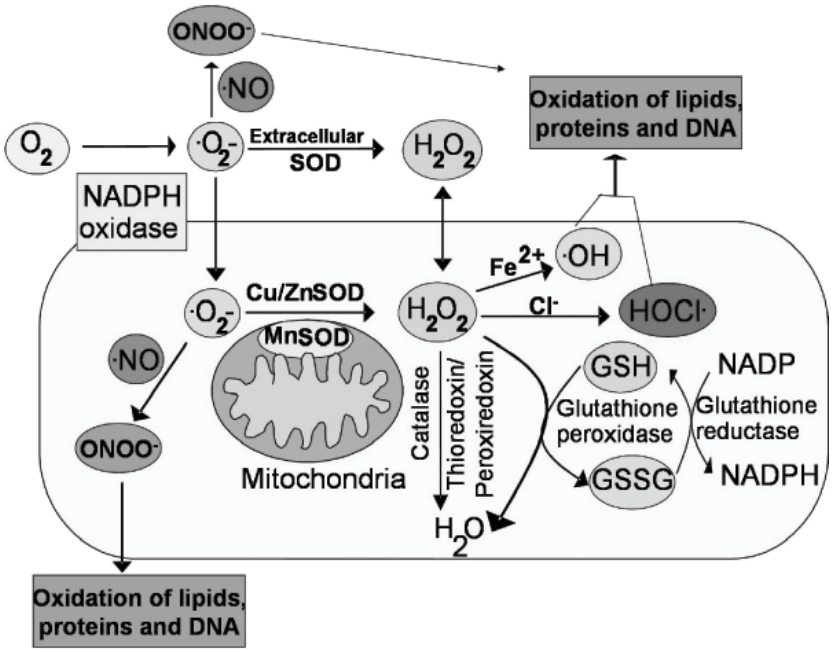

Figure 1.3: Schematic overview of the intracellular formation of reactive oxygen species, during aerobe metabolism. From Azad et al.[23].

Excess ROS and RNS can cause damage to proteins, lipids, membranes, DNA and RNA in the cells. Damage to DNA includes single and double strand breaks in DNA and oxidative modification of bases such as 8-oxoguanin adducts. Lipid peroxidation is another effect of ROS/RNS exposure, which can lead to membrane and DNA damage [22, 23]. ROS production also affects cell signaling cascades, and causes activation of gene expression through activation of specific transcription factors, most importantly nuclear factor kappa B (NF-κB) and activating protein 1 (AP-1). AP-1 is activated through mitogen-activated protein kinase (MAPK) pathways and may lead to initiation of transcription of genes involved in proliferation, cell differentiation, inflammation and apoptosis. NF-κB is a central transcription factor involved in the induction of inflammatory responses, proliferation and in repression of apoptosis. NF-κB is activated by ROS/RNS via redox sensitive mechanisms, or via MAPK signaling[23].

1.4.2 Formation of ROS/RNS in response to CNTs

Because of their small size, nanoparticles are thought to be transported easily into the cells by various mechanisms. Inside the cells, nanoparticles may be able to interact with mitochondria, which can lead to overloading or interfering with antioxidant defenses, causing oxidative stress. In addition, metal contaminants such as iron or cupper in the nanoparticles could increase the ROS/RNS formation. Transition metals cause formation of the highly reactive hydroxyl radicals via Haber-Weiss reactions, causing increased levels of oxidative stress. Extracellular ROS and metal contaminations can also affect membrane receptors like epidermal growth factor receptor (EGFR) on the cell surface, causing activation of signaling pathways, including MAPK pathways leading to the activation of AP-1 and NF-κB [1, 22]. Particles can also induce inflammatory signaling pathways leading to recruitment of inflammatory cells such as macrophages and neutrophils which produce ROS/RNS[22].

Some *in vitro* studies have been performed to investigate involvement of ROS/RNS in the toxicity of MWCNTs. In a study by Garza et al, there were shown significant increased levels of ROS in the human lung cancer cell line A549 following exposure to MWCNTs. However, ROS formation differed greatly between MWCNTs produced by different production methods. Particles produced using a nickel catalyst method gave a significantly higher level of ROS compared to particles produced by arc discharge. These results illustrate the effect of production method and level of metal impurities in the cytotoxic effects of various MWCNTs [24]. A study by Srivastava et al. has also shown generation of ROS by MWCNTs in a dose-dependent manner in the A549 lung cell line after 6, 12 and 24 hours exposure[25]. On the other hand, in a study by Tsukahara et al, there was shown no significant ROS production in BEAS-2B human lung epithelial cells after 24 hours exposure to MWCNTs. There was, however, high toxicity and induction of inflammatory responses, with increased expression of pro-inflammatory cytokines/chemokines such as Interleukin 6 (IL-6) and Interleukin 8 (IL-8) [26]. This study used a highly purified type of MWCNT, with very low contaminations of iron.

1.5 Induction of inflammatory responses by CNTs

Inflammation is a normal physiological process that normally occurs as a response to cell- and tissue damage or to infection, and is a response with the goal to heal the wounded tissue, remove the infectious agents and to maintain homeostasis. Inflammation is mediated by chemical signals, the release of pro-inflammatory cytokines and chemokines. The action of cytokines/chemokines leads to activation and directed migration of leukocytes from the circulation to the site of damage [27]. Two main pathways for activating inflammation are regulated by interleukin 1(IL-1) and tumor necrosis factor (TNF) both of which activate the NF-κB pathway. A schematic overview over the induction of inflammatory genes by IL-1 and TNF are shown in Figure 1.4.

Studies have shown different effects of exposure to carbon nanotubes regarding inflammation. Carbon nanotubes are thought to induce inflammation, leading to increased expression of pro-inflammatory cytokines. The inflammatory effect seems to differ with different carbon nanotubes. SWCNTs have been shown to decrease the protein levels of pro-inflammatory cytokines/chemokines like IL-6, IL-8 and Monocyte chemotactic protein-1 (MCP-1) in the human lung cell lines A549 and normal human bronchial epithelial cells (NHBE), indicating reduction of inflammatory responses [28]. For MWCNTs, several studies have shown induction of inflammation via activation of the central transcription factor NF-κB and the increased expression of pro-inflammatory mediators like IL-6 and IL-8 [29, 30].

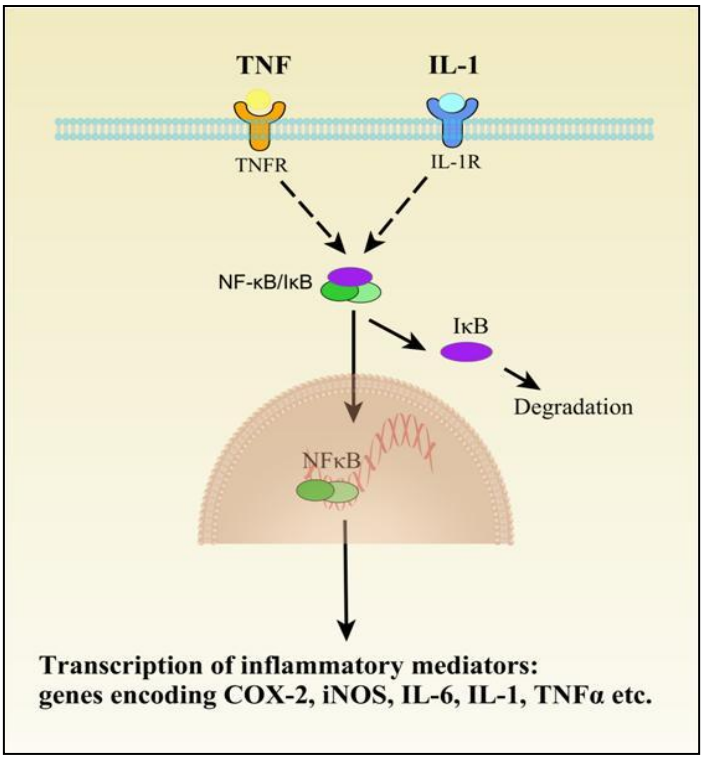

Figure 1.4 Schematic illustration of the induction of inflammation via the TNF/IL-1 pathways. Activation of the IL1/TNF receptors causes phosphorylation/degradation of IκB and translocation of NF-κB to the nucleus where it functions as a transcription factor. NF-κB activates genes involved in the inflammatory response, including genes encoding COX-2, iNOS, IL-6, IL-1, TNFα and other cytokines/chemokines.

Furthermore, chronic inflammation has been linked to development of several cancers including cancer in liver, colon, stomach, ovary, urinary bladder, esophagus and lung. Chronic inflammation contributes to a favorable microenvironment for tumor growth, promotion, angiogenesis and genetic instability through which activation of inflammatory cells leads to release of growth factors, activated stroma and DNA damaging agents which increase the risk for neoplastic transformation [27, 31].

1.5.1 Interleukin 1

The IL-1 family of cytokines is involved in the innate immune response, and includes Il-1α, IL-1β and IL-1Ra (receptor antagonist) [32]. IL-1α and IL-1β bind to the IL-1 receptor, leading to activation of inflammatory pathways. The IL-1Ra acts as a negative regulator binding to the IL1 receptor without activating further signaling.

Several studies have implicated IL-1β as the most important cytokine of the IL-1 family. Unlike *IL-1A* which is constitutively expressed, *IL-1B* is only transcribed in response to inflammatory stimuli. *IL-1B* mRNA is translated into pro-IL-1β, which requires cleavage to be activated, through the action of caspase-1 in the cytoplasm. After cleavage, Il-1β is secreted out of the cell. The gene expression of *IL-1B* is highly inducible in response to pro-inflammatory stimuli, e. g. as a consequence of activation of the central transcription factor NF-κB by Toll-like receptor (TLR)- or TNFR-signaling [33]. IL-1β activates gene expression and production of several other important inflammatory mediators like Cyclooxygenase-2 (COX-2), phospholipase A and inducible nitric oxide synthethase (iNOS). The increased

expression of these enzymes leads to increased levels of prostaglandin-E2, platelet activating factor and nitric oxide resulting in increased production of ROS/RNS. Like several other pro-inflammatory cytokines, IL-1 functions by activating the NF-κB pathway [32, 34]. At post-transcriptional level, IL-1 also functions by regulating the mRNA stability of several inflammatory mediators such as IL-6, COX-2 and cellular adhesion molecules. IL-1 also inhibits the protein expression of the Il1R type 1, by decreasing the mRNA half-life, causing negative feedback regulation [35].

The role of IL-1 in tumor development and its importance in the tumor microenvironment has been demonstrated in several studies. In one study, different *Il1* knock-out mice were generated by homologous recombination in BALB/c mice [36]. Cancer development was studied in the wild-type and knock-out mice by subcutaneous injection with 3-methylcholanthrene (3-MCA). Local fibrosarcomas developed in the mice after three to five months. The different knock-out mice showed great differences in the rate of tumor development as illustrated in Figure 1.5. The most rapid tumor development was seen in the *Il1rn*- knockout mice. The *Il1a* knock-out mice and the wild-type mice, showed a similar intermediate level of tumor development. The mice where *Il1b* was knocked out, showed a reduced frequency of tumor development, and longer time was required for a carcinogenic effect than in the other cell lines. These results indicate the importance of *Il1b* in cancer development; knocking out this gene reduces tumorigenicity compared to the wild-type. The fact that knocking down the receptor antagonist causes increased tumorigenicity also proves the carcinogenic role of IL-1, since IL-1Ra acts as a negative regulator of IL-1 signaling [37]. Fibrosarcoma cell lines from the same mice are used in the experiments in this thesis.

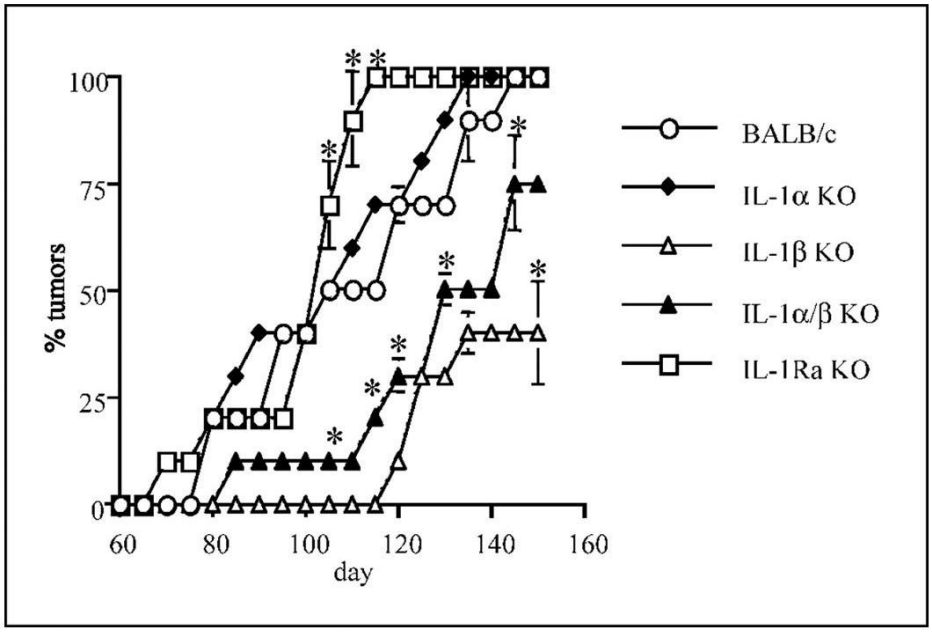

Krelin Y et al. Cancer Res 2007;67:1062-1071

Figure 1.5 Frequency of 3-MCA-induced tumors in IL-1/IL-Ra$^{-/-}$ mice. From Krelin et al [37].

IL-1β has also been closely linked to tumor development and carcinogenesis in human populations. Epidemiological studies have shown that genetic variation within the promoter

region of *IL-1B* is an important risk factor for the development of lung cancer. There has been shown that a specific combination of single nucleotide polymorphisms (SNP) in the promoter region of the *IL-1B* gene is overrepresented in patients with lung cancer. These SNPs have been shown to give a generally higher transcriptional activity of *IL-1B*, causing increased levels of inflammation [38, 39]. Polymorphisms in regions affecting *IL-1B* expression have also been linked to several other cancers, including gastric cancer [40].

1.5.2 Tumor Necrosis Factor alpha

The tumor necrosis factor alpha (TNFα) induced pathway of inflammation, is one of the main pathways in initiation of inflammation, in addition to the IL-1 induced pathway. TNFα binds to TNFRI on the cell surface of most cells, and TNFRII on blood cells. Under normal conditions, activation of the TNF receptor causes activation of the transcription factor AP-1 or activation of the IκB-kinases which leads to activation of NF-κB. This pathway gives much of the same response as for IL-1 activation, leading to increased transcription of genes involved in inflammation, inhibition of apoptosis and cell proliferation. The TNFRI can also function as a death receptor, activating the extrinsic pathway of apoptosis. If for some reasons, NF-κB is not activated following TNFRI activation, transcription of anti-apoptotic proteins will not be initiated and the apoptotic process will be activated through caspase 8 [41]. Mice deficient in TNFα or the TNF receptors are more resistant to several cancers, including liver and skin cancer, indicating an important role for this cytokine in carcinogenesis [42, 43].

1.5.3 Other important inflammatory mediators

NF-κB is a transcription factor which is central in regulation of inflammation, in addition to regulation of many other cellular processes. NF-κB is normally present as an inactive form in the cytoplasm of the cell, bound to inhibitory IκB proteins. Phosphorylation of IκB in response to stimuli, leads to release of NF-κB and translocation to the nucleus, where it functions as a transcription factor, initiating transcription of specific genes (Fig.1.4). NF-κB is activated by the binding of pro-inflammatory cytokines or other ligands to specific receptors on the cell surface, most importantly TLRs, the TNF receptors, and the IL-1 receptors. In the nucleus, NF-κB initiates transcription of genes involved in inflammation, including genes encoding COX-2, IL-6, TNFα and IL-1, giving a positive feedback loop and amplification of the inflammatory response. NF-κB also regulates genes involved in cell proliferation and genes that are involved in negative regulation of apoptosis [34, 44].

Multiwalled carbon nanotubes have been shown to induce expression of NF-κB in several cell culture studies, including studies performed with human lung epithelial cell lines. Hirano et al. (2010) showed significant increased transcriptional factor activity of NF-κB in cells of the BEAS-2B cell line exposed to doses of 1 – 10 μg/ml MWCNT using transient expression vectors. For the cancer cell line A549, Ye et al, found a dose-dependent increase in the DNA binding activity of NF-κB following exposure to 50 – 150 μg/ml MWCNT using the electrophoretic mobility shift assay (EMSA) [29, 30].

IL-6 is a pro-inflammatory cytokine, belonging to the IL-6 like family of cytokines. IL-6 binds to gp130 receptors on the cell surface, activating JAK/STAT and MAPK signaling, which causes activation of gene expression of specific genes involved in cell growth,

proliferation and activation of adaptive immune responses. IL-6 expression has been shown to induce growth and differentiation of B cells, and is also involved in the activation of CD4 positive T cells, inhibiting apoptosis in these cells [45, 46].

The cyclooxygenase (COX) family of enzymes catalyzes the formation of prostaglandins from arachidonic acid. Prostaglandins function as the precursors for eicosanoids which are important signal molecules in inflammation. There are two isoforms of COX-enzymes: COX-1 and COX-2, where COX-2 is the inducible form. COX-2 is particularly inducible by IL-1. The expression of COX-2 is also induced by a variety of other stress signals, including ROS/RNS and DNA damaging reagents [35, 47]. Polymorphisms located in the 3'UTR of COX-2 mRNA have been significantly linked to the development of non-small cell lung cancer in case-control studies [48]. There has also been shown that the use of non-steroidal anti-inflammatory drugs (NSAIDs) is associated with a decreased risk for development of several cancers, especially colorectal cancer. NSAIDs acts as selective inhibitors or covalently modify COX-2 enzymes, inhibiting the formation of prostaglandins [49].

1.6 Apoptotic cell death

Cell death can occur via several mechanisms, most commonly necrosis or apoptosis. Necrosis is an uncontrolled process of cell death, which is characterized by a ruptured cell membrane, and release of intracellular components, causing an inflammatory response in nearby cells [50]. Contrary, apoptosis is a form of programmed cell death which involves distinct changes in the cell architecture. Apoptosis is an essential mechanism for embryonic development, immune function and tissue homeostasis in multi cellular organisms. It is also a protective mechanism, preventing damaged cells to proliferate. Dysregulation of apoptotic pathways have been shown to be related to tumorigenesis. A common trait of most cancer cells is their resistance to undergo apoptosis [50, 51].

Morphologically, apoptotic cell death is recognized by cell shrinkage, detachment from neighboring cells and deformation. The chromatin in the nucleus becomes condensed and the plasma membrane is blebbing, causing formation of so-called apoptotic bodies. Apoptotic cells express specific surface molecules on the cell surface, including the phospholipid phosphatidylserine (PS), which increases recognition by macrophages [51, 52]. Apoptosis is initiated by the action of caspases. Inactive pro-caspases are present in the cytoplasm in normal cells. Proteolytic cleavage of the initiator pro-caspases causes activation of apoptosis, which is an irreversible process. Apoptosis is mainly regulated by proteins of the Bcl-2 family which include both pro- and anti-apoptotic members. Pro-apoptotic members include Bax and Bak, in addition to the BH3-only proteins Puma, Noxa, Bim, Bad and Bid. Anti-apoptotic proteins include the Bcl-2 proteins present in the mitochondrial membrane. The expression and localization of these proteins are tightly regulated [51]. Activation of apoptosis can occur in response to intracellular signals. Intrinsic signals cause increased expression of pro-apoptotic Bcl-2 proteins. This causes changes in the permeability of the mitochondrial membrane, leading to release of cytochrome c into the cytosol. Cytochrome c is a key signaling molecule in apoptosis, causing formation of the apoptosome, and activation of effector caspases. The intrinsic pathway of apoptosis is triggered by extracellular and intracellular stress, including hypoxia, growth factor withdrawal, DNA damage and oncogene

induction [50]. Apoptosis can also be induced by extracellular stimuli, like binding of TNFα or FAS Ligand to their respective receptors on the cell surface, activating pathways leading to activation of the initiator caspase 8. Independent of route of activation, apoptotic pathways lead to the activation of the effector caspases; caspase-3, caspase-6 and caspase-7, causing proteolytic events which are specific for apoptosis [51].

MWCNTs have been shown to induce apoptosis *in vitro*. Lung epithelial cells exposed to MWCNTs, have shown activation of AP-1 and NF-κB via MAPK signaling pathways, indicating a role of oxidative stress in induction of apoptosis. In these studies, there have also been shown activation of P53 and increased expression of apoptotic proteins like caspase-3 and Bax [16, 25].

TP53 is a tumor suppressor gene encoding a central transcription factor, which regulates genes involved in several important cellular mechanisms necessary for maintaining homeostasis and preventing tumor development. *TP53* has an important role in tumorigenesis and has been found to be mutated in over 50% of human cancers, resulting in loss of apoptotic function[53]. P53 is activated by phosphorylation following different stress stimuli like DNA damage, hypoxia, and over-expression of oncogenes. Activation causes translocation to the nucleus where P53 activates transcription of genes involved in cell cycle arrest, senescence and apoptosis. A schematic overview of signals causing P53 activation and the cellular response is shown in Figure 1.6. P53 activates apoptosis via activation of genes involved in death receptor pathways, mitochondrial pathways and by inhibition of survival signals [53, 54].

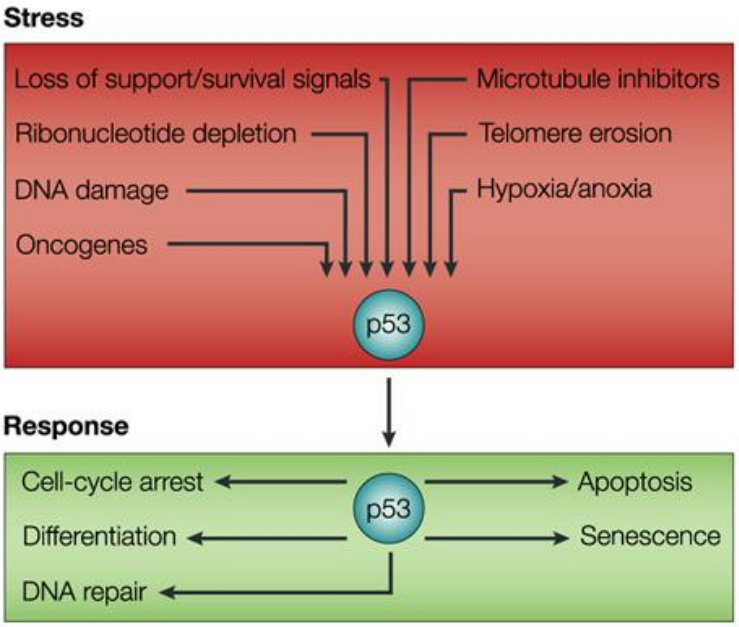

Figure 1.6 Schematic overview over the P53 response. P53 is activated following various stress signals, initiating processes like senescence, apoptosis and cell-cycle arrest. From Vousden and Lu [53].

Mice deficient in P53 have been shown to develop mesothelioma in response to MWCNT exposure, a response similar to that following asbestos exposure. There was found 87.5 % and 77.8 % incidence of mesothelioma following MWCNT and crocidolite exposure respectively, compared to no incidence in the control group. The $P53^{(+/-)}$ mice model has increased sensitivity for cancer development, because of the reduced activity of P53, impairing the activation of apoptotic processes or cell cycle arrest following DNA damage [55]. This study has however been subject to criticism, among others due to a very high dose of particles used (3 mg/mouse), lack of characterization of the particles used, and lack of knowledge of the P53-deficient mouse model [56].

1.7 Project aims and hypothesis

Inhalation of fiber-like compounds such as asbestos has been shown to lead to several adverse health effects including fibrosis and cancer. Due to the structural similarities with asbestos, it is possible that CNTs may lead to the same adverse effects following exposure. Similar to asbestos, CNTs in particular MWCNTs, have been shown to induce biological responses such as oxidative stress, inflammation, DNA damage/repair and cell death. However, it has been hypothesized that the biological responses may vary between CNTs produced by different producers and even varying from batch to batch from the same producer. It is also hypohesized that genetic factors may modulate the cellular responses following CNT exposure, especially genes regulating inflammatory reactions such as the IL1 gene family.

The aims of this study was to investigate the cellular responses, and some of the molecular mechanisms involved in CNT exposure, using MWCNTs from two different producers, located in Norway and in Japan. The responses were compared with a known asbestos fiber (UICC crocidolite) and an oxidative agent (hydrogen peroxide). Furthermore, an *Il1* knock-out model system was used to investigate the effect of IL-1 on endpoints such as cytotoxicity, apoptosis and gene expression of inflammatory/apoptotic genes following the exposures. IL-1β is an important mediator of inflammation, and differential expression of this cytokine has been associated with the risk of developing cancers where chronic inflammation is an important factor. A flow diagram illustrating the work performed in this thesis is shown in figure 1.7.

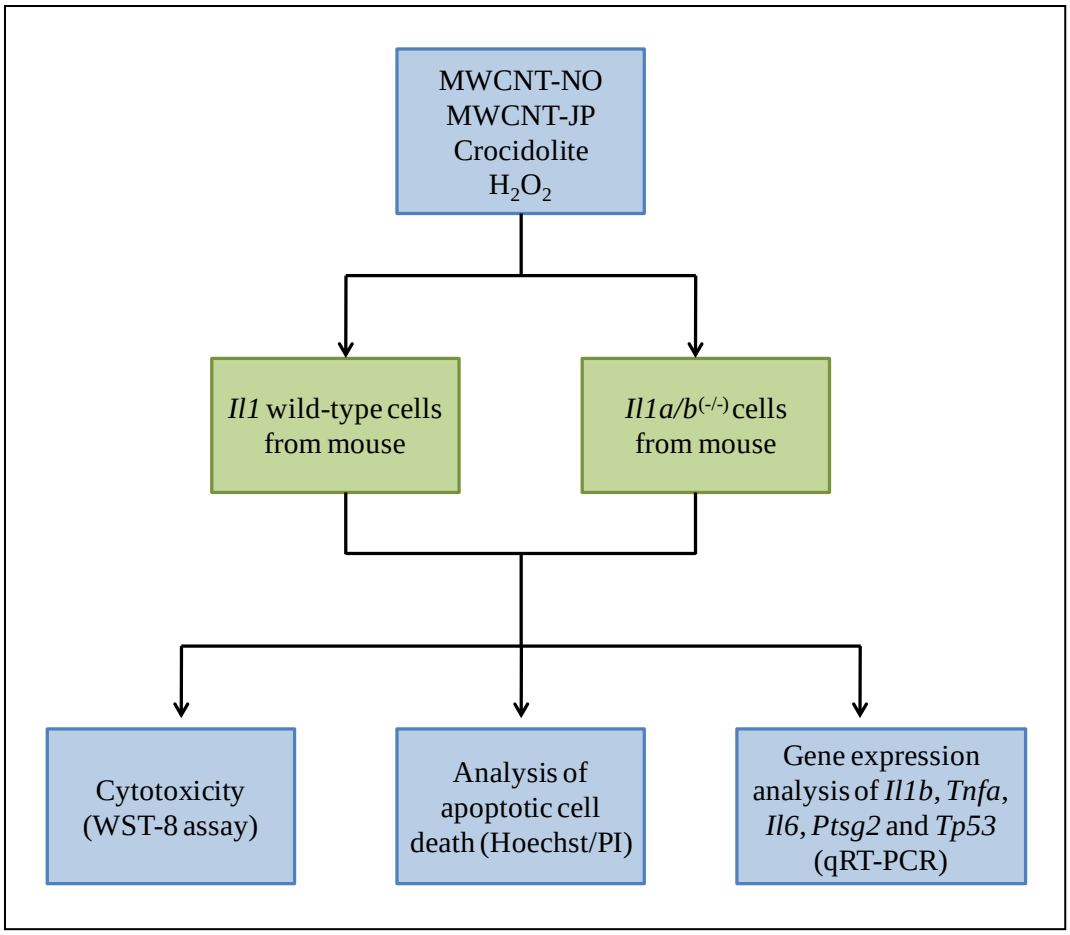

Figure 1.7 Overview of the work performed in this thesis.

2. Materials and Methods

2.1 Materials

A complete list of chemicals, solutions and instruments used in the experiments can be found in appendix I

2.1.1 Cell lines

The cell lines used in these experiments were kindly provided by Professor R.N Apte (Department of Microbiology and Immunology, NIBN, Israel). The cell lines originate from wild-type (WT) and IL1α/β$^{(-/-)}$ mice from a BALB/c strain. Tumors were induced in the mice by subcutaneous injection with 3-methylcholanthrene (3-MCA) as described by Krelin et al. (2007). After incubation, a majority of the mice developed fibrosarcomas as described in chapter 1.5.1. The tumors were removed, and parts of the tumor tissue were processed with trypsin for establishment of cell lines [37].

The cell lines used are the wild-type cell line (WT), and the *Il1a/b* double knock-out cell line (*Il1a/b* KO). Fibrosarcomas were initiated by the same method, and cell lines were established under same conditions in the two mice, it is therefore expected that also the cell lines are genetically similar, the only parameter differing between the cell lines is the presence or abscence of *Il1* [36, 37]. The two cell lines displayed different morphology under normal conditions when observed by a phase contrast microscope, with WT cells (Fig. 2.1A) generally being smaller than the *Il1a/b* KO cells (Fig. 2.1B). The cells also exhibited different growth patterns, with WT cells being clustered, while *Il1a/b* KO cells generally seemed to be evenly distributed in culture.

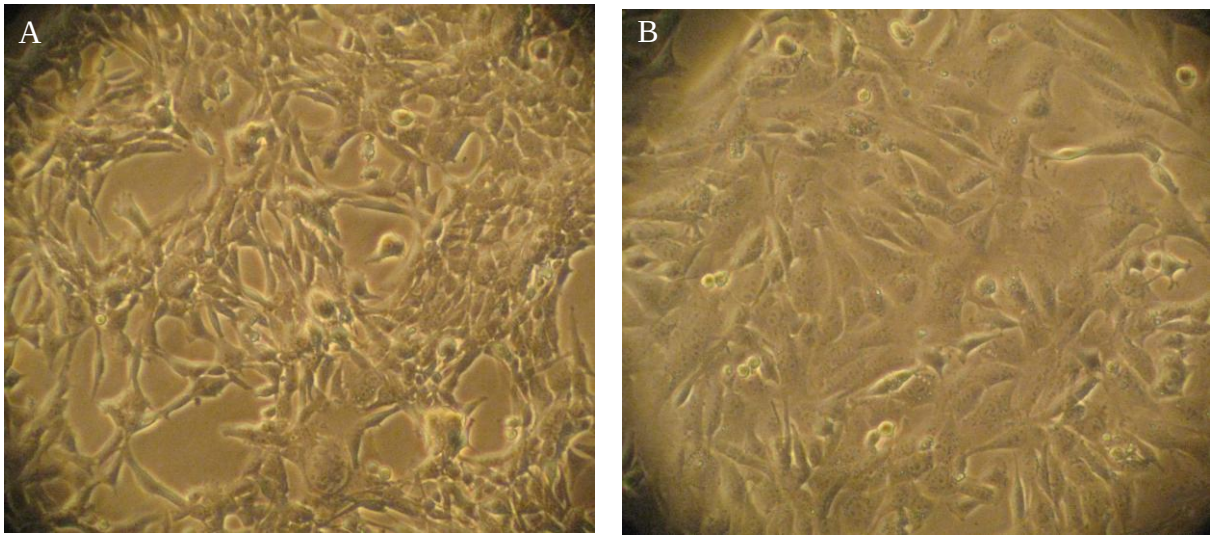

Figure 2.1: Photographs from phase contrast microscopy of the cell lines used in this project at normal morphology, 70 – 80 % confluency. Figure A: WT cell line, B: *Il1a/b* KO cell line.

2.1.2 Particles

Multi-walled carbon nanotubes (MWCNT) from two different producers were used in the experiments, MWCNTs produced in Norway (MWCNT-NO), and MWCNTs produced in

Japan (MWCNT-JP). The MWCNT-NO particles, have not yet been subject to characterization or toxicity studies. These particles are produced using the arc discharge method. Data obtained from the distributor, states that the length of the MWCNT-NO lies in the size range 0.2 -5.4µm, with a mean length of 1.4 µm ±0.1. The diameter lies in the size range 2-67 nm and the mean diameter is stated to be 26.7 nm ±3.4.

MWCNT-JP has earlier been subject to both *in vivo* and *in vitro* toxicity studies, and is relatively well characterized. The particles are synthesized using CVD. In a characterization study by Takaya et al.(2010) using Scanning electron microscopy (SEM) and dynamic light scattering, the MWCNT-JP have been found to have a length of 5 ± 4.5µm and a diameter of 88 ± 5 nm where 38.9 % of the fibers were shown to be longer than 5 µm. The particles contained some contaminations of iron, chromium and nickel [57]. In another characterization study, the general length of the particles were somewhat shorter, with mean length at about 2 µm, and a mean diameter at about 100 nm. 27. 5 % of the fibers in this study were longer than 5 µm. There were found contaminations of iron also in this study [55].

The MWCNTs used in the experiments were characterized using scanning electron microscopy (SEM). SEM was kindly performed by Scientist Asbjørn Skogstad at NIOH.

The crocidolite asbestos (UICC Crocidolite reference sample) was used as a positive control in this study, and was provided by the Medical Research Council (England).

2.2 Work with eukaryote cell culture

Cell culture work was performed under sterile conditions in an OAS LAF bench. Cell cultures were incubated at 37°C, with 95 % humidity and 5 % CO_2. Only sterile or autoclaved equipment and solutions were used in the experiments.

2.2.1 Thawing of cells from storage in liquid nitrogen

The following protocol was used when taking up cell lines from storage in liquid nitrogen.

1. Cells were removed from storage in liquid nitrogen, and thawed in a water bath at 37°C.
2. The cell suspension was transferred to a 15 ml falcon tube, 5 ml PBS was added.
3. The tube was sentrifuged at 1000 rpm for 4 minutes.
4. The supernatant was carefully removed and the cell pellet was resuspended in 3 ml medium
5. The suspension was transferred to a 100 mm petri dish, 5 ml medium was added, giving a total of 8 ml medium.
6. After 24 hours, the cell culture media was removed, 8 ml fresh media was added.

2.2.2 Maintaining cell cultures

Cells were replated when reaching 70 – 80 % confluency, and medium was replaced 2-3 times per week. Cells were replated using trypsin. This enzyme degrades cell adhesion molecules, which connects the cells to the petri dish, causing the cells to detach from the plate. The general procedure for replating cell cultures is described below. The given amounts of reagents are suitable for 100 mm cell culture dishes.

1. Medium was removed from the cells.
2. Cells were cleaned twice with 10 ml phosphate buffered saline(PBS).
3. The cell cultures were added 1 ml trypsin.
4. The trypsinated cells were placed in a 37°C incubator for a few minutes until the cells had detached from the dish.
5. The cell culture dish was added 5 ml medium to stop the enzymatic activity of trypsin. The cell suspension was transferred to a 15 ml sentrifuge tube. The dish was then cleaned once more with 5 ml media, giving a total of 10 ml cell suspension.
6. The cell suspension was centrifuged by 1000 rpm for 4 minutes.
7. The supernatant was carefully removed
8. When to be used in an experiment, the cell pellet was first added 20µl of DNase, then 10 ml medium was added. DNase was used to prevent clustering of the cells, which can cause uncorrect concentration measurements. 10 µl of the cell suspension was transferred to a vial and 10 µL Trypane Blue stain was added. Trypane Blue distinguishes between viable and dead cells, dead cells are stained blue because of an unintact plasma membrane.10 µL of this solution was applied to a counting slide or Bürcher cell counting chamber. Cells were counted automatically using the Countess automated cell counter (Invitrogen) or manually using a Bürcher counting chamber in a phase contrast microscope. The concentration of cells in the suspension was calculated, and cells were distributed to new dishes in known numbers.
9. When cells were not to be used in an experiment, the cell pellet was directly resuspended in medium and the cell suspension was transferred directly to new petri dishes. The amount of cell suspension which was transferred to new plates depended on the wanted degree of dilution. Usually, cells were diluted 1:10 or 1:20. Media was added to yield a total amount of 8ml.

Other petri dishes than 100 mm plates were also used in experiments. Table 2.1 summarizes the surface areas of the plates, and the amount of medium that was used for plating out cells and used for exposure. The amount of medium used for exposure was calculated according to the surface area of the dish, so that the amount of particles per surface area should be the same between the different types of dishes.

Table 2.1 Overview of amount of medium used for plating out cells in different types of plates, and amount of medium used for exposure.

Plates	**Surface area per well (cm^2)**	**Amount of medium(µl)**	
		For plating out cells	**For exposure**
100 mm	100	8000	-
6 well plates	9.6	1500	2500
12 well plates	3.5	700	900
96 well plates	0.4	100	100

2.2.3 Preparing cells for storage in liquid nitrogen

For long term storage, cells were stored in liquid nitrogen in a suspension of aseptic media (AF media) and dimethylsulfoxide (DMSO). DMSO was added to make the cell membrane permeable, thereby preventing osmotic pressure and lysis of the cells. Cells were trypsinized

from a petri dish as described in chapter 2.2.2. After centrifugation and removal of the supernatant (step 7), the following procedure was followed.

1. The cell pellet was carefully resuspended in 500 µl AF-media. The cell suspension was transferred to a 1.8 ml freezing vial.
2. 500 µL 8 % DMSO was added to the freezing vial. The suspension was mixed thoroughly.
3. The vial was placed in the Cool Cell box, which was placed at -80°C for 4-6 hours. The Cool Cell box provides gradual decrease in temperature, about 1° C decrease per minute.
4. The vial was placed for storage in liquid nitrogen

2.3 Dispersion of particles and exposure to cell cultures

MWCNTs and Crocidolite were dissolved in dispersion medium (DM) followed by sonication. DM contains PBS supplemented with 0.6 mg/ml Bovine Serum Albumin (BSA), 0.01 mg/ml 1,2-dipalmitoyl-sn-glycero-3-phosphocholine(DPPC) and 5.5 mM d-Glucose. For more information, see appendix I.

2.3.1 Dispersion and sonication of MWCNTs and Crocidolite

Particles were dissolved in DM according to the following procedure.

1. An appropriate amount of particles were transferred to a tube. The weight of the tube was measured before and after addition of particles, and the weight of the particles was calculated.
2. Dispersion media was added to the tube, giving a 1 mg/ml stock solution.
3. 2 droplets of Tween 80 were added.
4. Samples were sonicated (20 % duty cycle, 6W) on ice for 3x5 minutes.
5. The stock solutions of particles were used for exposing cells immediately after sonication.

2.3.2 Exposure of cells to MWCNTs, Crocidolite and H_2O_2.

Exposure to cell culture was performed using the following protocol

1. Cells were seeded out approximately 24 hours before exposure as described in chapter 2.2.2.
2. The 1 mg/ml stock solution of MWCNTs (chapter 2.3.1) and crocidolite were diluted in cell culture media, gaining specific concentrations (5 -100 µg/ml). DM was added to yield a total of 10 % for each concentration, including the control. H_2O_2 (8.8 M) were diluted to a 1mM stock solution in dH2O, the stock solution was diluted to specific concentrations (1-10 µM) in cell culture media.
3. Cell culture media was removed from the cell culture plates. Particle/H_2O_2 solutions were added in various concentrations. Volumes of exposure solution used for the different cell culture plates are shown in table 2.1.
4. Exposed cells were incubated at 37°C for various periods of time including 6, 24, 48 and 72 hours.

2.4 Cytotoxicity studies

Cytotoxicity tests were performed for 4 different test materials including MWCNT-NO, MWCNT-JP, UICC Crocidolite and hydrogen peroxide (H_2O_2).

For determination of cell viability, the WST-8 assay was used (Sigma). This is an absorbance based method, which measures the dehydrogenase activity of metabolically active cells. The WST-8 assay is based on the water soluble tetrazolium salt WST-8 [2-(2-methoxy-4-nitrophenyl)-3-(4-nitrophenyl)-5-(2, 4-disulfophenyl)-2H-tetrazolium, monosodium salt] which is reduced to yellow colored formazan by metabolically active cells. The amount of formazan produced is directly proportional to the amount of living cells, and can be measure spectrophotometrically. WST-8 has its absorbance peak at 460 nm, which causes low interference with the OD of nanoparticles (OD ≈ 600 nm).

The cytotoxicity assays were performed using 96-wells plates with a density of 5000 cells per well, cells were seeded out as described in chapter 2.2.2. In the 96 well plates, cells were also seeded out with different densities (500, 1000, 2000, 3000, 4000, 5000, 10000 and 20000 cells per well) for the generation of a standard curve. These cells were exposed to the control solution (cell culture + DM), and were used as a quality control for each experiment. Examples of standard curves for the WT and *Il1a/b* KO cell lines are shown in appendix II.

Exposure was performed 24 hours after seeding out cells, as described in chapter 2.3. The WT and the *Il1a/b* KO cell lines were exposed to five different concentrations of each compound in addition to a control sample with no exposure. The doses used for exposure were 5, 10, 20, 50 and 100 µg/ml for MWCNT-NO, MWCNT-JP and Crocidolite, and 1, 2, 4, 5 and 10 µM for H_2O_2. Three replicates were carried out for each of the different concentrations. For cytotoxicity assays, cell culture media without phenol red was used for exposure because of potential interference of phenol red with absorbance readings.

After exposure (6, 24, 48 or 72 hours), media was removed from the 96 well plates, and the cells were washed twice with 200 µl PBS to remove excess particles. There was added 100µl cell culture media (without phenol red) and 10µl WST-8 solution to each well. Cells were incubated at 37°C for 4 hours. The absorbance at 450 nm and 750 nm was measured using the Modulus Microplate Reader. Three to five independent experiments were performed for each substance and time point.

The data from the cytotoxicity studies were used to determine the doses and time of exposure to be used for studies of apoptosis and gene expression. Doses and time of exposure that gave low levels of toxicity (80 – 90 % viability) were used in the further studies.

2.5 Hoechst/PI staining and fluorescence microscopy

Hoechst/PI-staining combined with fluorescence microscopy was used to determine the contribution of apoptotic cell death compared to necrotic cell death in exposed and control samples. Cells were stained by the use of two different fluorescent dyes; Hoechst 33342 and propidium iodide (PI). Hoescht 33342 binds to DNA, giving blue fluorescence. The compound is lipophilic, and passes through the plasma membrane of all cells. PI binds to both RNA and DNA, giving red fluorescence. Unlike Hoechst 33342, PI is not able to permeate the

plasma membrane and can only interact with DNA/RNA in cells that do not have an intact plasma membrane. When observed in a fluorescence microscope after staining, the nucleus of live cells will be stained blue, with both light and dark areas. The nucleus of apoptotic cells will also be stained blue, but because of the nuclear condensation which is a hallmark of apoptotic cells, the nucleus will appear more intense, with clear spots. Necrotic cells, which do not have an intact plasma membrane will stain red.

The following procedure was followed for staining and visualization of apoptotic cells.

Cells were seeded out in 12-well plates in a density of $1.1*10^5$ cells per well, as described in chapter 2.2.2. After attachment of the cells to the surface (about 24 hours incubation), cells were exposed to MWCNT-NO (5, 10, 20 µg/ml), MWCNT-JP (5 µg/ml), Crocidolite (20 µg/ml), H_2O_2 (4µM), Thapsigargin (100 nM) and control (cell culture media + 10% DM) as described in chapter 2.3.2. 2 parallel samples were made per experiment, 3 independent experiments were performed.

After 24 hours exposure, the following procedure was performed

1. The cell culture media from each well (900 µL) was transferred to eppendorf vials (1.5 ml), one for each well.
2. Wells were cleaned twice with 250 µL PBS, this was transferred to the eppendorf vials.
3. 90 µL trypsin was added to each well
4. Cells were incubated at 37°C for 2-3 minutes
5. The media/PBS solution in the eppendorf vials was used to clean the wells after treatment with trypsin, the solution was then transferred back into the vials.
6. 20 µL staining solution was added to each vial (Hoechst 33342(1 mg/ml) + PI(0,5mg/ml), scale 1:1)
7. The cell suspension was mixed thoroughly and incubated dark at room temperature for 30 minutes
8. The cell suspension was centrifuged at 3000 rpm for 10 minutes at 4°C
9. The supernatant was removed carefully
10. The pellet was resuspended in 10 µL FBS
11. Two droplets were dispersed and smeared out on a microscopic slide, and were left to dry.
12. The microscopic slides were observed in a fluorescence microscope. The number of apoptotic, necrotic and live cells was counted. A total number of 300 cells were counted per slide.

2.6 Isolation of RNA

Total RNA from cell cultures for use in cDNA synthesis and qRT-PCR was isolated using Isol-RNA lysis agent (5-prime). This reagent contains phenol and guanidine thiocyanate, which causes lysis of cells, and inhibits the activity of RNases. When adding chloroform to the lysate, followed by sentrifugation, the solution will be divided into two phases, an organic phase at the bottom and an aqueous phase on top. The organic phase contains lipids and

proteins, the interphase contains DNA, while the aqueous phase contains RNA. RNA is precipitated when adding isopropanol.

The cells used for isolation of RNA were plated out in 6 well plates with a density of $3*10^5$ cells per well as described in chapter 2.2.2. After 24 hours incubation, cells were exposed to MWCNT-NO (5, 10 µg/ml), MWCNT-JP (5 µg/ml), Crocidolite (20 µg/ml), H_2O_2 (4µM) and control (cell culture media + 10% DM) as described in chapter 2.3.2. After 24 hours exposure, cells were washed three times with ice cold PBS, and stored at -80°C. The following procedure was performed under sterile, RNase free conditions in an OAS LAF bench.

1. 1 ml Isol-solution was added to each well of the 6 well plate. The cell lysate was pipetted up and down several times, and transferred to an eppendorf vial. The lysate was incubated for 5 minutes at room temperature.
2. 200 µl chloroform was added to each vial, the vials were shaken powerfully for 15 seconds. The samples were incubated for 2-3 minutes at room temperature.
3. Samples were centrifuged at 12000 g for 15 minutes at 4°C.
4. The water soluble phase of the samples (on top) was transferred carefully to new tubes. 500 µL iso-propanol was added to each vial, and the samples were mixed thoroughly. Samples were incubated at room temperature for 10 minutes.
5. Samples were centrifuged at 12000 g for 15 minutes at 4°C.
6. The supernatant was removed carefully. The RNA pellet was then added 1 ml 75 % EtOH (in DEPC-H_2O). The samples were mixed thoroughly and vortexed.
7. Samples were centrifuged at 12000 g for 5 minutes at 4°C.
8. The supernatant was removed. The tubes were then centrifuged for additional 10 seconds for spinning down the last ethanol. The supernatant was removed carefully.
9. The pellet was left to dry for 5 – 10 minutes. The pellet was resuspended in 10 µL DEPC water, and the vials were placed on ice.
10. Samples were incubated at 65°C for 10 minutes. The contents of each vial were mixed using a pipette. RNA samples were stored at -80°C.

2.7 Measurements of RNA concentration and quality

RNA concentration and quality was measured using the Eppendorf Biophotometer. The RNA concentration was measured at OD 260 nm. The $OD_{260/280}$ and $OD_{260/230}$ ratios were used to determine quality of the isolated RNA, and indicate contaminations with proteins and solvents respectively. Both of these ratios should ideally lie round 2.0. RNA concentrations were used to calculate dilutions of RNA to be used in cDNA synthesis and were measured using the following procedure.

1. Isolated RNA was taken up from storage at -80°C, and was incubated at 65°C for 10 minutes. RNA samples were placed on ice.
2. RNA was diluted in TE-buffer; 1µl RNA + 80 µl TE-buffer.
3. 70 µl diluted RNA was added to a quartz cuvette, and RNA concentration and quality was measured using the Eppendorf biophotometer.

2.8 cDNA synthesis

Complimentary DNA (cDNA) was synthesized from isolated RNA using the qScript™ cDNA Synthesis Kit (Quanta Biosciences). Before cDNA synthesis, RNA samples were diluted in nuclease free water to yield 1µg RNA/5 ml. Dilutions were calculated using the measured RNA concentration (chapter 2.7).

The experiments were performed according to the protocol, adding 10 µl nuclease free water, 4 µl qScript reaction mix and 1 µl qScript reverse transcriptase(RT) per RNA sample. The qScript reaction mix includes all reagents needed for the cDNA synthesis, including optimized buffer, magnesium, primers (oligo(dT)20 + random primers), and dNTPs (Quanta Biosciences). The cDNA synthesis was performed using the Perkin Elmer Cetus DNA Cycler 480 with the program shown in table 2.2. After synthesis, cDNA was added 80 µL TE-buffer, giving a total of 100 µl with the cDNA concentration 10µg/µl. cDNA samples were stored at -20°C.

Table 2.2 Program used for cDNA synthesis.

Step	Temperature(°C)	Time(min)
Incubation	22	5
cDNA synthesis	45	30
Enzyme denaturation	85	5
Cooling	4	5

2.9 Quantitative reverse transcriptase PCR

Quantitative RT PCR (qRT-PCR), is an effective method for measuring gene expression of specific genes. qRT-PCR is a specialized version of the original polymerase chain reaction (PCR). It is a quantitative method, which is used to measure the relative expression of genes. The method facilitates detection of eventual differences in gene expression between samples. The method is based on the detection and quantification of a fluorescent reporter during the PCR reaction. In these experiments, SYBR® green is used, this dye binds to double stranded cDNA, and emits light upon excitation. During the PCR reaction, the level of fluorescence will increase proportionally to the amount of PCR product [58].

2.9.1 Primer design

For this project, primers for the genes *Actb*, *Il1b*, *Il6*, *Ptgs2*, *Tnfa* and *Tp53* in mice were used. The primers were designed specifically for this project, using the Primer 3 program (http://frodo.wi.mit.edu/primer3/) and the beacon designer (Premier Biosoft) followed by testing of specificity with Primer BLAST (NCBI). Primers were ordered from Thermo Fischer Scientific. The primers were specifically designed for qRT-PCR by including two or more exons, which makes eventual contaminations with genomic DNA easily detectable. Eventual genomic DNA contains introns, which would give much larger amplicons, and can be detected in the dissociation curve for the qRT-PCR products.

The primer sequences used in the experiments are shown in table 2.3. The primers were tested for specificity by qRT-PCR (dissociation curve) and for correct amplicon size by agarose gel electrophoresis of PCR products. Because of the low specificity of SYBR Green, it is important to prevent eventual double stranded DNA structures that can form between primers.

The primers used in this project (table 2.3), were shown to be functional, although there was observed some formation of primer dimers for the *Tp53* primer. However, these dimers did not seem to be formed in samples containing cDNA. For more information, see appendix III.

Table 2.3: Primer sequences used in real time PCR.

Primer		Sequence (5'→3')	GC(%)	Tm(°C)	Amplicon size(bp)
Actb, *Mus musculus*	Forward	GCTTCTTTGCAGCTCCTTCGT	52.38	55.69	75
	Reverse	CCAGCGCAGCGATATCG	64.71	53.02	
Il1b, *Mus musculus*	Forward	TGAAATGCCACCTTTTGACA	40.00	50.21	189
	Reverse	TTCTCCACAGCCACAATGAG	50.00	52.00	
Il6, *Mus musculus*	Forward	GTTCTCTGGGAAATCGTGGA	50.00	51.44	84
	Reverse	TTCTGCAAGTGCATCATCGT	45.00	52.42	
Ptgs2, *Mus musculus*	Forward	GGCCATGGAGTGGACTTAAA	50.00	51.62	110
	Reverse	ACCTCTCCACCAATGACCTG	55.00	53.09	
Tnfa, *Mus musculus*	Forward	CCACCACGCTCTTCTGTCTA	55.00	53.33	103
	Reverse	AGGGTCTGGGCCATAGAACT	55.00	53.88	
Tp53, *Mus Musculus*	Forward	AGAGACCGCCGTACAGAAGA	55.00	60.01	304
	Reverse	TATGGCGGGAAGTATACTGG	55.00	60.09	

2.9.2 qRT-PCR setup

The following procedure was followed when preparing 96 well plates for qRT-PCR. The procedure was performed under RNase free conditions, and all reagents were put on ice during the experiment, preventing degradation. For qRT-PCR, Perfecta SYBR Green fast mix was used. This mix contains all reagents necessary for the qRT-PCR reaction (except for primers), including optimized concentrations of $MgCl_2$, dNTPs, Taq DNA Polymerase, SYBR Green I dye, ROX Reference Dye, and stabilizers (Quanta Biosciences).

1. Master mix was made for each gene to be examined, using the reagents shown in table 2.4.
2. cDNA samples were diluted in various concentrations for the different genes, depending on the expression level of the gene. For *Il1b*, *Tnfa* and *Il6*, undiluted cDNA (50ng/sample) were used because of low expression levels. For *Ptgs2*, *Tp53* and *Actb*, cDNA was diluted to concentrations of 10 ng, 5 ng and 2.5 ng per sample, respectively.
3. The template dilution series for the standard curve was prepared. For the standard curve, a cDNA sample with high expression of the genes of interest was used. In the standard curve for *Actb*, *Il6* and *Ptgs2*, cDNA from the unexposed *Il1a/b* KO cell line were used. For *Tnfa* and *Tp53*, cDNA from the unexposed WT cell line was used. There was not found a cDNA sample with a sufficiently high expression of *Il1b* in mice, there was not included a standard curve in the setup for this gene. cDNA was diluted in 5 steps, diluting the cDNA 4 * per step. The setup and concentrations of cDNA for the dilutions are shown in table 2.5. For *Actb*, dilutions from 0.049 -12.5 ng were used (because of high expression), while for the other genes, dilutions from 0.195 – 50 ng were used.

4. The cDNA samples were transferred to a 96 well plate. 5 µl template was added to each well, two parallels of each cDNA sample was included. For each gene, the standard curve, a non template control (dH_2O) and cDNA samples were added. 15 µl Mastermix specific for each gene was added to each well. The 96 well plates were covered with ampicillin film, and the plate was centrifuged at 2500 rpm for 25 seconds.

Table 2.4 Mastermix used in Real Time PCR, reagents used per cDNA sample.

Reagents	**Amount per sample(µL)**
dH_2O	4.6
2 * Perfecta SYBR Green FastMix	10
Forward primer (25 pmol/µL)	0.2
Reverse primer (25 pmol/µL)	0.2
Total	15.0

Table 2.5 Setup for standard curve solutions, one gene.

Dilution	**cDNA(µl)**	**dH_2O(µl)**	**Concentration(ng/well)**
0	5 from cDNA stock		50
1	4 from cDNA stock	12	12.5
2	4 from dilution 1	12	3.13
3	4 from dilution 2	12	0.78
4	4 from dilution 3	12	0.195
5	4 from dilution 4	12	0.049

The 96 well plate was inserted into the ABI PRISM 7900 HT Sequence detection system, and PCR was run using the program shown in table 2.6. The initiation step of the PCR reaction involves activation of the thermostable DNA polymerase and denaturation of the DNA strands. The amplification step involves denaturation of the DNA strand (95°C) followed by annealing of primers and extension of the DNA strand (60°C) which is repeated 40 times. The qRT-PCR reaction is terminated with a dissociation step, which is used for the creation of a dissociation curve.

Table 2.6 Program used for performing qRT-PCR.

Step	**Temperature (°C)**	**Time (sec)**
1 Initiation	95	120
2 Amplification – repeated 40 times	95	5
	60	30
3 Dissociation	95	15
	60	15
	95	15

2.9.3 Processing of data obtained from qRT-PCR.

The data obtained from qRT-PCR was processed using SDS 2.4 software and presented in a semi-logaritmic plot as shown in figure 2.2. For gene expression analysis, the CT value was used. The CT value can be defined as the number of cycles where the PCR kinetic curve reaches a threshold amount of fluorescence [59]. The CT value lies in the exponential phase of the PCR reaction, where the fluorescence increases the most compared with the background fluorescence. The CT value will depend on the original concentration of cDNA template in the sample; cDNA which is present in high concentrations in the cDNA template

will have a low CT-value, while cDNA which is present in low concentrations will have a high CT value. In the experiments, the fluorescence threshold value ΔRn was set to 1.0 as shown in figure 2.2.

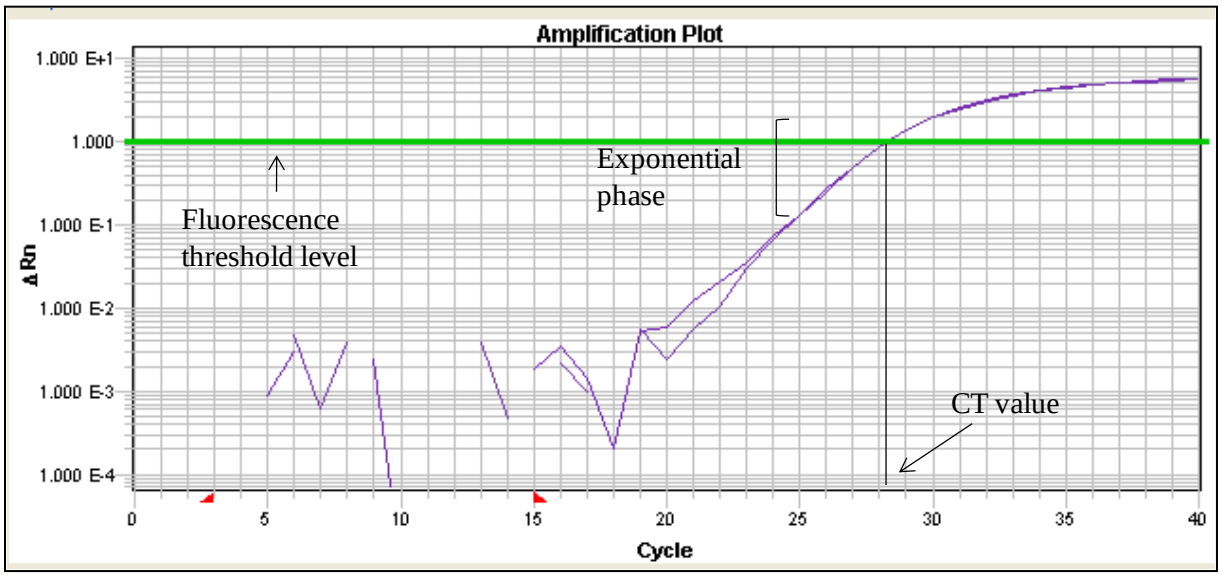

Figure 2.2 Amplification plot for a qRT-PCR reaction, illustrating the CT-value of the sample, the fluorescence threshold level and the exponential phase of the PCR reaction.

The standard curve for each gene was used as a quality control for the PCR reaction. A slope value between -3.1and -3.6 and $R^2 > 0.95$ was generally accepted. Figure 2.3 shows an example of a valid standard curve for the gene *Ptgs2*.

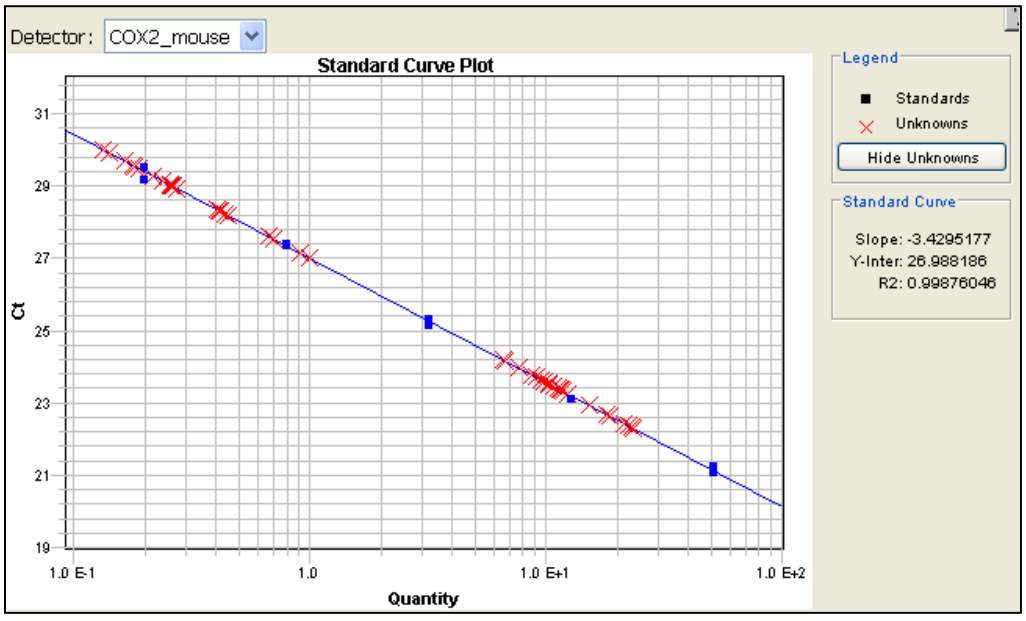

Figure 2.3 Example of a standard curve obtained from Real-time PCR, with quantity of template on the x axis, and CT value on the y-axis.

All gene expression data were normalized to the expression of the gene encoding β-actin (*Actb)*, which was used as an endogenous control. *Actb* is a housekeeping gene, which is assumed to be expressed in similar levels between cells of the same cell line, and not to be affected by exposure. When normalizing the gene expression to the expression of *Actb*,

eventual differences in concentration of cDNA template are taken into account. The relative expression of each gene was calculated using equation 2.1.

$$\text{Relative expression} = 2^{(Ct_{gene} - Ct_{Actb})} * 10^4 \quad (2.1)$$

By using equation 2.1, there is assumed a doubling in template for each PCR cycle, the PCR efficiency is not taken into account. For each experiment, two parallel cDNA samples were run, the mean relative expression value of the two parallels were used. For more detailed information about calculations used in gene expression analysis, see appendix IV.

2.10 Agarose Gel Electrophoresis

Agarose gel electrophoresis is a much used method within molecular biology for separation of DNA/RNA fragments based on size. In this thesis, agarose gel electrophoresis was used in combination with qRT-PCR for determination of the specificity of the primers (Chapter 2.9.1). The 1.5 % agarose gel was prepared as described below.

1. 2.4g agarose powder was mixed in 160 ml 1*TAE-buffer. The solution was heated in a microwave oven until the powder had dissolved.
2. The solution was cooled down, and 7 µl GelRed was added. The Agarose solution was poured into a tray and a comb was applied at the end of the tray for creation of wells. The gel was left to set for 15-20 minutes.
3. The comb was removed, and the gel was transferred to an electrophoresis tray and covered with 1*TAE-buffer.
4. The PCR products were added 5 µL of loading buffer, giving a total volume of 25 µL.
5. In the first well on the gel, 3 µL of 100 bp ladder was applied. For the rest of the samples, 10 µl was applied to each well.
6. The gel was applied a current of 120 V, and was run for 45 minutes.
7. The gel was photographed using the Kodak Image Station 440Cf.

2.11 Statistical methods

The statistical analysis in this study was performed using the SPSS version 18 (from PASW Statistics) and Sigmaplot version 11.0.

2.11.1 Standard deviations and standard errors

Standard deviations (SD) and standard errors (SE) are both measures for variations within the samples. SD reflects the variability of individual data points, while the SE reflects variability of mean values, and is often called the standard error of mean [60]. In this thesis, SD was used for the results where only one experiment was performed. SE was used when using the mean values of several experiments.

2.11.2 P-values

The P-value is used for determination of significantly different values. The P-value is defined as the probability to have obtained the observed data if the null hypothesis was true. A P-value is normally considered significant if $P < 0.05$. A P-value of 0.05 means that there is only 5 % probability that the null-hypothesis is true [61]. In this thesis, differences between

groups with $P < 0.05$ are marked with one asterix whereas highly significant differences with $P < 0.01$ are marked with two asterixes.

2.11.3 The T-test

The t-test is used for hypothesis testing relating to the means of groups of observations. Two different variants of the t-test are used in this thesis; the Students t-test for related samples, and the independent sample t-test.

When comparing the effect before and after exposure, the Students t-test is often used. This test is also called the paired t-test. Two observations are said to be paired when the same sample is studied more than once, only at different circumstances. When using a paired test, only variance within groups is compared, between samples variations are not taken into account. This test requires normally distributed data [61]. The Students t-test has been used in this thesis for the cytotoxicity experiments and in gene expression analysis, when comparing exposed samples to controls.

For comparison of two independent groups of observations, an independent sample t-test is often used. Unlike the paired t-test, the variances between different samples are taken into account (variances between experiments of the same group). The test requires normally distributed data, and equal variances between observations. If the variances are not equal, a modified version of the t-test must be performed [61]. In this thesis, the independent sample t-test was used when comparing results from groups with different exposure, e.g. when comparing the response in cells exposed to MWCNT-NO compared to the response to MWCNT-JP. The test was also used for comparison of effects following exposure between cell lines.

3 Results

The raw data for the experiments and formulas used are enclosed in appendix IV and V.

3.1 Scanning electron microscopy of MWCNTs

Carbon nanotubes from two different producers were used in the experiments; MWCNTs produced in Norway (MWCNT-NO) and MWCNTs produced in Japan (MWCNT-JP). The MWCNT-NO particles have not been studied earlier whereas the MWCNT-JP particles have been studied to some extent and are included in the experiments to compare the effects with the MWCNT-NO particles.

The two MWCNTs were subjected to Scanning Electron Microscopy (SEM). Judging from the gross SEM pictures (Figure 3.1) it was observed that the MWCNT-NO particles (Fig. 3.1 A and B) were shorter than the particles from MWCNT-JP (Fig. 3.1 C and D). There was also observed some non-fiberous structures in the MWCNT-NO samples that were not characterized in further detail. Crocidolite asbestos (a known biopersistent fiber) and H_2O_2 (a known oxidative agent) were also included in the experiments.

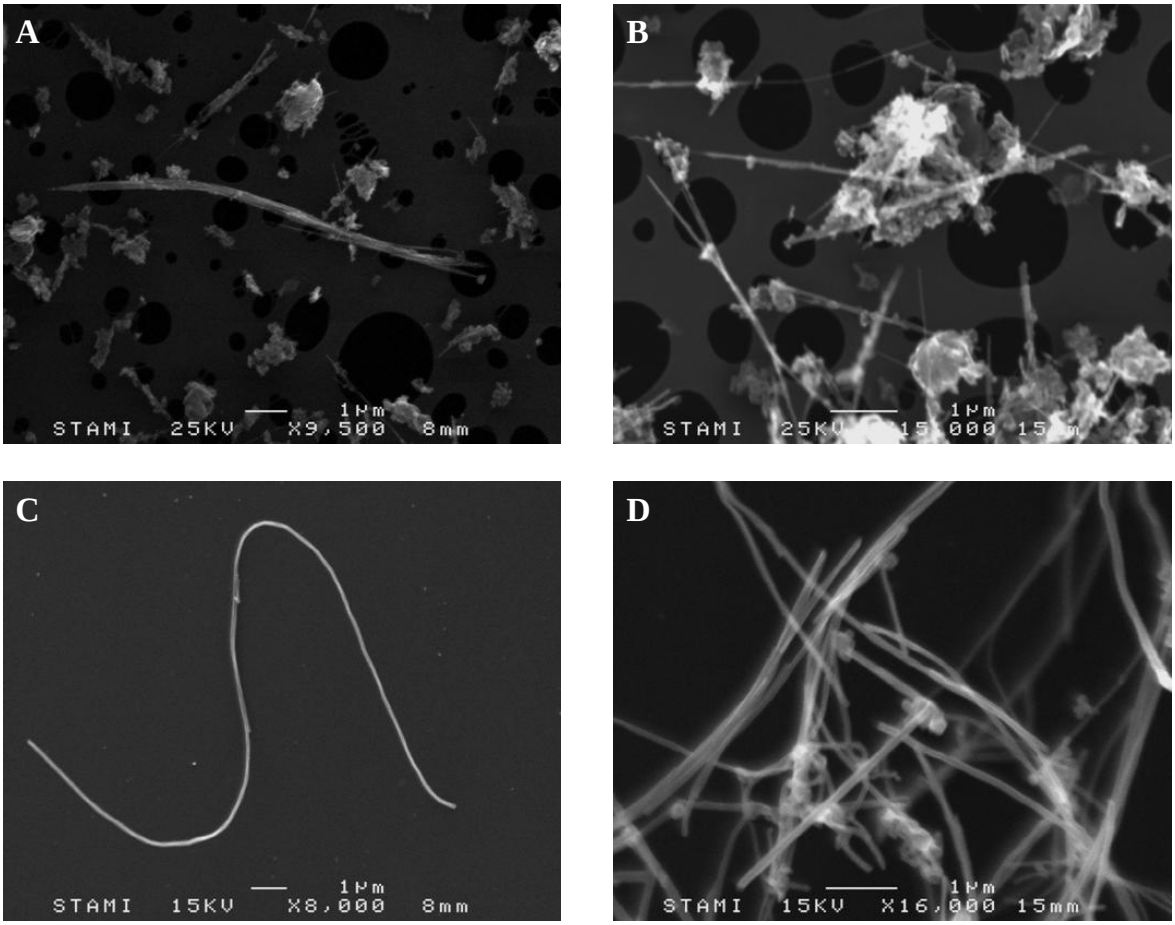

Figure 3.1 SEM images of MWCNT particles used in the experiments. A, B: MWCNT-NO, C, D: MWCNT-JP.

3.2 Cytotoxicity of MWCNTs, crocidolite and H_2O_2 in WT and *Il1a/b* KO cells

The cytotoxic effects of the MWCNTs, crocidolite and H_2O_2 were studied in wild-type (WT) and *I1a/b* knock-out (KO) cell lines derived from a BALB/c mouse strain. Cell viability was measured after 6, 24, 48 and 72 hours exposure. The detailed characteristics of cell lines, the WST-8 cytotoxicity assay and other experimental procedures are described in the materials and methods section. Differences in cell growth and proliferation of the two cell lines over time were observed, especially after 48 and 72 hours exposure. The detailed growth curve is shown in Appendix II.

3.2.1: Cytotoxicity of MWCNTs

In cells exposed to MWCNT-NO (Fig. 3.2), there were observed significant toxicity at all time points, with significant toxicity after exposure to concentrations of 20 µg/ml and higher. The two cell lines showed similar toxicity after 6 and 24 hours (Fig. 3.2 A, B). In the *Il1a/b* KO cell line (red bars), there was a trend of increased toxicity of MWCNT-NO with increased exposure time.

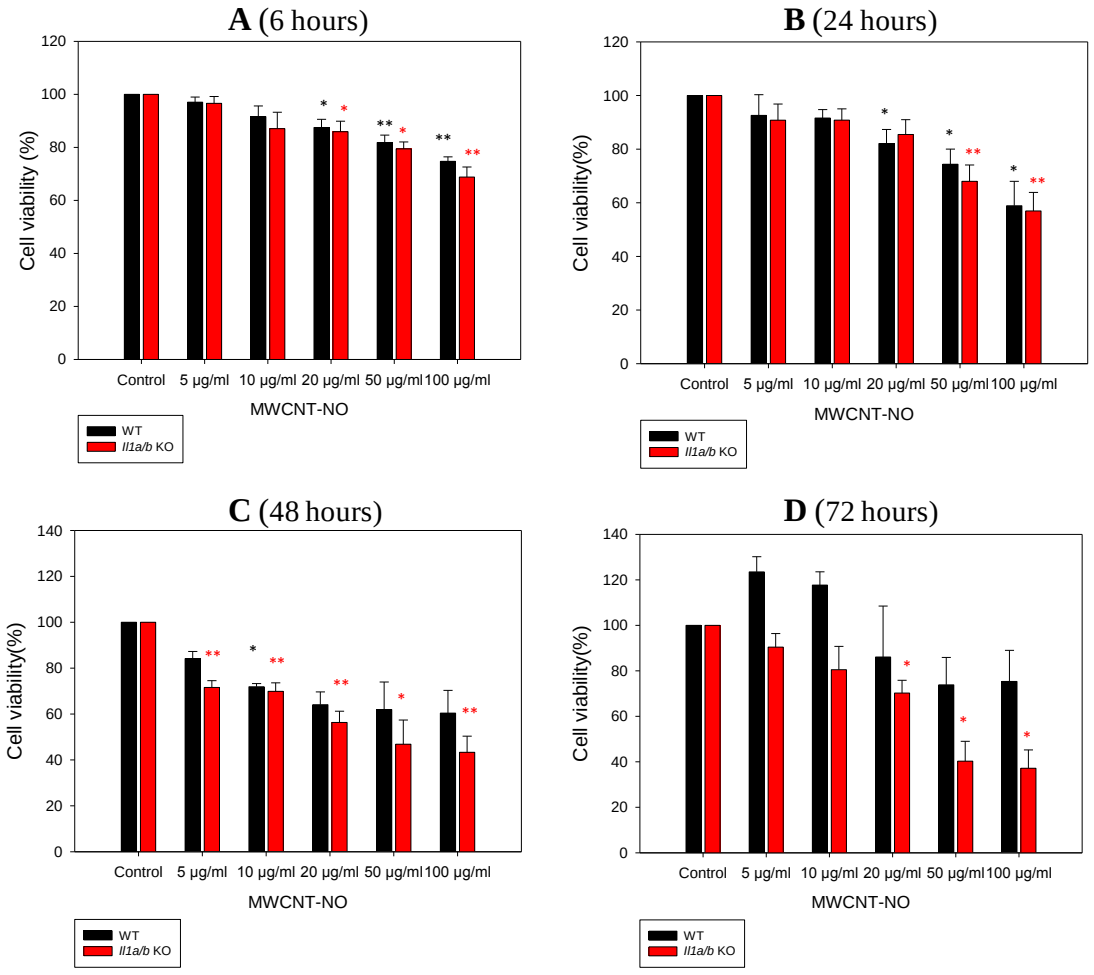

Figure 3.2 Cytotoxicity of MWCNT-NO in WT (black bars) and *Il1a/b* KO cells (red bars). Exposure for A: 6 hours, B: 24 hours, C: 48 hours and D: 72 hours. Percentage of cell viability = 100 x (OD of exposed/OD of control). Statistical analysis performed with the Student's t-test for paired samples. Error bars= SE; *, $P < 0.05$; **, $P < 0.01$

MWCNT-JP (Fig. 3.3) generally seemed to have a high toxic effect on the cells, with significant toxicity after exposure to concentrations of 5 µg/ml and higher for 6 and 24 hours (Fig. 3.3A, B). There were some differences between the cell lines, with higher toxicity in the *Il1a/b* KO cell line compared to the WT cells after 24 hours exposure (Fig. 3.3.B). Similar to MWCNT-NO, there was a trend of increased toxicity of MWCNT-JP with increased exposure time in the *Il1a/b* KO cell line (red bars). For the 48 and 72 hours experiments (Fig. 3.3C, D), only one experiment was performed, since toxicity was too high to use for further studies.

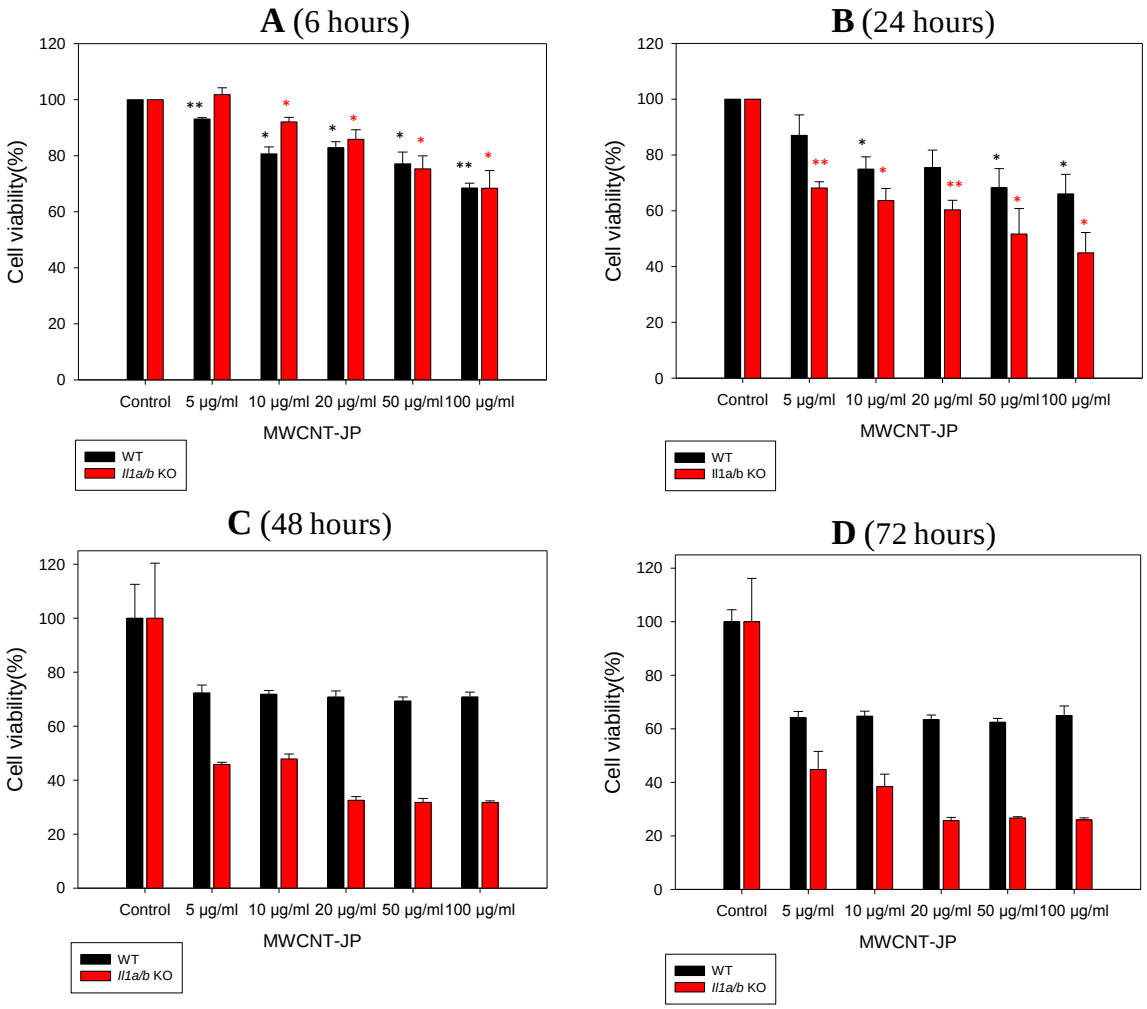

Figure 3.3 Cytotoxicity of MWCNT-JP in WT (black bars) and *Il1a/b* KO cells (red bars). Exposure for A: 6 hours, B: 24 hours, C: 48 hours and D: 72 hours. The percentage of cell viability = 100 x (OD of exposed/OD of control). Statistical analysis performed with the Student's t-test for paired samples. A, B: Error bars= SE, C, D: Error bars = SD; *, $P < 0.05$; **, $P < 0.01$

3.2.2: Cytotoxicity of H_2O_2 and Crocidolite

Crocidolite (blue asbestos) was used as a positive control for fiber toxicity while H_2O_2 was used as a positive control for a non-fiber and oxidative-stress inducing agent. The cytotoxicity results after exposure to crocidolite are shown in figure 3.4. Crocidolite showed, unlike the MWCNTs, low toxicity after 6 hours (Fig.3.4A), with some toxicity in the WT cell line, and no toxicity in the *Il1a/b* KO cell line. Toxicity was higher in both cell lines after 24 hours

(Fig. 3.4B). Similar to the MWCNTs, toxicity increased over time regarding the *Il1a/b* KO cell line (red bars).

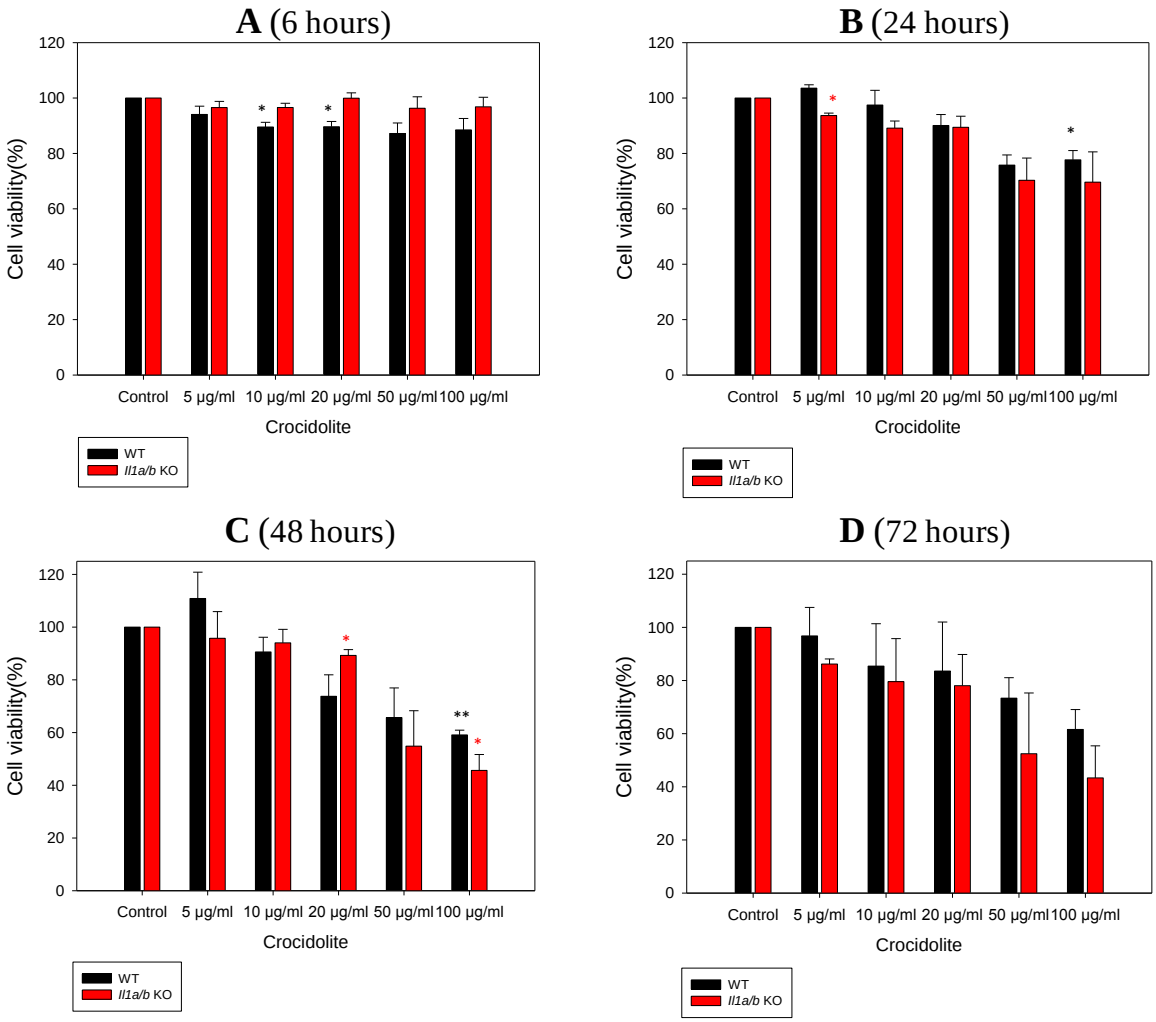

Figure 3.4 Cytotoxicity of Crocidolite in WT (black bars) and *Il1a/b* KO cells (red bars). Exposure for A: 6 hours, B: 24 hours, C: 48 hours and D: 72 hours. The percentage of cell viability = 100 x (OD of exposed/OD of control). Statistical analysis performed with the Student's t-test for paired samples. Error bars= SE; *, $P < 0.05$; **, $P < 0.01$

The cytotoxicity of H_2O_2 in the WT and *Il1a/b* KO cell line is shown in figure 3.5. Both cell lines were generally very sensitive to H_2O_2, resulting in significant toxicity at concentrations of 4 µM and higher after 6 hours exposure (Fig. 3.5 A). A similar tendency was observed after 24 hours exposure (Fig. 3.5 B). When observing the *Il1a/b* KO cell line (red bars), H_2O_2 did not induce increased toxicity over time at the low concentrations (1 – 4 µM) (Fig. 3.5A-D) like was observed for the fibers.

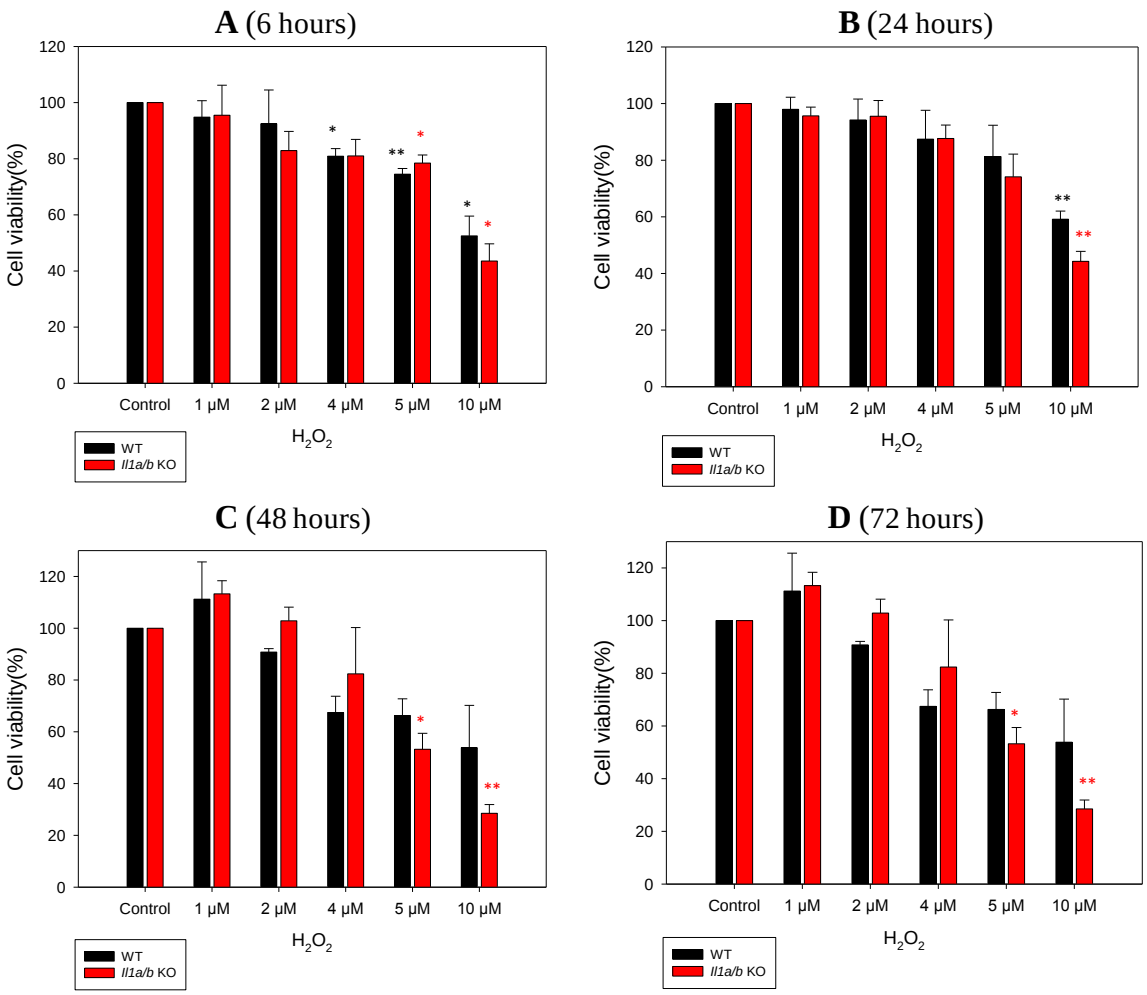

Figure 3.5 Cytotoxicity of H_2O_2 in WT (black bars) and *Il1a/b* KO cells(red bars). Exposure for A: 6 hours, B: 24 hours, C: 48 hours and D: 72 hours. The percentage of cell viability = 100 x (OD of exposed/OD of control). Statistical analysis performed with the Student's t-test for paired samples. Error bars= SE; *, $P < 0.05$; **, $P < 0.01$

3.2.3: Comparison of the toxicity of MWCNTs and crocidolite

In order to investigate differences in toxicity between particles, cytotoxicity of MWCNT-NO, MWCNT-JP and Crocidolite after 24 hours exposure was compared in WT and *Il1a/b* KO cells as shown in figure 3.6. The data for 24 hours exposure were used since these results had less variation.

For the WT cell line (Fig. 3.6A), MWCNT-JP was the most toxic, followed by MWCNT-NO and crocidolite, respectively. MWCNT-JP also was the most toxic for the *Il1a/b* KO cell line (Fig. 3.6B), while MWCNT-NO and crocidolite seemed to cause similar toxicity in this cell line. The toxicity of MWCNT-JP was higher in the *Il1a/b* KO (Fig. 3.6B) compared to the WT cell line (Fig. 3.6A). No clear differences in toxicity between cell lines were observed for MWCNT-NO or crocidolite.

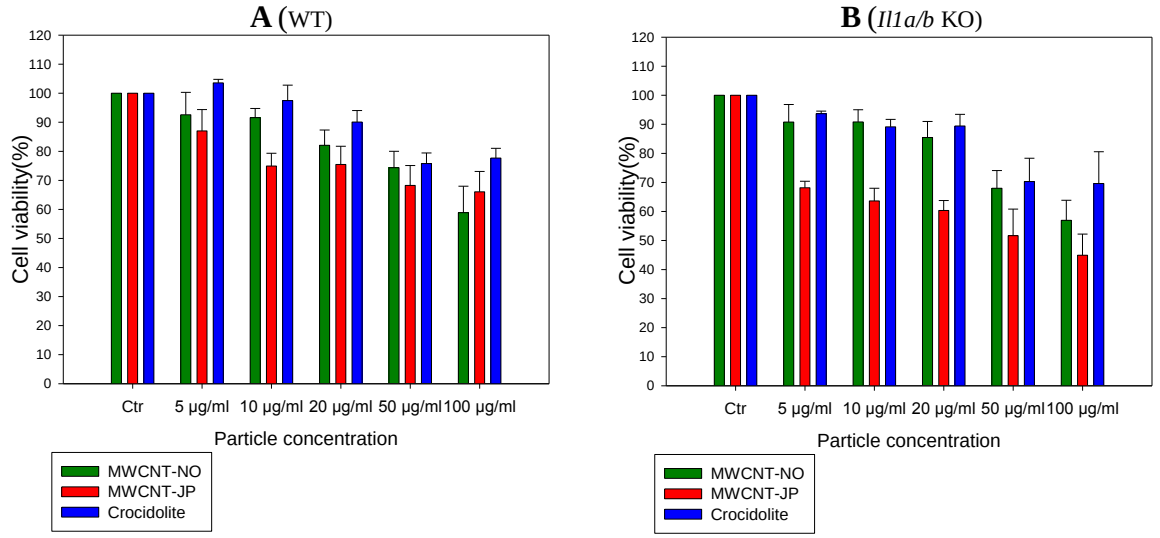

Figure 3.6 Cytotoxicity after 24 hours exposure to MWCNT-NO (green bars), MWCNT-JP (red bars) and Crocidolite (blue bars) in the A: WT cell line, B: *Il1a/b* KO cell line. The percentage of cell viability = 100 x (OD of exposed/OD of control), error bars = SE.

The results from the cytotoxicity experiments of 24 hours exposure were also used to choose the appropriate doses for apoptosis and gene expression experiments. Doses which resulted in relatively low cell toxicity were preferred since these doses may not have many adverse effects on cellular functions. For MWCNT-NO, which is the main focus in the experiments, it was determined to use the concentrations 5, 10 and 20 µg/ml for fluorescence microscopy (apoptosis), and 5 and 10 µg/ml for qRT-PCR (gene expression). For MWCNT-JP, the concentration used was 5 µg/ml, for Crocidolite 20 µg/ml was used, and for H_2O_2 4 µM was used. Based on the results from the cytotoxicity assays (Fig. 3.5B, 3.6), these concentrations seemed to result in 10 – 20 % cell death after 24 hours exposure. The exception is the *Il1a/b* KO cells exposed to MWCNT-JP, where the toxicity seemed to be somewhat higher with about 30-35 % cell death.

3.3 Analysis of apoptotic cell death

To study apoptotic cell death following exposure, cells were exposed to the appropriate doses of MWCNTs, Crocidolite and H_2O_2 for 24 hours and stained with Hoescht 33432 and propidiumiodide (PI) dyes. Thapsigargin, a known apoptosis-inducing chemical was included in the experiments as a positive control.

In this assay, the nucleus of viable cells were stained blue (Fig. 3.7), the nucleus of apoptotic cells were also stained blue, but with intense spots (encircled cell in Fig. 3.7E and F), and the nucleus of necrotic cells were stained red (rectangled cell in Fig. 3.7E and F), when visualized by a fluorescence microscope. Figure 3.7 shows representative photographs from fluorescence microscopy of cells from the WT and *Il1a/b* KO cell line unexposed (Figure 3.7A and B), exposed to 10 µg/ml MWCNT-NO (Fig. 3.7 C and D) and exposed to 100 nM thapsigargin (Fig. 3.7E and F). The unexposed (control) cells (Fig. 3.8 A and B), contained a significant number of necrotic cells.

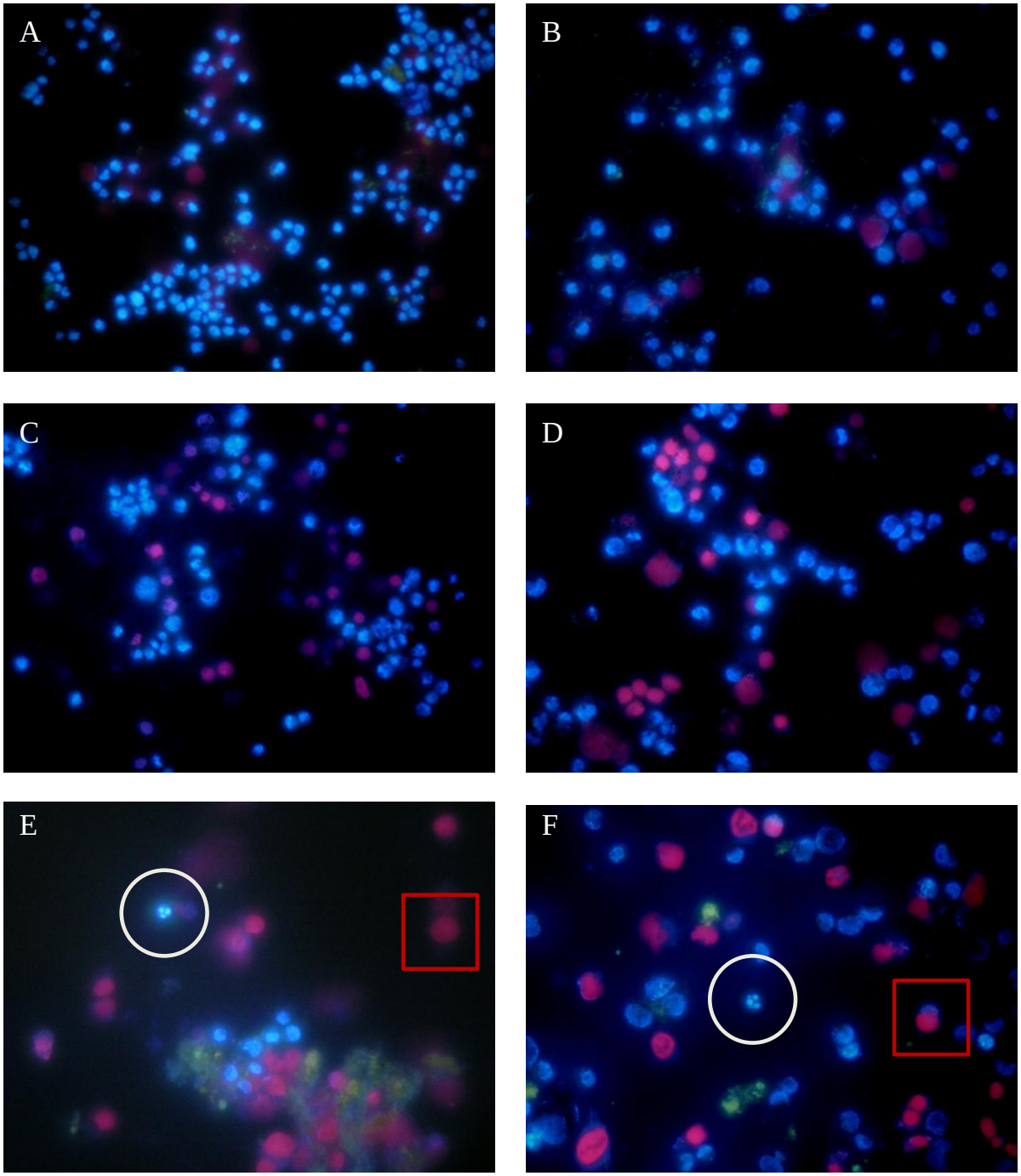

Figure 3.7 Example photographs from fluorescence microscopy of cells from the WT and *Il1a/b* KO cell lines stained with PI/Hoecsht 33432 after 24 hours exposure. A: WT cells unexposed, B: *Il1a/b* KO cells unexposed, C: WT cells exposed to 10 µg/ml MWCNT-NO, D: *Il1a/b* cells KO exposed to 10 µg/ml MWCNT-NO, E: WT cells exposed to 100 nM thapsigargin, F: *Il1a/b* KO cells exposed to 100 nM thapsigargin.

A summary of the results from the counting of cells is illustrated in figure 3.8. The experiments generally showed a very low occurrence of apoptosis in all the exposed as well as in the unexposed cells for both cell lines (Figure 3.8 A). In the MWCNT-NO exposed cells, there was shown a maximal level of 0.6%±0.6 cells undergoing apoptosis in the WT cell line and 2.1%±1.7 in the *Il1a/b* KO cell line, respectively. MWCNT-JP induced 1.9%±0.7 and 2.1%±1.3% apoptotic cell death in the WT and *Il1a/b* KO cell line, respectively. Similar results were observed for crocidolite and H_2O_2 (For further details see Appendix V). There

was a higher number of apoptotic cells in the thapsigargin-exposed cells in general, and this was higher in the WT cells (16.9% ±3.4) compared to the *Il1a/b* KO cell line (10.1%±1.7), although this difference was not statistically significant (P>0.05).

Regarding cell death due to both necrosis and apoptosis (Fig. 3.8 B), there were differences in toxicity levels between the cell lines after exposure to the MWCNT-JP, where there was about a two-fold higher cell death in the *Ila/b* KO cells (21.2% ±5.1) compared to the WT (9.9% ±3.3) (P>0.05). Similar results were seen in the toxicity assay for 24 hours (figure 3.6A, B), where MWCNT-JP seemed to be more toxic for the *Il1a/b* KO cell line than for the WT cells.

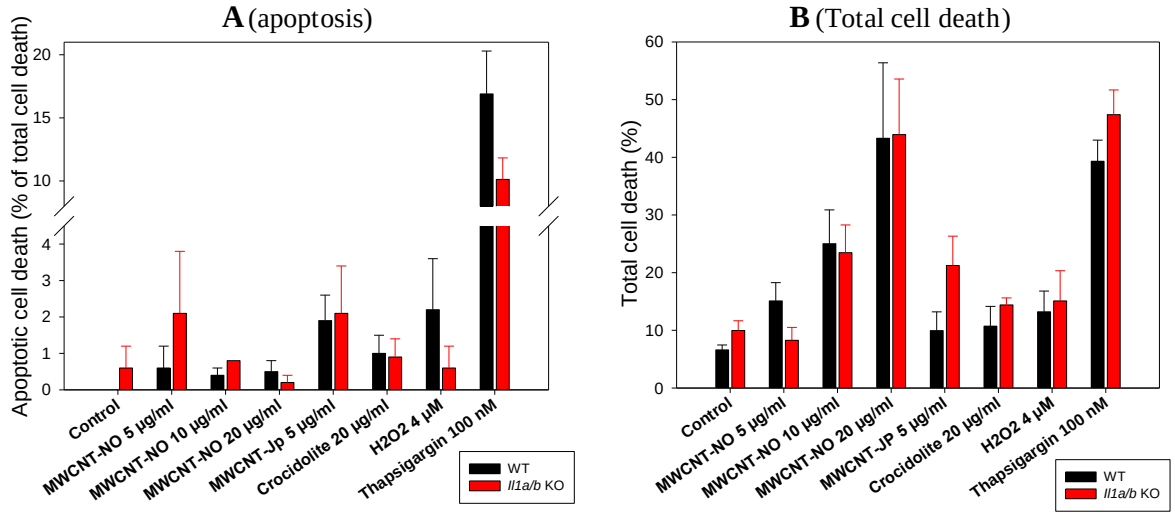

Figure 3.8 Results from counting of cells from the WT(black bars) and the *Il1a/b* KO(red bars) cell lines, 24 hours exposure. Cells were stained with Hoecsht/PI, and counted in a fluorescence microscope. A: Percentage apoptotic cell death after exposure (apoptotic cells/(apoptotic +necrotic cells) *100). B: Total cell death in the exposed samples ((apoptotic + necrotic cells)/(total number of cells)*100). Statistical analysis performed with the independent sample t-test. Error bars = SE; *, P < 0.05; **, P < 0.01

3.4: Effects on expression of genes involved in inflammation and apoptosis

Expression analysis of the genes *Il1b*, *Tnfa*, *Il6*, *Ptgs2*, and *Tp53* in the WT and *Il1a/b* KO cell lines was investigated using RNA isolated from unexposed cells and cells exposed to appropriate doses of MWCNTs, crocidolite and H_2O_2 for 24 hours.

The results from qRT-PCR showed significant differences in basal gene expression of inflammatory genes between the WT (black bars) and the *Il1a/b* KO cell lines (red bars), as shown in figure 3.9. The *Il1a/b* KO cell line had significantly reduced expression of *Tnfa*, and significantly increased expression of *Il6* and *Ptgs2* compared to the WT cell line (Fig. 3.9 B, C and D). The *Il1a/b* KO cell line showed no expression of *Il1b* (Fig. 3.9A), which confirms successful knock-out of the gene in these cells. There were no significant changes in the expression of *Tp53* between the cell lines, indicating that knocking out *Il1a/b* does not affect the expression of *Tp53* directly.

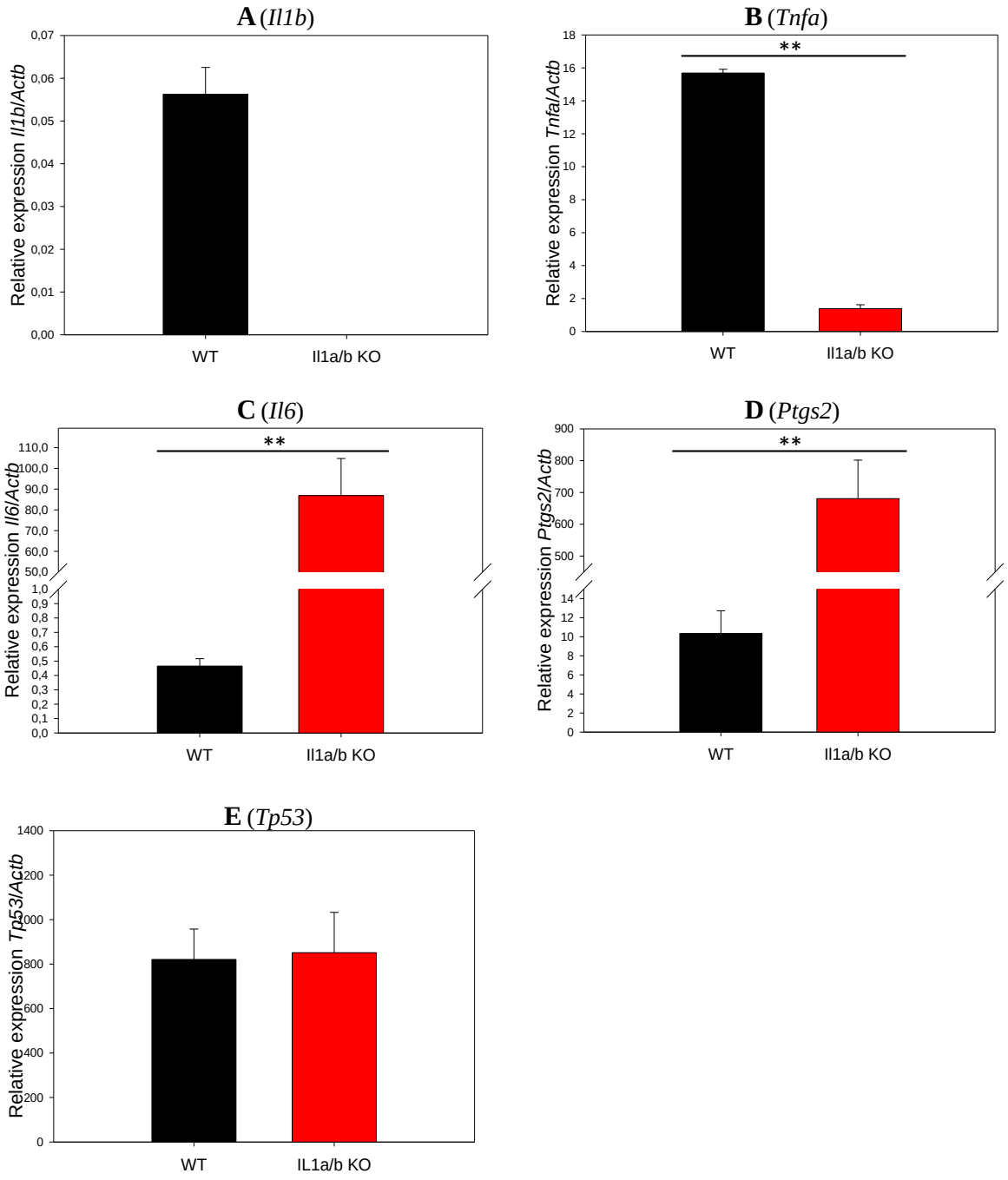

Figure 3.9 The level of basal gene expression in the WT (black bars) and *Il1a/b* KO (red bars) cell lines: Relative expression of A: *Il1b*, B:*Tnfa*, C: *Il6*, D: *Ptgs2* and E: *Tp53* in unexposed samples, 24 hours incubation. Relative expression = 2^ (-ΔCt)* 10^4, with *Actb* expression as endogenous control. Statistical analysis performed with the independent sample t-test. Error bars = SE; *, P < 0.05; **, P < 0.01

The relative expression of genes after exposure to MWCNTs, Crocidolite and H_2O_2 in the WT and *Il1a/b* KO cell line is shown in figure 3.10 and 3.11, respectively. The figures show the relative expression of genes normalized to the expression of *Actb*.

In the WT cell line (Fig. 3.10), MWCNT-NO exposure gave a trend of dose-dependent reduction of *Il1b* and dose-dependent increase of *Ptgs2* expression (Fig. 3.10 A, D) (P>0.05) when compared to unexposed cells. There were no changes in gene expression of *Tnfa* or *Il6* (Fig. 3.10B, C). In WT cells exposed to MWCNT-JP, there was seen induced expression of *Il6* (P>0.05) and *Ptgs 2*(Fig. 3.10C, D). There was no differential gene expression of *Il1b* or *Tnfa* (Fig. 3.10A, B) when compared to the control. In crocidolite exposed cells there was reduced expression of *IL1b* (P>0.05), *Tnfa* and *Il6* (3.10A, B, C), but no change in gene expression of *Ptgs2* (Fig. 3.10D). H_2O_2-exposed WT cells showed a possibly reduced expression of *Il1b* and *Il6* (Fig. 3.10A, C, P>0.05), but no changes in gene expression of *Tnfa* or *Ptgs2* (Fig 3.10B, D). The expression of *Tp53* does not seem to be influenced by any of the test materials (Fig. 3.10E).

In *Il1a/b* KO cells exposed to MWCNT-NO (Fig. 3.11), there was a significant reduction in *Tnfa* and *Il6* expression (Fig 3.11A, B), and a trend of dose-dependent induction of *Ptgs2* expression (Fig. 3.11C), with significant induction at 10 µg/ml. There were no changes in the expression of *Tp53* (Fig. 3.11D). In MWCNT-JP exposed cells, there seemed to be an induction of *Tnfa, Il6, Ptgs2* and *Tp53* (Fig 3.11A-D), however none of these changes were shown to be statistically significant (P>0.05). The Crocidolite exposed cells showed reduced expression of *Tnfa* and *Il6* (Fig. 3.11A, B), a similar response to what is seen in the MWCNT-NO exposed cells. No changes in gene expression of *Ptgs2* or *Tp53* (Fig. 3.11C, D) were observed. For H_2O_2, there were no changes in gene expression following exposure.

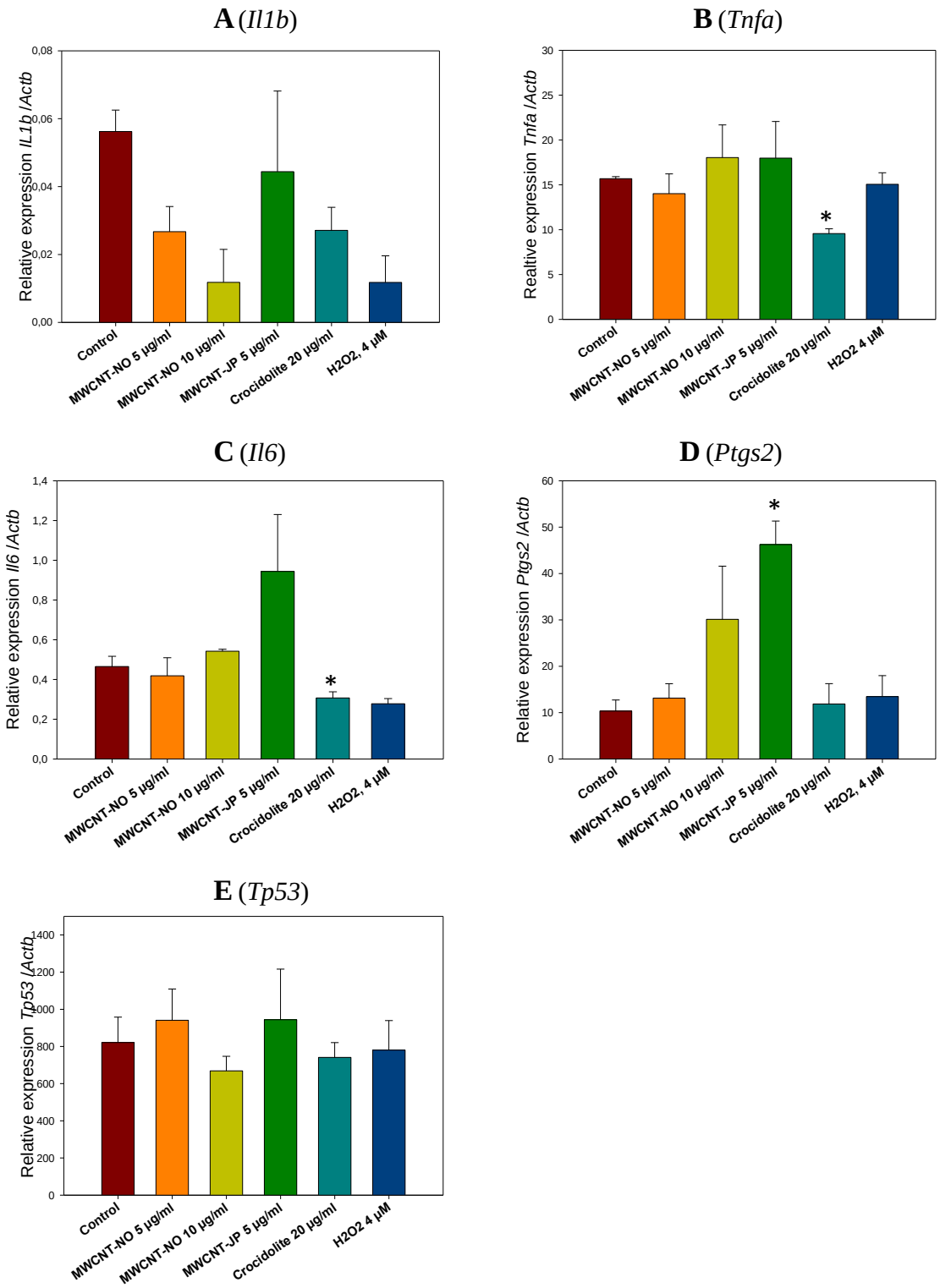

Figure 3.10 Relative expression of A: *Il1b*, B: *Tnfa*, C: *Il6*, D: *Ptgs2* and E: *Tp53* in the WT cell line after 24 hours exposure. Cells exposed to control (red bars), MWCNT-NO 5 µg/ml (orange bars), MWCNT-NO 10 µg/ml (yellow bars), MWCNT-JP 5 µg/ml (green bars), Crocidolite 20 µg/ml (turquoise bars) and H_2O_2 4 µM (blue bars). Relative expression = 2^ (-ΔCt)* 10^4, with *Actb* expression as endogenous control. Statistical analysis performed with the Students t-test for paired samples. Error bars = SE; *, P < 0.05; **, P < 0.01

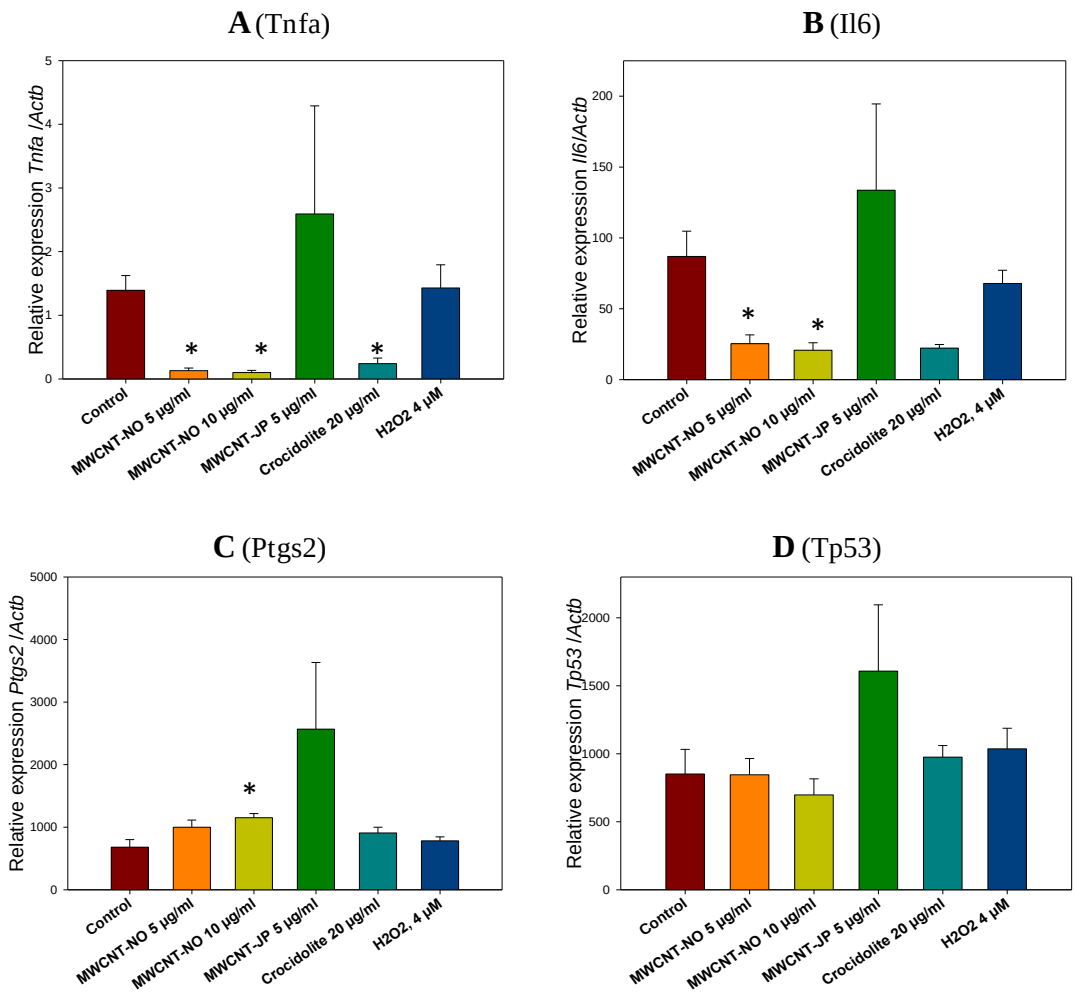

Figure 3.11 Relative expression of A: *Tnfa*, B: *Il6*, C: *Ptgs2* and D: *Tp53* in the *Il1a/b* KO cell line after 24 hours exposure. Cells exposed to control (red bars), MWCNT-NO 5 µg/ml (orange bars), MWCNT-NO 10 µg/ml (yellow bars), MWCNT-JP 5 µg/ml (green bars), Crocidolite 20 µg/ml (turquoise bars) and H_2O_2 4 µM (blue bars). Relative expression = 2^ (-ΔCt)* 10^4, with *Actb* expression as endogenous control. Statistical analysis performed with the Students' t-test for paired samples. Error bars = SE; *, P < 0.05; **, P < 0.01

Figure 3.12 illustrates the differential responses in gene expression in the WT and the *Il1a/b* KO cell lines following exposure to various test materials. The results are presented as the fold change in mRNA expression in exposed cells compared to control (unexposed) cells of each cell line. There are significant differences in expression of *Tnfa* and *Il6* between the cell lines following exposure to MWCNT-NO and Crocidolite (Fig. 3.12 A and B). The expression of these genes is strongly reduced in response to exposure in the *Il1a/b* KO cell line while the same effect is not observed in the WT cell line. There were no significant differences in gene expression between cell lines following exposure to MWCNT-JP. For H_2O_2, there was observed a significantly different response in *Tp53* between the cell lines (Fig. 3.12D), with induced expression in the *Il1a/b* KO compared to the WT cells.

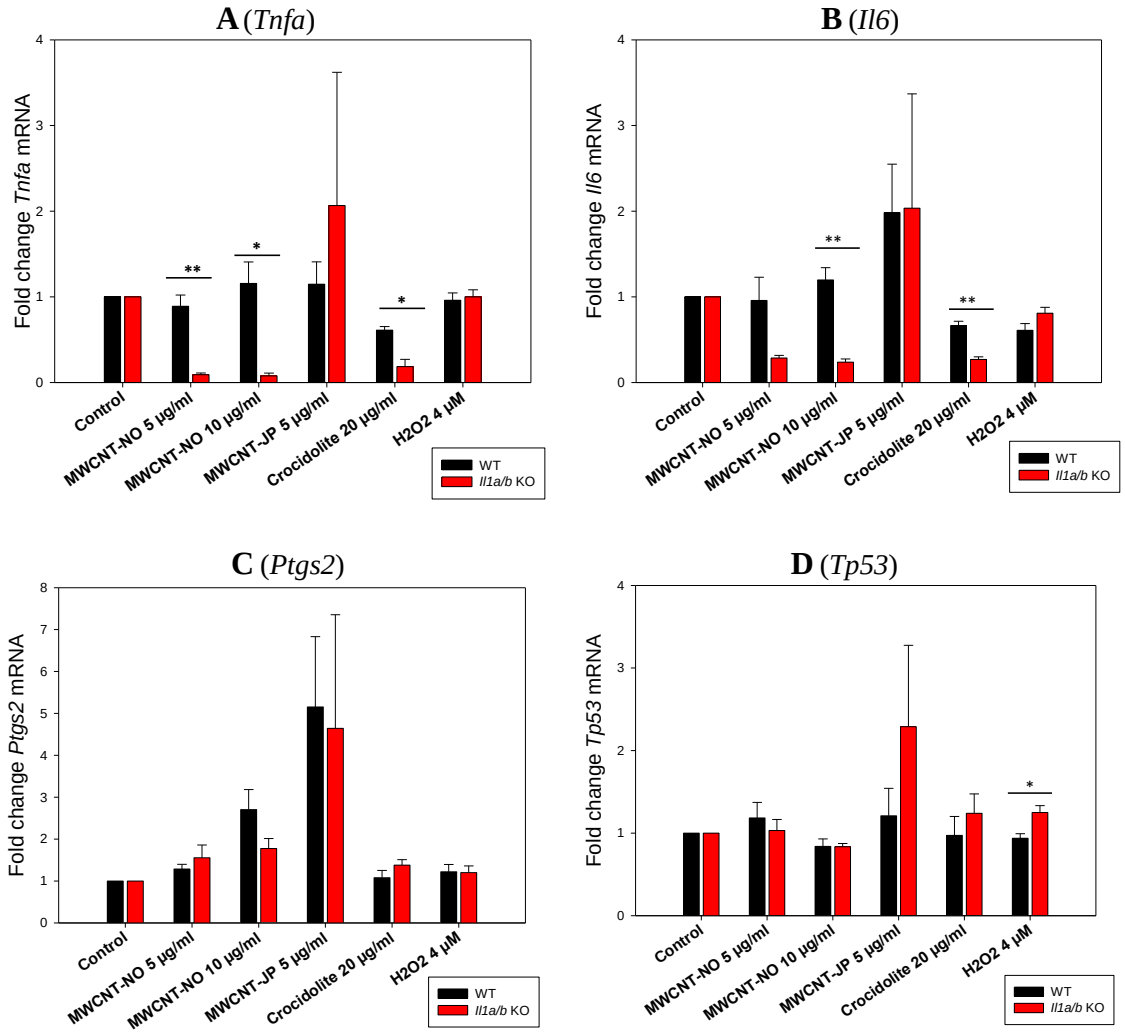

Figure 3.12: Fold change mRNA expression after exposure to MWCNT, Crocidolite and H_2O_2 in WT (black bars) and *Il1a/b* KO cell lines (red bars). A: *Tnf*a, B: *Il6*, C: *Pgst2*, D: *Tp53*. Fold change mRNA= relative expression of exposed sample/relative expression of control. Statistical analysis performed with the independent sample t-test. Error bars = SE; *, P < 0.05; **, P < 0.01

4. Discussion

The toxicological effects of nanoparticles are under increasing concern because of the highly increased number of products containing nanomaterials. A main concern is the ability of nanoparticles to induce inflammatory responses. IL-1 is a key regulator of the inflammatory processes, activating pro-inflammatory cytokines and other inflammatory mediators. The objective of this thesis was to study cytotoxic, apoptotic and inflammatory responses in wild-type and *Il1*-deficient cells from mice after exposure to different carbon nanotubes. It was aimed to study whether IL-1 is involved in modulation of the biological effects following carbon nanotube exposure. The model system used consisted of the WT and the *Il1a/b* KO cell lines derived from BALB/c mice. These cells were assumed to be genetically identical, except for the presence of *Il1*.

4.1 Cytotoxicity of MWCNTs, Crocidolite and H_2O_2

The results from the cytotoxicity experiments showed a dose-dependent toxicity of all test materials (Fig. 3.2 -3.5). MWCNTs and H_2O_2 showed immediate effects, giving significant cytotoxicity already after 6 hours. For Crocidolite, a clear toxic effect was first observed after 24 hours. In the particle exposed cells there was a general trend of increasing toxicity with increasing time (Fig. 3.2-3.4), when observing the *Il1a/b* KO cell line. The same trend did not seem to appear for the H_2O_2 exposed cells (Fig. 3.5), which may be due to the fact that H_2O_2 is not biopersistent, as it may have an acute effect on the cells, and be readily metabolized [62].

Toxicity levels in response to MWCNT-NO were similar in both cell lines after 6 and 24 hours. There were differences in toxicity between cell lines exposed to MWCNT-JP, with somewhat higher toxicity in the WT cell line at 6 hours, but higher toxicity in the *Il1a/b* KO cell line at 24 hours, indicating involvement of *Il1* in the toxicity of MWCNT-JP. The cells also responded differently to exposure by Crocidolite, the toxic effect appeared at an earlier stage for the WT cell line, with significant toxicity after 6 hours. Similar toxicity in both cell lines was observed after 24 hours. This may indicate that *Il1* is involved in the immediate response following Crocidolite exposure.

For studies regarding apoptosis and gene expression of inflammatory genes, only one time point of exposure was chosen. Apoptosis and gene expression of pro-inflammatory cytokines are acute events, which are potentially activated at an early stage after exposure. 24 hours of exposure was used, because of more stable results at this time point than for 6 hours. At 24 hours, there was significant toxicity for all exposed cells, unlike the cells exposed for 6 hours. The decision to use 24 hours exposure was also partly based on a study of cellular uptake of MWCNTs by Hirano et al. This study examined the cytotoxicity and uptake of MWCNTs in BEAS-2B human lung epithelial cells, and found a maximal cellular uptake of MWCNTs after 10 hours [29]. Based on these results, it is thought that at 24 hours of exposure, a maximum level of particles is internalized within the cells and the effects of particles are becoming evident.

When comparing the effect of particles after 24 hours at low concentrations (5, 10 and 20 µg/ml) in the WT cell line (Fig. 3.6A), MWCNT-JP seemed to cause the highest level of toxicity, followed by MWCNT-NO, and Crocidolite being least toxic at this time point. MWCNT-JP also seemed to be the most toxic when exposed to the *Il1a/b* KO cell line (Fig. 3.6B), while the toxicity of MWCNT-NO and Crocidolite seemed similar in this cell line, indicating a role of *Il1* in the difference in toxicity between MWCNT-NO and Crocidolite. The less toxic effect of crocidolite compared to MWCNTs in the WT cell line is confirmed by studies performed by Hirano et al. However, in this study, the differences in toxicity after 24 hours exposure are much larger, indicating higher toxicity of the CNTs vs. Crocidolite in these studies compared to our experiments [29].

MWCNT-JP seemed to be longer than MWCNT-NO particles when observed by SEM (Fig. 3.1). The higher length of MWCNT-JP was also confirmed when comparing what has been published in the literature (MWCNT-JP) and manufacturing information (MWCNT-NO). This may partly explain the more toxic effects of MWCNT-JP in both cell lines. The length of the fibers has been shown to be strongly related to the toxicity [17]. Additionally, other factors could be involved, like presence of metal contaminations or surface properties. Better characterization of the particles, especially the MWCNT-NO is needed to explain the differences in toxicity.

When comparing results between cell lines, these indicate that MWCNT-JP was more toxic to the *Il1a/b* KO cell line than to the WT cell line after 24 hours. The fact that MWCNT-JP was more toxic for the *Il1a/b* KO cell line, may suggest a role of *Il1* in preventing cell death in these cells.

The results for H_2O_2 at 24 hours (Fig. 3.5B) showed significant toxicity at 10 µM and a clear drop in cell viability between 5 and 10 µM. These results imply that the cells used in the experiments are very sensitive to ROS compared to other cell lines. Previous research with other cell types, show much higher tolerance to H_2O_2 exposure, with significant toxicity at concentrations from100-300 µM [62, 63]. The high sensitivity to H_2O_2 exposure in the cell lines used may be caused by high intrinsic ROS production within the cells or decreased catalase/antioxidant activity.

In previous cytotoxicity studies regarding MWCNTs, there were large differences in doses used, time of exposure and which doses that cause significantly toxic effects. Examples include studies using human fibroblasts, in concentrations from 40 – 400 µg/ml, where no significant toxicity was seen before 72 hours [64]. In contrast, in human bronchial epithelial cells (BEAS-2B), MWCNTs were shown to give drastic effects already after 24 hours, with an IC_{50} value of 12 µg/ml [29]. The MWCNT-JP particles used in this thesis have been subject to previous toxicity studies, including a study performed by Asakura et al. In this study, Chinese hamster lung cells were exposed to MWCNTs and there was shown a dose-dependent toxicity from 12.5 – 400 µg/ml after 24 hours [65]. The doses causing toxicity in this study are much higher than what was used in our experiments. Asakura et al. also observed toxicity at a later stage than what was observed in our studies, where significant toxicity was observed after exposure to 5 µg/ml for 6 hours. Differences in toxicity may be

due to several parameters, including cell type used, cell density, different characteristics of the particles and differences in dispersion.

Based on current literature, doses between 10 -100 µg/ml were used for cytotoxicity experiments. During the toxicity assays, it was observed that when exposing cells to high concentrations of nanoparticles (50 and 100 µg/ml), cells were partly covered with a layer of nanoparticles. This could cause indirect effects on toxicity through lower nutrient availability, hypoxia, lack of light etc. In current literature, doses up to 400 µg/ml [64] have been used for *in vitro* toxicity assays, the use of these high doses is questionable because of the above mentioned reasons.

4.2 Analysis of apoptotic cell death

The contribution of apoptotic vs. necrotic cell death in WT and *Il1a/b* KO cells exposed to MWCNTs, Crocidolite, H_2O_2 and thapsigargin for 24 hours was determined by Hoechst/PI staining followed by fluorescence microscopy. Cells exposed to MWCNTs, Crocidolite and H_2O_2, generally showed a very low degree of apoptotic cell death, compared to cells exposed to thapsigargin, which were used as a positive control (figure 3.8A). From these results, one can conclude that MWCNT, Crocidolite or H_2O_2 does not significantly induce apoptosis in the WT nor in the *Il1a/b* KO cell line after 24 hours exposure. The toxicity seen is due to necrotic cell death.

The cells used in the experiments are cancer cell lines. One main characteristic of the transformation of a normal cell into a cancer cell is a decreased or lost ability to undergo apoptosis. A low level of apoptotic cell death can therefore be expected. However, thapsigargin, which inhibits the Ca^{2+}- ATPase in the membrane of the endoplasmic reticulum [66], induces apoptosis both in the WT and in the *Il1a/b* KO cell line, indicating that induction of apoptosis is possible in the cell lines. In cells exposed to thapsigargin, there was observed a higher degree of apoptotic cell death in the WT cell line compared to the *Il1a/b* KO cell line. These results may correspond with the observation that the *Il1a/b* KO cells had a significantly lower basal expression of *Tnfa* than the WT (fig. 3.10), suggesting that TNF-α may be involved in the process of thapsigargin induced apoptosis. TNF-α is able to induce apoptosis through activation of Caspase-8 [41].

MWCNTs have been shown to induce apoptotic cell death in several cell lines, including rat epithelial cells (5µg/ml, 24 hours exposure) [16], normal human fibroblast cells (200 µg/ml, 48 hours exposure) [64] and the human lung cancer cell line A549 (10 and 50 µg/ml, 72 hours). The study using A549 also confirmed transcriptional changes in genes involved in apoptosis after 12 hours exposure, including increased transcription of P53, P21 and caspase-3 [25].

No significant effects on the level of apoptotic cell death were seen after 24 hours exposure in our experiments. There may have been observed more apoptotic cell death at a later time, as shown in studies by Srivastava et al. and Patlolla et al. [25, 64]. However, in the studies by Srivastava et al, there was a significant induction of P53 already after 12 hours. In gene expression analysis of MWCNT exposed cells in our experiments, there were no significant

changes in *Tp53* expression compared to control (Fig. 3.10, 3.11), something which could be expected if the particles caused induction of apoptosis through P53. There was however a possible induction of *Tp53* in *Il1a/b* KO cells exposed to MWCNT-JP ($P>0.05$), which may have caused these cells to enter apoptosis after a longer period of exposure.

4.3 Expression analysis of genes involved in inflammation and apoptosis

In this thesis, the expression of five genes was examined using qRT-PCR. The expression of *Il1b, Tnfa, Il6* and *Ptgs2* was used to study the induction of inflammation following particle exposure. *Tnfa* and *Tp53* were also included to study eventual induction of apoptosis, and pathways affected. For inducible cytokines, changes in mRNA expression generally seem to correlate well with changes in protein expression; changes seen in qRT-PCR were assumed to reflect protein levels.

4.3.1 Differences in basal gene expression in WT and *Il1a/b* KO cell lines

Inflammation has been shown to be an important factor in the development of cancer. The tumor microenvironment often contains a high level of inflammatory cells providing growth factors, ROS/RNS and cytokines which is favorable for tumor development. Cancer development involves mutations in important genes, genomic instability, dysregulation of apoptosis and uncontrolled growth. IL-1 has been shown to have an important regulatory effect in systemic inflammation, and is important for cancer development and the invasiveness of tumors [27, 37].

The results from qRT-PCR experiments showed a significantly different basal expression of inflammatory genes in the WT and *Il1a/b* KO cell lines (Fig. 3.9). Compared to the WT cell line, the *Il1a/b* KO cell line had significantly reduced expression of *Tnfa*, and significantly increased expression of *Ptgs2* and *Il6*. There was confirmed successful knock-out of *Il1b* in the *Il1a/b* KO cell line. No significant differences in the basal expression of *Tp53* between cell lines were observed. These results indicate a much higher basal level of inflammatory mediators in the *Il1a/b* KO compared to the WT cells. The high expression of *Il6* and *Ptgs2* does not correlate with expression of neither *Il1* nor *Tnfa*, where the basal expression was significantly higher in the WT.

IL-1β is a central cytokine, and is together with TNF-α a main regulator of inflammation. IL-1β induces the expression of several other important pro-inflammatory mediators including IL-6 and COX-2 [35]. One would expect that knocking out *Il1b* would cause decreased expression of genes downstream in the signaling cascade. In previous studies on similar cell culture systems, there was a significantly reduced production of IL-6 and induced production of TNFα in *Il1a/b* KO compared to WT fibrosarcoma cells from a C57BL/6 mouse strain. These results are the opposite compared to the results found in our experiments. The induction of tumors in mice, and the establishment of cell lines from C57BL/6 mice were executed by the same procedure as for the cells from the BALB/c strain used in this thesis [67, 68].

The effect of gene knockout on the establishment of 3-MCA induced tumors has been shown to be similar in BALB/c and C57BL/6 mice in previous studies, with reduced incidence and invasiveness of tumors derived from *Il1a/b* KO compared to WT mouse. The hypothesis for

the induced tumorigenicity and invasiveness in the WT cells is the fact that IL-1 is involved in maintaining a chronic inflammatory effect, inducing expression of inflammatory mediators like COX-2 and iNOS in the tumor microenvironment [37, 67]. The observations from basal expression of genes in our studies do not support this hypothesis with higher basal level of expression of *Il6* and *Ptgs2* in the *Il1a/b* KO cell line.

3-MCA, which is used to induce tumors in the BALB/c mice is known to be mutagenic. There may have occurred mutations during carcinogenesis in the mice, which affected the expression of inflammatory genes, favorable for tumor growth. The unexpected changes in gene expression in the *Il1a*/*b* KO compared to the WT cells may also be caused by evolution of the cells in culture. Cancer cells have high genomic instability, which have shown to accelerate in culture, causing rapid accumulations of mutations. Cells with a high rate of proliferation are often naturally selected in culture, causing selection of minor subpopulations of the tumor cells that are not characteristic for the original population [69]. High expression of *Il6* and *Ptgs2* can be beneficial for increased proliferation of cancer cells, and cells with high expression of these genes may have gained a selective advantage compared to the other original tumor cells. The cells used in the experiments had passage numbers of 17 and higher, and it is possible that the number of passages have influenced the gene expression in the cell lines. The cell lines used by Nazarenko et al. and Voronov et al, may not have gone through as many passages as the cells used in this thesis, however this is not known.

The basal expression of genes in the WT vs. the *Il1a/b* KO cells implicate that the presence of *Il1* may not be the only parameter differing between the cell lines, like first assumed. The differences between cell lines in gene expression and toxicity may also be due to other factors, which are not known at this point. This should be taken into consideration when comparing results between cell lines.

4.3.2 Responses in gene expression following exposure to MWCNTs

qRT-PCR was performed on RNA isolated from WT and *Il1a/b* KO cells exposed to 5 and 10 µg/ml MWCNT-NO, and to 5µg/ml MWCNT-JP for 24 hours.

In the WT cell line (Fig. 3.10), there seemed to be a dose-dependent reduction of *Il1b* expression after MWCNT-NO exposure. There was also dose-dependent increase in the expression of *Ptgs2*. None of these changes were significant. There were no apparent changes in expression of *Tnfa*, *Il6* or *Tp53* following MWCNT-NO exposure. The *Il1a/b* KO cell line (Fig 3.11) exposed to MWCNT-NO showed significantly reduced expression of both *Tnfa* and *Il6*. There was significant increased expression of *Ptgs2* (10 µg/ml), while there were no significant changes in the expression of *Tp53*. When comparing the effect of exposure to MWCNT-NO in the different cell lines (Fig. 3.12), there were significant differences in expression of *Tnfa* and *Il6*. No significant changes were seen for *Ptgs2* or *Tp53*. From these results, it seems like the presence of *Il1* affects the response in gene expression of *Tnfa* and *Il6* following MWCNT-NO exposure. There was also a trend of increased gene expression of *Ptgs2* in both cell lines following MWCNT-NO exposure, indicating that increased *Ptgs2* expression is a direct effect of particle exposure, independent of the presence of *Il1*.

The reduction of the pro-inflammatory cytokines *Tnfa* and *Il6* in the *Il1a/b* KO cell line after MWCNT-NO exposure, indicate that MWCNT may cause inhibition of inflammatory responses. Anti-inflammatory effects have been observed in previous *in vitro* studies regarding carbon nanotube toxicity. In a study performed by Herzog et al. (2009), SWCNTs were shown to reduce expression of IL-6 and IL-8 following SWCNT exposure in human lung epithelial cells (A549, NHBE) [28]. The reduction seen in the *Il1a/b* KO cell line may be caused by MWCNT-NO interfering with the TNF-α signaling pathway for induction of inflammation. In the WT, where IL-1 also is able to induce inflammation, the same reduction in *Tnfa* and *Il6* is not seen.

MWCNT-JP generally caused different effects on gene expression than MWCNT-NO, with trends of increased expression of inflammatory genes. The gene expression results for cells exposed to MWCNT-JP generally showed large variations, especially for the *Il1a/b* KO cell line. This may be due to the higher toxicity at this concentration compared to the other exposure. For the WT cell line exposed to MWCNT-JP, there was induced expression of *Il6* and significantly induced expression of *Ptgs2*. No significant changes in *Il1b*, *Tnfa* or *Tp53* were observed. In the *Il1a/b* KO cell line, there was induced expression of *Tnfa*, *Il6*, *Ptgs2* and *Tp53*, although none of these differences were considered to be significant. The results indicate an induction of inflammatory responses in the cell lines when exposed to 5 µg/ml MWCNT-JP, but more experiments are needed to be performed for confirmation of these results. The possible increase in transcription of *Tp53* in the *Il1a/b* KO cell line, may indicate genotoxicity of MWCNT-JP in this cell line. MWCNT-JP has previously been shown to be genotoxic in studies performed on cultured hamster lung cells [65].

When comparing the gene expression of cells exposed to MWCNT-NO and MWCNT-JP in the same dose (5µg/ml) one can see clear differences. MWCNT-JP seem to have a higher inflammatory potential, causing induced expression of genes encoding pro-inflammatory cytokines, while MWCNT-NO does not induce the expression of these gene, it actually causes reduced expression of *Tnfa* and *Il6* in the *Il1a/b* KO cell line. However, both MWCNTs seem to induce the expression of *Ptgs2*, an induction which is similar in both cell lines, and may be independent of *Il1* status (Fig.3.10D, 3.11C, 3.12C). The ability to induce *Ptgs2* expression is most likely a common property for the MWCNTs used in the experiments. The same effect was not observed for crocidolite or H_2O_2 exposed cells. There are not much data available on induction of COX-2 expression following CNT exposure *in vitro*, but *in vivo*, there has been found increased expression of COX-2 in BAL fluid from mice following CNT exposure, similar to what is found in our experiments [70].

4.3.3 Comparison of effects of MWCNTs with Crocidolite and H_2O_2

Crocidolite (20 µg/ml) caused reduced expression of *Tnfa* and *Il6* in both cell lines, and a trend of reduced *Il1b* expression ($P>0.05$) in the WT cell line. The reduction in expression was more apparent in the *Il1a/b* KO cell line, giving a significantly different response to exposure in the two cell lines (Fig. 3.13). The expression of *Ptgs2* and *Tp53* following crocidolite exposure was not significantly different from the control sample in neither of the cell lines. No induction of inflammatory genes was observed.

Previous *in vitro* studies with lung epithelial cells exposed to asbestos, have shown that their biological effect is mediated through oxidative stress and activation of inflammatory responses, through activation of transcription factors like NF-κB, NF-IL6 and AP-1. Exposure to asbestos has been shown to give induced expression of pro-inflammatory cytokines like TNFα, Il-1, IL-6 and IL-8 in alveolar macrophages, lung epithelial cells and mesothelial cells [71, 72]. The observation of decreased gene expression of *Il1b*, *Tnfa* and *Il6* in Crocidolite exposed cells in our experiments is not consistent with these studies. However, there have not been performed studies regarding the effect of crocidolite in the cell lines used in these experiments, the observed responses may be cell type specific. *Il1* seems to be involved in the changes in gene expression following exposure to Crocidolite, with significantly different responses in gene expression of *Tnfa* and *Il6* in the WT and *Il1a/b* KO cell lines.

The results showed a similarity between the effect of MWCNT-NO and crocidolite in the absence of *Il1*, with highly reduced expression of *Tnfa* and *Il6*. Unlike MWCNT-NO, there was no induced expression of *Ptgs2* in crocidolite exposed samples, suggesting that this effect was specific to MWCNT-NO exposure. The resemblance to MWCNT-NO exposure, both regarding toxicity, and in the gene expression, indicates that MWCNT-NO particles may share many common features with crocidolite regarding toxicity, and influence similar cellular responses. The presence of *Il1* seemed to influence the response following crocidolite exposure, with a less drastic reduction in the WT cell line. In the WT cells, where *Il1* is present, there was a more potent inflammatory response following MWCNT-NO exposure than for crocidolite, implicating a role for *Il1* in the inflammatory response induced by MWCNT-NO.

The effect of MWCNT-JP differed more from the effect of crocidolite. The MWCNT-JP exposed cells rather showed a tendency of increased expression of inflammatory genes including *Il6* and *Ptgs2*. Based on our experiments, MWCNT-JP has higher inflammatory potential compared to crocidolite after 24 hours exposure.

H_2O_2 (4µM) was included in the experiments as a known oxidative agent. Gene expression analysis of the WT cell line showed a possible reduced expression of *Il1b* and *Il6* compared to control. There were no differences in expression of *Tnfa*, *Ptgs2* or *Tp53*. In the *Il1a/b* KO cell line, there were no clear differences in expression of any of the genes. These findings suggest that H_2O_2 does not affect the expression of inflammatory genes to a large extent after 24 hours, except from a possible effect on expression of *Il1b* and *Il6* in the WT cell line. Compared with particle exposed cells, there was no effect on gene expression of inflammatory genes by H_2O_2 exposure. This indicates that the changes in gene expression after exposure to particles are not solely a consequence of ROS formation, but are also contributed to by other factors like fiber shape, metal contaminations, interactions with membrane receptors and biopersistence.

The expression following H_2O_2 exposure was measured after 24 hours, an inflammatory effect may have occurred at an earlier stage, e.g. at 6 hours exposure. In cytotoxicity experiments, the toxicity of H_2O_2 seemed to be acute after 6 hours, giving small changes in toxicity over time (Fig. 3.5). H_2O_2 is, unlike the other substances used in this thesis, a chemical which

diffuses easily through the plasma membrane of the cells and is metabolized by catalase and antioxidant defenses within the cell [23]. The effect of H_2O_2 is hence expected to be acute, and to be neutralized quite quickly. To confirm this hypothesis, gene expression analysis should be performed after a shorter period of exposure.

4.3.4 General trends in gene expression

When comparing the effects of exposures on expression of the different genes, there are similar patterns in the fold change gene expression of *Il6* and *Tnfa* (Fig 3.12A, B), which indicate co-expression of these cytokines through similar regulatory mechanisms, e.g. through the action of NF-κB. *Ptgs2* does not have the same trend, with increasing expression after MWCNT exposure in both cell lines. This indicates that other regulatory mechanisms than the ones involved in regulation for *Tnfa* and *Il6* are involved in the induction of *Ptgs2*, which are not examined in our experiments.

There was no significant induction of *Tnfa* or *Il1b* in any of the exposed cells, this may be due to the duration of exposure. IL-1β and TNF-α are short-lived signaling molecules, which are activated rapidly after inflammatory stimuli. Induction of expression of *Tnfa* and *Il1b* may have occurred at an earlier time than 24 hours e.g. after 6 hours.

4.4 Methodical considerations

Current *in vitro* test methods concerning nanoparticle toxicity are based on test methods established for the risk assessments of chemicals. Nanoparticles have unique properties that may interfere with these test methods, including high adsorption capacity, hydrophobicity, surface charge and optical properties [73]. In this section, there will be given an overview of methodical considerations concerning the methods used in this thesis, including dispersion of particles, cytotoxicity testing and fluorescence microscopy.

4.4.1 Dispersion of particles

For *in vitro* studies of toxicity of nanoparticles, good dispersion of the particles in cell culture media is important, because it is desirable to study the interactions of single particles with the cells. Dispersion medium (DM) as described by Porter et al, has been shown to give good dispersion of particles compared to PBS. DM has been shown to be non-toxic, to not interfere with particle toxicity, and to give low degree of particle agglomeration. The media contains serum albumin, which is shown to stabilize nanoparticles by preventing hydrophobic interactions. It also contains the phospholipid DPPC which provides additional stability to single particles in solution [74, 75]. Based on these observations, DM was used for dispersion of the particles used in the experiments. To exclude eventual adverse effects of DM, all cells, including controls were added a total of 10 % DM.

During experiments, it was observed that DM was not sufficient to dissolve the MWCNT-JP particles. In addition to DM, it was decided to use Tween 80 for optimal dispersion. Tween 80 was used to dissolve all the particles used, making the results from the different particles comparable.

All particles (MWCNT-NO, MWCNT-JP and Crocidolite) were dissolved in DM with Tween 80 to a stock solution of 1 mg/ml. Cells were sonicated before use, giving a homogenous solution. The method for dispersion and sonication of particles contains several steps which may cause loss of particles. Adding DM and Tween 80 to the tube containing particles caused in some cases loss of a small amount of particles, due to the static nature of the particles, and that they were handled in a LAF bench with high air flow. Additionally, particles attached to the probe during sonication. Some particles also were stuck in the cap of the eppendorf tube, and were not dissolved. This may have caused small differences in final concentration of particles between experiments.

4.4.2 WST-8 cytotoxicity assay

Cytotoxicity of nanoparticles and controls were measured using the WST-8 assay, which is an absorbance based method. Absorbance based methods are much used within *in vitro* toxicological testing, but have been subject to some criticism when used in the evaluation of toxicity of nanoparticles. This is mainly due to the optical properties of carbon nanotubes, which could possibly interfere with absorbance readings. The MTT assay, which is a much used assay for *in vitro* toxicity testing was determined not to be useful for our experiments, because of potential overlap with the absorbance spectra of carbon nanotubes with an absorbance at 570 nm. MTT has also been shown to react with carbon nanotubes, causing false negative results[76]. In this study, the MTT assay was used in some experiments (results not shown), because of high variances within the results, the WST-8 assay was used instead. This assay gave more stable results, with lower variations. WST-8 has an absorbance at 460 nm, which most likely does not overlap with the absorbance spectra of the MWCNTs.

The media used in cell culture work in this thesis was added 10 % serum (FBS). The presence of serum in cell culture media used for *in vitro* toxicity assays have previously been shown to interfere with toxicity testing, binding to nanoparticles and giving false negative results [77]. The effects of the CNTs on WT and *Il1a/b* KO may therefore be different in the absence of serum. However, serum is used in all the experiments performed, making the results within experiments comparable.

4.4.3 Cell growth and proliferation

The WT and *Il1a/b* KO cell line showed some differences in morphological and proliferative properties when observed in cell culture. The *Il1a/b* KO cells were observed to have a lower rate of proliferation than the WT cell line under normal conditions. The WT cells also were observed to be more clustering than the *Il1a/b* KO cells. These results are consistent with the literature, where expression of *Il1* has been associated with increased cell proliferation and expression of cellular adhesion molecules [35, 78].

However, the growth and proliferation of the WT and *Il1a/b* KO cells in 96-well plates, which was used in cytotoxicity experiments, was shown to differ from each other, as shown in appendix II. The WT cell line did not grow well in these plates, no increased proliferation was observed after 48 and 72 hours. When observed in a phase-contrast microscope after 48 and 72 hours, cells were observed to have an abnormal morphology. The *Il1a/b* KO cell line however, grew well, with proliferation after 48 and 72 hours. These differences are most

likely contributed by the plates used, and the number of cells seeded out. The density of cells per well may have been too low (5000 cells/well), the proliferation in the WT cells may be dependent of cell-cell communication.

The cell density is a parameter that may affect the toxic effect of particles. In toxicity studies with particles, lower cell density has shown to cause higher toxicity because of an increased number of particles per cell [29]. High cell density can also cause increased toxicity. If the toxicity of the test substance involves metabolism or some of the processes involved in mitosis and cell division, the substance may be more toxic to cells with high proliferation rate. Activation of cell cycle checkpoints and apoptotic processes can also increase toxicity in highly proliferating cells. If comparison of cells is desirable, it is important that the cell density and level of proliferation is approximately the same. At 48 and 72 hours of exposure, a comparison of toxicity in the two cell lines can be difficult because of the large difference in cell density. The results from the WT cell line seemed quite unstable after 48 and 72 hour exposure (Fig. 3.2- 3.5), and should be interpreted with caution.

4.4.4 PI/Hoecsht staining and fluorescence microscopy

The contribution of apoptotic vs. necrotic cell death was determined by Hoechst/PI staining followed by fluorescence microscopy. This is a method which facilitates easy discrimination between viable, apoptotic and necrotic cells. Thapsigargin exposed cells were used as a positive control; the definition of the appearance of an apoptotic cell was determined from these cells. The percentage of total cell death obtained by fluorescence microscopy (Fig 3.8B) seemed to correspond relatively well with results from cytotoxicity assays, with similar trends in toxicity. However, the toxicity seemed to be somewhat higher at the higher concentrations of MWCNT-NO compared to results from the WST-8 assays.

The method used is a subjective method, and there will be individual differences in the definition of an apoptotic cell and in the choice of which areas that are to be counted. In the MWCNT exposed cells, the particles caused the picture to be less clear, making identification of apoptotic cells in these cells more difficult. Many of the apoptotic cells in the particle exposed cells were on the borderline in being defined as an apoptotic cell, causing uncertainties. Automatic counting of cells, e.g. by flow cytometry, would have removed the parameter of subjectivity.

5 Conclusion and further work

In this study, it was shown that MWCNTs from different producers caused different cellular responses in WT and *Il1a/b* KO cells, including differences in toxicity and in expression of genes encoding inflammatory mediators. MWCNT-JP was shown to cause a higher cytotoxic and inflammatory response at low doses after 24 hours exposure, compared to MWCNT-NO. The response to MWCNT-NO and crocidolite exposure was similar in the *Il1a/b* KO cells, both regarding cytotoxicity and gene expression. A common property of the MWCNTs seemed to be the ability to induce expression of *Ptgs2*. This induction was shown in both cell lines and was not observed for crocidolite or H_2O_2. MWCNTs were not observed to induce apoptotic cell death in the cell lines used.

The presence of *Il1* seemed to influence both cytotoxic and inflammatory responses following MWCNT exposure. For MWCNT-JP, there was differential toxicity between the cell lines with higher toxicity in the *Il1a/b* KO cell line compared to the WT after 24 hours, which suggests a role of *Il1* in cell survival following MWCNT-JP exposure. Exposure to MWCNT-NO caused reduced expression of *Tnfa* and *Il6 in the Il1a/b* KO cell line, an effect which was not observed in the WT cell line.

To further investigate the mechanisms for toxicity induced by MWCNTs, it is suggested to study the intracellular formation of ROS in cells following exposure. Formation of ROS/RNS and oxidative stress is together with inflammatory responses thought to be important mechanisms for the toxicity of nanoparticles. The difference in the MWCNT's effect on cytotoxicity and inflammatory responses may be due to the different ability of the particles to induce ROS. To explain which properties that are responsible for the different effects observed between the Norwegian and Japanese MWCNTs, particles must be better characterized. Characterization of length/diameter distribution, amount of contaminations, surface properties, and differential dispersion in DM/cell culture media, should be examined in future studies.

To provide additional information, gene expression at an earlier time after exposure should be studied, e.g. after 6 hours exposure, providing further information about the changes in gene expression over time. Also other genes should be included, e.g. genes encoding other inflammatory cytokines/chemokines, genes involved in MAPK signaling or DNA repair pathways. To support the gene expression data, it is suggested to see whether differences in gene expression are reflected at the protein level, using Western Blot or ELISA. It would also be interesting to examine the activity of central transcription factors like NF-κB and AP-1 following MWCNT exposure. There should also be studied whether the responses following CNT exposure *in vitro* is correlated with the response *in vivo*, using BALB/c WT and *Il1a/b* KO mice.

References

1. Oberdorster, G., E. Oberdorster, and J. Oberdorster, *Nanotoxicology: an emerging discipline evolving from studies of ultrafine particles.* Environ Health Perspect, 2005. **113**(7): p. 823-39.
2. Warheit, D.B., et al., *Health effects related to nanoparticle exposures: environmental, health and safety considerations for assessing hazards and risks.* Pharmacol Ther, 2008. **120**(1): p. 35-42.
3. Iijima, S., *Helical Microtubules of Graphitic Carbon.* Nature, 1991. **354**(6348): p. 56-58.
4. Aschberger, K., et al., *Review of carbon nanotubes toxicity and exposure--appraisal of human health risk assessment based on open literature.* Crit Rev Toxicol, 2010. **40**(9): p. 759-90.
5. Donaldson, K., et al., *Asbestos, carbon nanotubes and the pleural mesothelium: a review of the hypothesis regarding the role of long fibre retention in the parietal pleura, inflammation and mesothelioma.* Part Fibre Toxicol, 2010. **7**: p. 5.
6. Baughman, R.H., A.A. Zakhidov, and W.A. de Heer, *Carbon nanotubes--the route toward applications.* Science, 2002. **297**(5582): p. 787-92.
7. Donaldson, K., et al., *Carbon nanotubes: a review of their properties in relation to pulmonary toxicology and workplace safety.* Toxicol Sci, 2006. **92**(1): p. 5-22.
8. Lam, C.W., et al., *A review of carbon nanotube toxicity and assessment of potential occupational and environmental health risks.* Crit Rev Toxicol, 2006. **36**(3): p. 189-217.
9. Shvedova, A.A., V.E. Kagan, and B. Fadeel, *Close encounters of the small kind: adverse effects of man-made materials interfacing with the nano-cosmos of biological systems.* Annu Rev Pharmacol Toxicol, 2010. **50**: p. 63-88.
10. Firme, C.P., 3rd and P.R. Bandaru, *Toxicity issues in the application of carbon nanotubes to biological systems.* Nanomedicine, 2010. **6**(2): p. 245-56.
11. Muhlfeld, C., et al., *Interactions of nanoparticles with pulmonary structures and cellular responses.* Am J Physiol Lung Cell Mol Physiol, 2008. **294**(5): p. L817-29.
12. Mossman, B.T., et al., *Pulmonary endpoints (lung carcinomas and asbestosis) following inhalation exposure to asbestos.* J Toxicol Environ Health B Crit Rev, 2011. **14**(1): p. 76-121.
13. Jaurand, M.C., A. Renier, and J. Daubriac, *Mesothelioma: Do asbestos and carbon nanotubes pose the same health risk?* Part Fibre Toxicol, 2009. **6**: p. 16.
14. Poland, C.A., et al., *Carbon nanotubes introduced into the abdominal cavity of mice show asbestos-like pathogenicity in a pilot study.* Nat Nanotechnol, 2008. **3**(7): p. 423-8.
15. Donaldson, K., et al., *The limits of testing particle-mediated oxidative stress in vitro in predicting diverse pathologies; relevance for testing of nanoparticles.* Part Fibre Toxicol, 2009. **6**: p. 13.
16. Ravichandran, P., et al., *Multiwalled carbon nanotubes activate NF-kappaB and AP-1 signaling pathways to induce apoptosis in rat lung epithelial cells.* Apoptosis, 2010. **15**(12): p. 1507-16.
17. Yamashita, K., et al., *Carbon nanotubes elicit DNA damage and inflammatory response relative to their size and shape.* Inflammation, 2010. **33**(4): p. 276-80.
18. Unfried, K., C. Schurkes, and J. Abel, *Distinct spectrum of mutations induced by crocidolite asbestos: clue for 8-hydroxydeoxyguanosine-dependent mutagenesis in vivo.* Cancer Res, 2002. **62**(1): p. 99-104.
19. Wallin, H., et al., *Mutagenicity of carbon nanomaterials.* J Biomed Nanotechnol, 2011. **7**(1): p. 29.
20. Lindberg, H.K., et al., *Genotoxicity of nanomaterials: DNA damage and micronuclei induced by carbon nanotubes and graphite nanofibres in human bronchial epithelial cells in vitro.* Toxicol Lett, 2009. **186**(3): p. 166-73.
21. Oberdorster, G., *Safety assessment for nanotechnology and nanomedicine: concepts of nanotoxicology.* J Intern Med, 2010. **267**(1): p. 89-105.
22. Knaapen, A.M., et al., *Inhaled particles and lung cancer. Part A: Mechanisms.* Int J Cancer, 2004. **109**(6): p. 799-809.
23. Azad, N., Y. Rojanasakul, and V. Vallyathan, *Inflammation and lung cancer: roles of reactive oxygen/nitrogen species.* J Toxicol Environ Health B Crit Rev, 2008. **11**(1): p. 1-15.

24. Garza, K.M., K.F. Soto, and L.E. Murr, *Cytotoxicity and reactive oxygen species generation from aggregated carbon and carbonaceous nanoparticulate materials.* Int J Nanomedicine, 2008. **3**(1): p. 83-94.
25. Srivastava, R.K., et al., *Multi-walled carbon nanotubes induce oxidative stress and apoptosis in human lung cancer cell line-A549.* Nanotoxicology, 2010.
26. Tsukahara, T. and H. Haniu, *Cellular cytotoxic response induced by highly purified multi-wall carbon nanotube in human lung cells.* Mol Cell Biochem, 2011.
27. Coussens, L.M. and Z. Werb, *Inflammation and cancer.* Nature, 2002. **420**(6917): p. 860-7.
28. Herzog, E., et al., *SWCNT suppress inflammatory mediator responses in human lung epithelium in vitro.* Toxicol Appl Pharmacol, 2009. **234**(3): p. 378-90.
29. Hirano, S., et al., *Uptake and cytotoxic effects of multi-walled carbon nanotubes in human bronchial epithelial cells.* Toxicol Appl Pharmacol, 2010.
30. Ye, S.F., et al., *ROS and NF-kappaB are involved in upregulation of IL-8 in A549 cells exposed to multi-walled carbon nanotubes.* Biochem Biophys Res Commun, 2009. **379**(2): p. 643-8.
31. Aggarwal, B.B., et al., *Inflammation and cancer: how hot is the link?* Biochem Pharmacol, 2006. **72**(11): p. 1605-21.
32. Dinarello, C.A., *Immunological and inflammatory functions of the interleukin-1 family.* Annu Rev Immunol, 2009. **27**: p. 519-50.
33. Dinarello, C.A., *Interleukin-1beta.* Crit Care Med, 2005. **33**(12 Suppl): p. S460-2.
34. Shen, H.M. and V. Tergaonkar, *NFkappaB signaling in carcinogenesis and as a potential molecular target for cancer therapy.* Apoptosis, 2009. **14**(4): p. 348-63.
35. Dinarello, C.A., *Biologic basis for interleukin-1 in disease.* Blood, 1996. **87**(6): p. 2095-147.
36. Horai, R., et al., *Production of mice deficient in genes for interleukin (IL)-1alpha, IL-1beta, IL-1alpha/beta, and IL-1 receptor antagonist shows that IL-1beta is crucial in turpentine-induced fever development and glucocorticoid secretion.* J Exp Med, 1998. **187**(9): p. 1463-75.
37. Krelin, Y., et al., *Interleukin-1beta-driven inflammation promotes the development and invasiveness of chemical carcinogen-induced tumors.* Cancer Res, 2007. **67**(3): p. 1062-71.
38. Landvik, N.E., et al., *A specific interleukin-1B haplotype correlates with high levels of IL1B mRNA in the lung and increased risk of non-small cell lung cancer.* Carcinogenesis, 2009. **30**(7): p. 1186-92.
39. Zienolddiny, S., et al., *Polymorphisms of the interleukin-1 beta gene are associated with increased risk of non-small cell lung cancer.* Int J Cancer, 2004. **109**(3): p. 353-6.
40. Persson, C., et al., *Polymorphisms in inflammatory response genes and their association with gastric cancer: A HuGE systematic review and meta-analyses.* Am J Epidemiol, 2011. **173**(3): p. 259-70.
41. Balkwill, F., *TNF-alpha in promotion and progression of cancer.* Cancer Metastasis Rev, 2006. **25**(3): p. 409-16.
42. Moore, R.J., et al., *Mice deficient in tumor necrosis factor-alpha are resistant to skin carcinogenesis.* Nat Med, 1999. **5**(7): p. 828-31.
43. Knight, B., et al., *Impaired preneoplastic changes and liver tumor formation in tumor necrosis factor receptor type 1 knockout mice.* J Exp Med, 2000. **192**(12): p. 1809-18.
44. Aggarwal, B.B., *Nuclear factor-kappaB: the enemy within.* Cancer Cell, 2004. **6**(3): p. 203-8.
45. Heinrich, P.C., et al., *Principles of interleukin (IL)-6-type cytokine signalling and its regulation.* Biochem J, 2003. **374**(Pt 1): p. 1-20.
46. Dienz, O. and M. Rincon, *The effects of IL-6 on CD4 T cell responses.* Clin Immunol, 2009. **130**(1): p. 27-33.
47. Williams, C.S., M. Mann, and R.N. DuBois, *The role of cyclooxygenases in inflammation, cancer, and development.* Oncogene, 1999. **18**(55): p. 7908-16.
48. Campa, D., et al., *Association of a common polymorphism in the cyclooxygenase 2 gene with risk of non-small cell lung cancer.* Carcinogenesis, 2004. **25**(2): p. 229-35.
49. Cuzick, J., et al., *Aspirin and non-steroidal anti-inflammatory drugs for cancer prevention: an international consensus statement.* Lancet Oncol, 2009. **10**(5): p. 501-7.

50. Okada, H. and T.W. Mak, *Pathways of apoptotic and non-apoptotic death in tumour cells.* Nat Rev Cancer, 2004. **4**(8): p. 592-603.
51. Taylor, R.C., S.P. Cullen, and S.J. Martin, *Apoptosis: controlled demolition at the cellular level.* Nat Rev Mol Cell Biol, 2008. **9**(3): p. 231-41.
52. Saraste, A. and K. Pulkki, *Morphologic and biochemical hallmarks of apoptosis.* Cardiovasc Res, 2000. **45**(3): p. 528-37.
53. Vousden, K.H. and X. Lu, *Live or let die: the cell's response to p53.* Nat Rev Cancer, 2002. **2**(8): p. 594-604.
54. Toledo, F. and G.M. Wahl, *Regulating the p53 pathway: in vitro hypotheses, in vivo veritas.* Nat Rev Cancer, 2006. **6**(12): p. 909-23.
55. Takagi, A., et al., *Induction of mesothelioma in p53+/- mouse by intraperitoneal application of multi-wall carbon nanotube.* J Toxicol Sci, 2008. **33**(1): p. 105-16.
56. Donaldson, K., et al., *Re: Induction of mesothelioma in p53+/- mouse by intraperitoneal application of multi-wall carbon nanotube.* J Toxicol Sci, 2008. **33**(3): p. 385; author reply 386-8.
57. Takaya, M., et al., *Characteristics of multiwall carbon nanotubes for an intratracheal instillation study with rats.* Ind Health, 2010. **48**(4): p. 452-9.
58. Kubista, M., et al., *The real-time polymerase chain reaction.* Mol Aspects Med, 2006. **27**(2-3): p. 95-125.
59. Schefe, J.H., et al., *Quantitative real-time RT-PCR data analysis: current concepts and the novel "gene expression's CT difference" formula.* J Mol Med, 2006. **84**(11): p. 901-10.
60. Streiner, D.L., *Maintaining standards: differences between the standard deviation and standard error, and when to use each.* Can J Psychiatry, 1996. **41**(8): p. 498-502.
61. Altman, D.G., *Practical statistics for Medical Research*. 1991, London: Chapman & Hall.
62. Schroder, E. and P. Eaton, *Hydrogen peroxide as an endogenous mediator and exogenous tool in cardiovascular research: issues and considerations.* Curr Opin Pharmacol, 2008. **8**(2): p. 153-9.
63. Wang, X.Y., et al., *Quercetin in combating H2O2 induced early cell apoptosis and mitochondrial damage to normal human keratinocytes.* Chin Med J (Engl), 2010. **123**(5): p. 532-6.
64. Patlolla, A., B. Knighten, and P. Tchounwou, *Multi-walled carbon nanotubes induce cytotoxicity, genotoxicity and apoptosis in normal human dermal fibroblast cells.* Ethn Dis, 2010. **20**(1 Suppl 1): p. S1-65-72.
65. Asakura, M., et al., *Genotoxicity and cytotoxicity of multi-wall carbon nanotubes in cultured Chinese hamster lung cells in comparison with chrysotile A fibers.* J Occup Health, 2010. **52**(3): p. 155-66.
66. Davidson, G.A. and R.J. Varhol, *Kinetics of thapsigargin-Ca(2+)-ATPase (sarcoplasmic reticulum) interaction reveals a two-step binding mechanism and picomolar inhibition.* J Biol Chem, 1995. **270**(20): p. 11731-4.
67. Voronov, E., et al., *Effects of IL-1 molecules on growth patterns of 3-MCA-induced cell lines: an interplay between immunogenicity and invasive potential.* J Immunotoxicol, 2010. **7**(1): p. 27-38.
68. Nazarenko, I., et al., *Tumorigenicity of IL-1alpha- and IL-1beta-deficient fibrosarcoma cells.* Neoplasia, 2008. **10**(6): p. 549-62.
69. Gazdar, A.F., B. Gao, and J.D. Minna, *Lung cancer cell lines: Useless artifacts or invaluable tools for medical science?* Lung Cancer, 2010. **68**(3): p. 309-18.
70. Park, E.J., et al., *A single intratracheal instillation of single-walled carbon nanotubes induced early lung fibrosis and subchronic tissue damage in mice.* Arch Toxicol, 2011.
71. Luster, M.I. and P.P. Simeonova, *Asbestos induces inflammatory cytokines in the lung through redox sensitive transcription factors.* Toxicol Lett, 1998. **102-103**: p. 271-5.
72. Mossman, B.T., et al., *Cell signaling pathways elicited by asbestos.* Environ Health Perspect, 1997. **105 Suppl 5**: p. 1121-5.
73. Kroll, A., et al., *Current in vitro methods in nanoparticle risk assessment: limitations and challenges.* Eur J Pharm Biopharm, 2009. **72**(2): p. 370-7.

74. Porter, D., et al., *A biocompatible medium for nanoparticle dispersion.* Nanotoxicology, 2008. **2**(3): p. 144-154.
75. Wang, X., et al., *Quantitative techniques for assessing and controlling the dispersion and biological effects of multiwalled carbon nanotubes in mammalian tissue culture cells.* ACS Nano, 2010. **4**(12): p. 7241-52.
76. Belyanskaya, L., et al., *The reliability and limits of the MTT reduction assay for carbon nanotubes-cell interaction.* Carbon, 2007. **45**(13): p. 2643-2648.
77. Geys, J., B. Nemery, and P.H. Hoet, *Assay conditions can influence the outcome of cytotoxicity tests of nanomaterials: better assay characterization is needed to compare studies.* Toxicol In Vitro, 2010. **24**(2): p. 620-9.
78. Apte, R.N., et al., *The involvement of IL-1 in tumorigenesis, tumor invasiveness, metastasis and tumor-host interactions.* Cancer Metastasis Rev, 2006. **25**(3): p. 387-408.

Appendix

Appendix I - Materials

Cell lines

Cell line	Media	Tissue origin	Distributor
WT	DMEM w. 50 mL FBS, 5 mL Pen Strept, 2 mL Fungizone/ 500 mL	Fibrosarcoma, WT BALB/c mouse	Professor R.N. Apte (Department of of Microbiology and Immunology, NIBN, Israel)
Il1a/b KO	DMEM w. 50 mL FBS, 5 mL Pen Strept, 2 mL Fungizone/ 500 mL	Fibrosarcoma, *Il1a/b*$^{(-/-)}$ BALB/c mouse	Professor R.N. Apte (Department of of Microbiology and Immunology, NIBN, Israel)

Particles

Particle	Provided by
MWCNT-NO	nTec Norway
MWCNT-JP	Mitsui & Co. (XNRI MWNT-7, lot#05072001K28)
Crocidolite Asbestos	Medical Research Council(England)

Kits

Sigma Aldrich

Measuring cytotoxicity by the CCK-8® assay

Biotium

Measuring cytotoxicity by the MTT® assay

Quanta

cDNA synthesis from isolated RNA using the qScript™ cDNA Synthesis Kit

qRT-PCR using Perfecta SYBR Green Fast Mix

Instruments

Cell counter	Countess automated cell counter (Invitrogen)
Centrifuges	Eppendorf centrifuge 5702
	Sigma 2-6E
Cooler centrifuges	Eppendorf centrifuge 5417R
	Sigma 4K15
Heating block	Grand instruments QBT2

Imaging system	Kodak Image Station 440Cf
Spectrophotometer	Eppendorf biophotometer
Microscope	Nikon Diaphoto light microscope
	Nikon Labophot fluorescence microscope
Multimode reader	Modulus microplate reader , Pronova
Real-time instrument	ABI Prism 7900 HT sequence detection system, Applied Biosystems
Sonicator	Labsonic M, Sartorius Stedim Biotech
Thermal cyclers	Perkin Elmer Cetus DNA Cycler 480

Chemicals

Acetic acid (glacial),	Merck	Hoechst 33342	Sigma Aldrich
Agarose (SeaKem GTG)	Lonza	Isol RNA Lysis reagent	5’ prime
Bovine Serum Albumin	Sigma Aldrich	Leibovitz’s L15 media	Invitrogen
Chloroform	Sigma Aldrich	Loading buffer	New England Biolabs
Dubeccos modified Eagles Medium (DMEM)	Sigma Aldrich	KCl	Merck
Dimethylsulfoxide (DMSO)	Sigma Aldrich	$MgSO_4$	Sigma Aldrich
DNA ladder(100 bp)	New England Biolabs	NaCl	Merck
DNase I (bovine pancreas)	Sigma Aldrich	NaOH	Merck
d-Glucose(10 %)	Sigma Aldrich	$NaHPO_4$* H_2O	Merck
1,2-dipalmitoyl-sn-glycero-3-phosphocholine (DPPC)	Sigma Aldrich	Penicillin Streptomyocin	Gibco
EDTA (triplex III)	Merck	Phenol red	Sigma Aldrich
Ethanol (rectified, absolute)	Kemethyl	Propidiumiodide (PI)	Merck
Fetal Bovine serum (FBS)	Gibco	Propane-2-ol (isopropanol)	Merck
Fungizone	Gibco	Thapsigargin	Sigma-Aldrich
GelRed	Biotium Inc.	Tris base 7-9®	Sigma Aldrich
HEPES	Sigma Aldrich	Trypane Blue stain	Invitrogen
Hydrogen Peroxide (H_2O_2), 8,8M	Sigma Aldrich	Trypsin	Sigma Aldrich
HCl	Merck	Tween 80	Sigma Aldrich

Solutions

All solutions are made with ddH2O and sterile filtered before use where needed.

AF-media

76 % L-15 medium, 2 % 1M HEPES, 2 % PS, 20 % FBS

BSA 60 mg/mL stock

60 mg BSA, 1 mL PBS

DEPC water

0.1 % DEPC in ddH_2O

DPPC 10 mg/mL stock

10 mg DPPC, 1 mL absolute ethanol

Disperging medium (for nanoparticles)

1000 µl BSA solution**,** 100 µl DPPC solution, 991 µl d-Glucose**,** PBS to 100 ml.

DMSO for cell culture storage

50 % L-15 medium, 2 % 1 M HEPES, 8 % DMSO, 40 % FBS

DNase (4mg/ml)

4 g DNase I, 87.66 mg NaCl, 5.06 mg $MgSO_4$, water to 1 ml

Ethanol in DEPC water (75%)

12,5 mL DEPC water, Absolute ethanol to 50 ml

EDTA

9.3 EDTA, 50 ml H2O, pH adjusted to 8.

Fetal Bovine Serum (FBS)

Heat inactivated at 56°C for 45 minutes.

Glutamax 100 x

2.9 g glutamine, 100 ml H_2O

HEPES

238.3 g HEPES, 1 ml 0.12% phenol red in 1 L ddH_2O, pH 7.3.

Hoechst 33342 (1 mg/ml) + PI (0,5mg/ml)

1 ml Hoescht 33432 (10*), 1 ml PI (5*), ddH_2O to 10 ml

Phenol red

125g phenol red, 360 µl 1M NaOH, 100 ml H_2O

Phosphate Buffered Saline (PBS)

7.07 g NaCl, 0.20 g KCl, 1.94 g $NaHPO_4$ * H_2O, H_2O to 1L.

TE-buffer (Tris-EDTA buffer) 10x, pH 8

100 mM Tris-Cl pH 8, 10 mM EDTA pH 8

TAE buffer (Tris-acetate-EDTA buffer) 50x, 1 L

242 g Tris base, 57.1 ml glacial acetic acid, 100 ml 0.5 M EDTA pH 8.

Thapsigargin

100 µM in DMSO

Tris-Cl 1M pH 8, 1L

121,1 g Tris base, 42 ml HCl, H_2O to 1L

Trypsin 1%

50 mg trypsin, 5 ml PBS

Cell culture media

Two different types of DMEM was used; For most cell culture work DMEM with phenol red was used (D5796). For absorbance readings, DMEM without phenol red was used (D1145). After 2 months, 5 mL 100x Glutamax was added.

DMEM w 10 % FBS

- 500 ml DME
- 50 ml FBS
- 5 ml PS
- 2 ml Fungizone

DNA ladders

100 bp ladder (New England Biolabs)

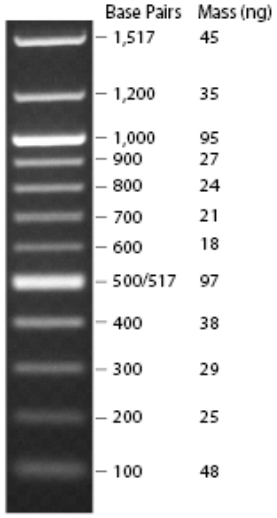

Appendix II: WST-8 cytotoxicity assay

Standard curves

A standard curve was applied in the setup for all of the cytotoxicity experiments, as a quality control for the cell culture work. Good examples of standard curves for the WT and *Il1a/b* KO cell lines after 24 hours incubation with cell culture media + 10 % DM are shown in figure A2.1A and B respectively.

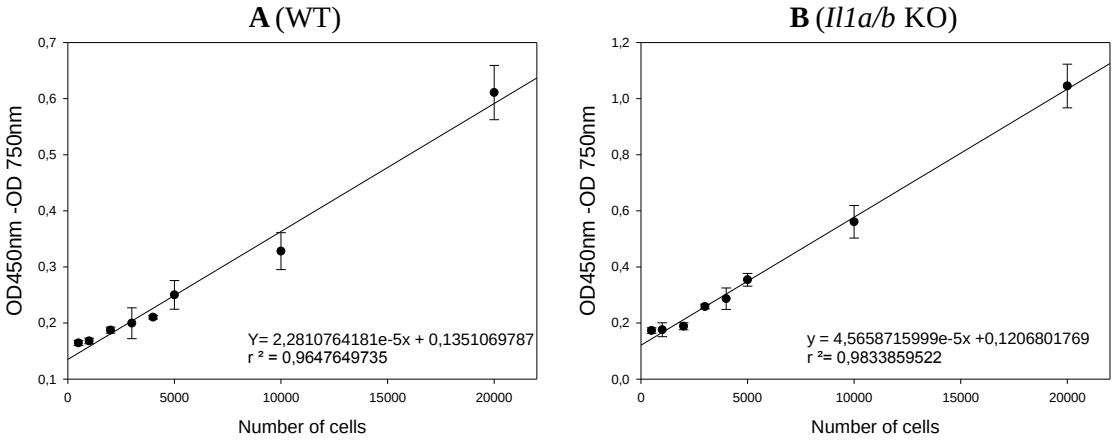

Figure A2. 1 Example of standard curves used for quality control in WST-8 experiments. OD 450nm – OD 750nm after 24 hours incubation in the A: WT and B: *Il1a/b* KO cell line. Error bars = SD.

Characterization of proliferation of WT and *Il1a/b* KO cells in 96-well plates.

For cytotoxicity assays, BalbC WT and *Il1a/b* KO cell lines were seeded out in 96 well plates with same cell densities (5000 cells/well). The cell lines ability to grow and proliferate was monitored, and seemed to differ from each other, causing different cell density in the two cell lines over time. The differences in cell proliferation between the cell lines are illustrated in figure A2.2. The figure shows the average OD (450 nm – 750 nm) for unexposed samples (cell culture media + 10% DM) as a function of incubation time. The *Il1a/b* KO cell line showed an increase in optical density with increasing time indicating cell proliferation. The WT cell line in contrast seems to have no increase in OD after 48 and 72 hours, indicating low levels of proliferation.

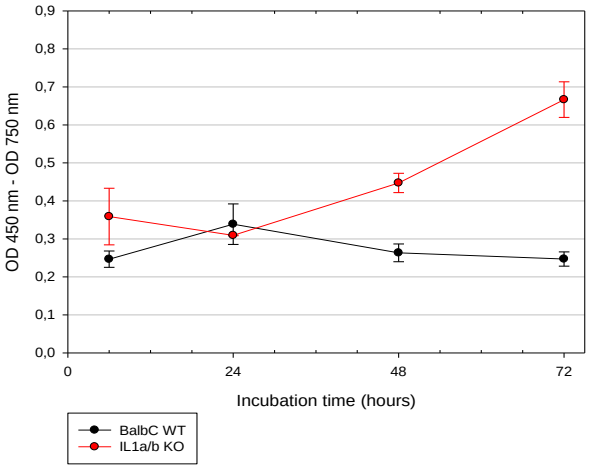

Figure A2.2 OD (450 nm- 750 nm) vs. hours of incubation in non-exposed samples of the WT and the *Il1a/b* KO cell lines. . The mean OD values for each of the experiments are used. Error bars = SE.

Appendix III - Test of primers used in qRT-PCR

The qRT-PCR primers for the genes *Il1b, Tnfa, Il6, Ptgs2, Tp53* and *Actb* in mice cells (table 2.3) were specifically designed for this project.

Before used in experiments, primers were tested for specificity by analyzing the dissociation curve from the qRT-PCR reaction and by agarose gel electrophoresis of the PCR products. For the genes *Il1b, Il6, Ptgs2* and *Actb*, qRT- PCR was performed for 3 cDNA samples from the WT cell line; cDNA from cells exposed to 10µg/ml nTec MWCNT, a mix of all exposed samples, and a control sample (unexposed). For the *Tp53* and *Tnfa*-primers, cDNA from both the WT and the *Il1a/b* KO cell lines were used, with one control sample and one cDNA mix from exposed samples.

The melting curves from the qRT- PCR reaction are shown in figure A3.1, and pictures from the agarose gel electrophoresis of the PCR products are shown in figure A3.2(*Il1b, Il6, Ptgs2* and *Actb*) and A3.3(*Tnfa* and *Tp53*).The primers generally seemed to be functioning well, giving single peak melting curves, and distinct bands on the gel after electrophoresis. The bands on the gel seemed to correspond with the given amplicon size(table 2.3). The different primers and their expected amplicon size are indicated in figure A3.2 and 3. In the NTC for the *Tp53* primer, there were some disruptions in the melting curve, indicating formation of primer dimers. This was confirmed when running the samples on a gel, giving an extra band in the NTC, (encircled band in Fig. A3.3). However, since this band only occurred in the NTC, this indicates that there are low levels of primer dimerization in samples containing cDNA, the primers can therefore be used.

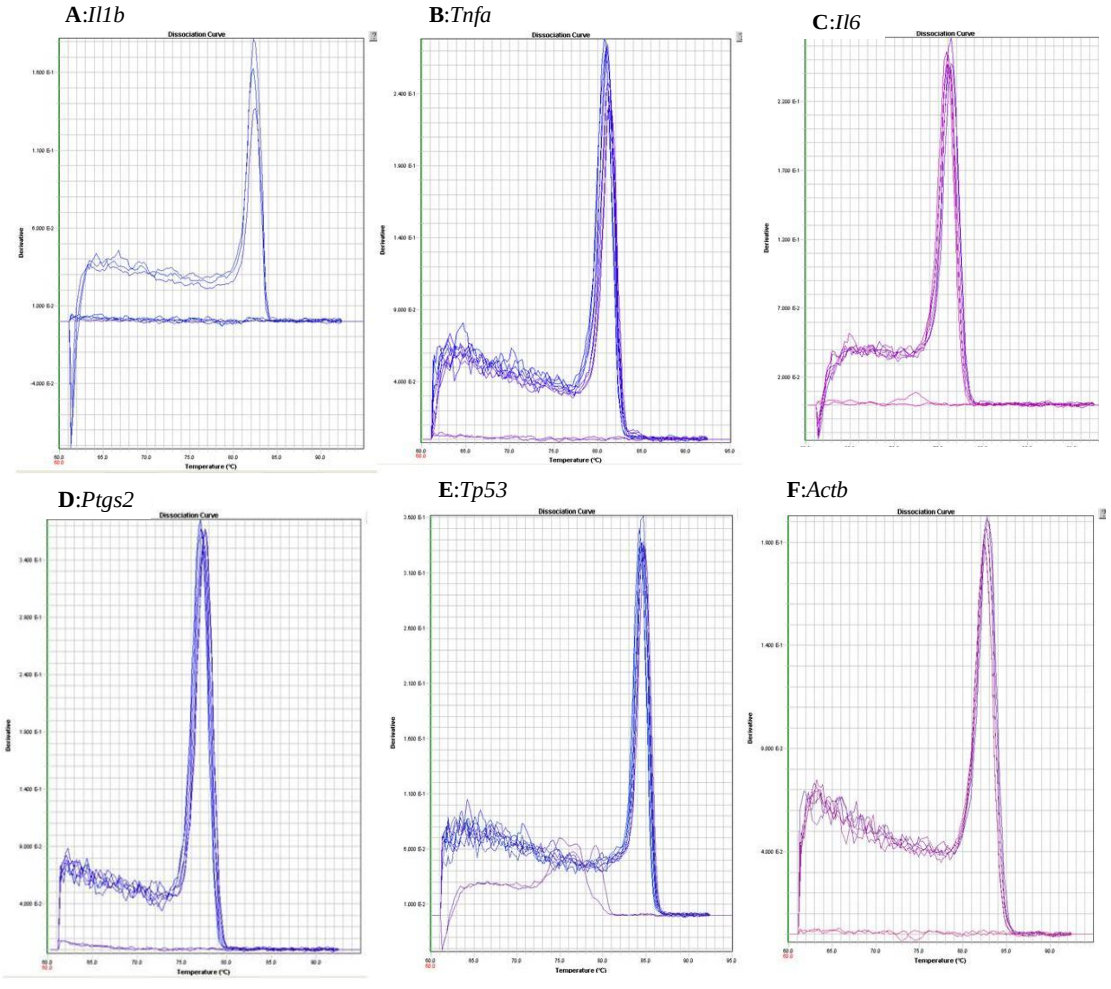

Figure A3. 1 Test of primers for real-time PCR: Dissociation curve for PCR products from real-time PCR. Primers for A: *Il1b*, B: *Tnfa*, C: *Il6*, D: *Ptgs2*, E: *Tp53*, F: *Actb*.

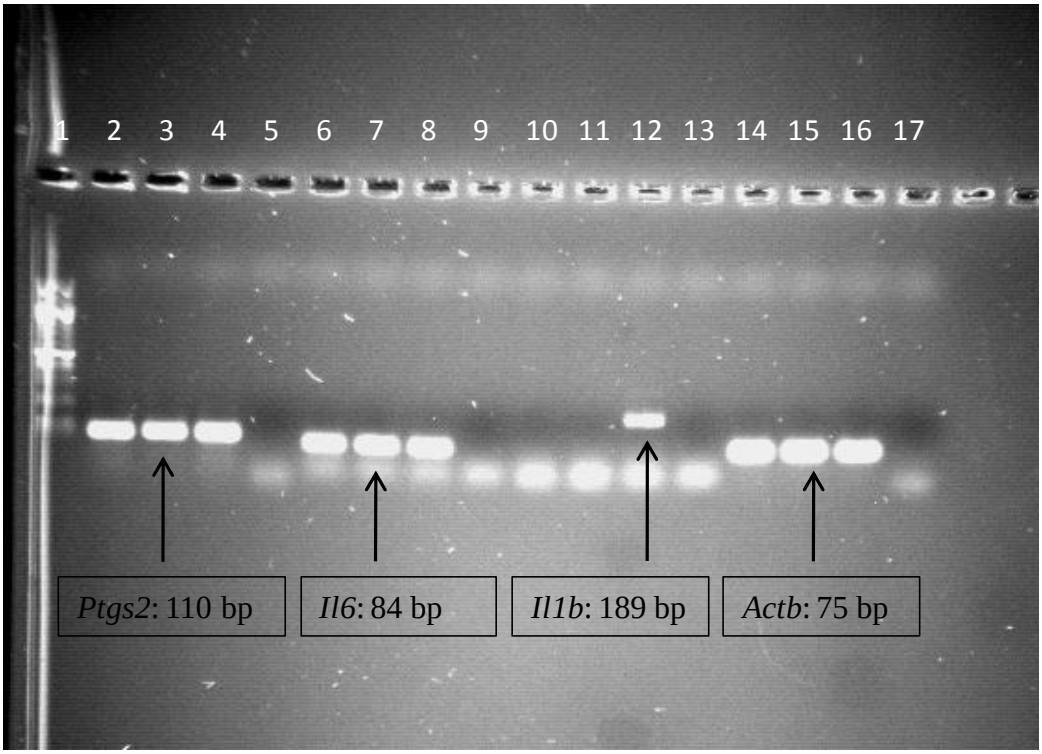

Figure A3.2: Agarose gel electrophoresis of PCR products, test of primers for *Ptgs2*, *Il6*, *Il1b* and *Actb*. Expected amplicon size is illustrated in the figure. The wells contained: 1: 100 bp ladder, 2: Ctr *Ptgs2*, 3: nTec *Ptgs2*, 4: Mix *Ptgs2*, 5: NTC *Ptgs2*, 6: Ctr *Il6*, 7: nTec *Il6*, 8: Mix *Il6*, 9: NTC *Il6*, 10: Ctr *Il1b*, 11: nTec *Il1b*, 12: Mix *Il1b*, 13: NTC *Il1b*, 14: Ctr *Actb*, 15: nTec *Actb*, 16: Mix *Actb*, 17: NTC *Actb*.

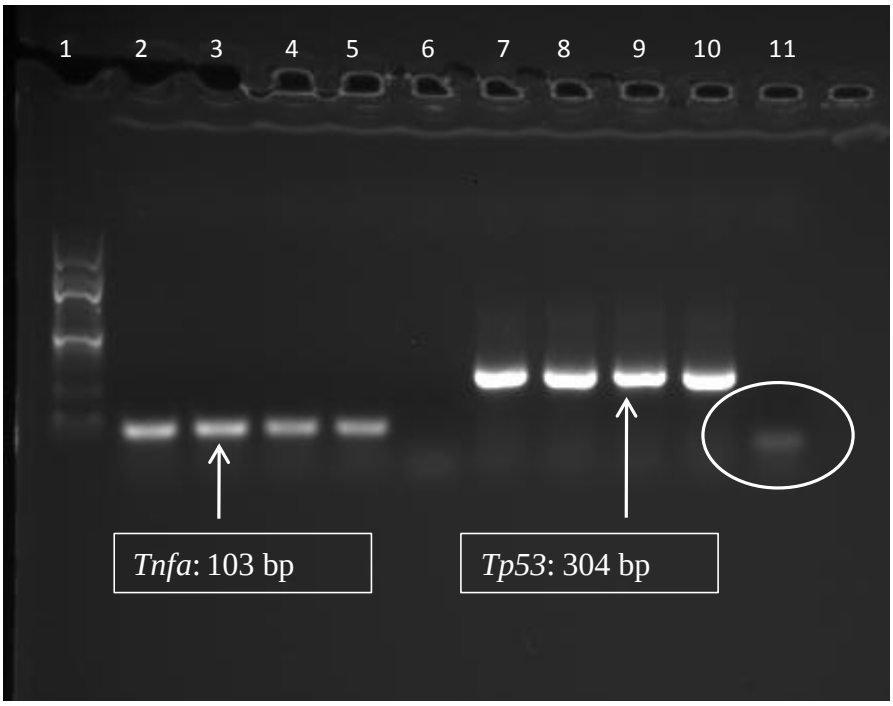

Figure A3.3: Agarose gel electrophoresis of real-time PCR products; test of primers for *Tnfα* and *Tp53*. Expected amplicon size is illustrated in the figure. The wells contained: 1: 100 bp ladder, 2: BalbC Ctr *Tnfa*, 3: BalbC mix exposed *Tnfa*, 4: IL1α/β Ctr *Tnfa*, 5: IL1α/β Mix exposed *Tnfa*, 6: NTC *Tnfa*, 7: BalbC Ctr *Tp53*, 8: BalbC Mix exposed *Tp53*, 9: IL1α/β Ctr *Tp53*, 10: IL1α/β Mix exposed *Tp53*, 11: NTC *Tp53*.

Appendix IV – Calculations

Cytotoxicity experiments:

For the cytotoxicity experiments, 3 independent experiments were performed. For each experiment, the mean $OD_{(450nm-750nm)}$ value of three parallels were calculated, and percentage viability was calculated using equation 1.

$$\text{Cell viability} = \frac{OD_{(450nm-750nm)}\text{exposed}}{OD_{(450nm-750nm)}\text{control}} * 100\% \quad (1)$$

Fluorescence microscopy:

The percentage of apoptotic, necrotic dead and viable cells was calculated from the total number of cells in each parallel according to equation 2 -5.

$$\text{Percentage apoptosis} = \frac{\text{apoptotic cells}}{\text{apoptotic + necrotic cells}} * 100\% \quad (2)$$

$$\text{Percentage necrosis} = \frac{\text{necrotic cells}}{\text{apoptotic + necrotic cells}} * 100\% \quad (3)$$

$$\text{Percentage cell death} = \frac{\text{apoptotic + necrotic cells}}{\text{total number of cells}} * 100\% \quad (4)$$

$$\text{Percentage viability} = \frac{\text{viable cells}}{\text{total number of cells}} * 100\% \quad (5)$$

Real-time PCR:

The relative expression of genes was calculated using *Actb* expression as an endogenous control, and was calculated using equation 6 and 7. The mean CT value from the parallels originating from the same cDNA template was used.

$$\Delta CT = CT_{Gene} - CT_{Actb} \quad (6)$$

$$\text{Relative expression} = 2^{(-\Delta Ct)} * 10^4 \quad (7)$$

Using equation 7, there is assumed that there is a doubling of DNA for each PCR cycle, PCR efficiency is not taken into account. The mean relative expression value of the 2 parallel cDNA samples used was used as the result for each experiment. When comparing response in gene expression between cell lines, fold change was used. Fold change is calculated using equation 8, the mean relative expression value for each experiment is used.

$$\text{Fold change mRNA} = \frac{\text{Relative expression}_{\text{exposed}}}{\text{Relative expression}_{\text{control}}} \quad (8)$$

Appendix V – Raw data.

Cytotoxicity studies

The OD values (OD 450 nm – OD 750 nm) obtained from the WST-8 assays following exposure to MWCNT-NO, MWCNT-JP, crocidolite and H_2O_2 is shown in table A5.1-4. Only experiments with valid standard curves (see appendix II) are applied in the tables.

Table A5. 1: OD values following MWCNT-NO exposure

			OD 450 nm - 750 nm(mean value of 3 parallells)					
Exposure time	Cell line	Concentration	Exp 1	Exp 2	Exp 3	Exp 4	Exp 5	Exp 6
6 hours	WT	Control	0.2955036		0.206947973	0.209866083	0.200539486	
		5 µg/ml	0.28521623		0.208469483	0.19268953	0.198721663	
		10 µg/ml	0.28490223		0.17408795	0.21065667	0.17151446	
		20 µg/ml	0.23327343		0.180583856	0.193256313	0.184037503	
		50 µg/ml	0.21858173		0.179899043	0.175858566	0.16576863	
		100 µg/ml	0.2185943		0.14697513	0.1662711	0.149773967	
	Il1a/b KO	Control	0.43276993	0.306283023	0.274968706		0.23910409	
		5 µg/ml	0.4073002	0.31605457	0.26914449		0.21837662	
		10 µg/ml	0.45635883	0.24015399	0.226792843		0.195816243	
		20 µg/ml	0.42031363	0.26229961	0.22425346		0.18979176	
		50 µg/ml	0.3507562	0.253691946	0.22598681		0.171304823	
		100 µg/ml	0.26399326	0.23227626	0.2055197		0.152277267	
24 hours	WT	Control			0.219381783	0.301729593	0.654132306	0.79057323
		5 µg/ml			0.22870103	0.309405886	0.60751871	0.55812793
		10 µg/ml			0.21073807	0.248049376	0.609619833	0.750100316
		20 µg/ml			0.201733967	0.227475833	0.589565	0.5597787
		50 µg/ml			0.19349707	0.219400613	0.4956632	0.480533866
		100 µg/ml			0.17567339	0.19017045	0.368852567	0.284869866
	Il1a/b KO	Control	0.322808083	0.400952386		0.401333623	0.38732868	0.43452116
		5 µg/ml	0.28923084	0.290584416		0.378302463	0.425724716	0.381261133
		10 µg/ml	0.2876718	0.315381693		0.36182273	0.4072253	0.395246767
		20 µg/ml	0.277138533	0.260897566		0.3484033133	0.378296	0.399420667
		50 µg/ml	0.2589861	0.210005186		0.2163912033	0.2952961	0.335629426
		100 µg/ml	0.27101996	0.2235347		0.1881511	0.192034966	0.211424867
48 hours	WT	Control			0.213400886	0.2373215367		
		5 µg/ml			0.172880026	0.20714704		
		10 µg/ml			0.1563744466	0.1674289867		
		20 µg/ml			0.148638863	0.1387863		
		50 µg/ml			0.157802946	0.1185432133		
		100 µg/ml			0.15006706	0.119871767		
	Il1a/b KO	Control	0.42220785	0.576469423	0.486218563	0.486927343		
		5 µg/ml	0.308085853	0.364616926	0.353192807	0.37709036		
		10 µg/ml	0.321963587	0.352973373	0.369327807	0.321865037		
		20 µg/ml	0.291975833	0.27433109	0.242360807	0.28566618		
		50 µg/ml	0.28806746	0.35419202	0.15391757	0.126806367		
		100 µg/ml	0.2332637	0.30781125	0.1925598	0.1223693		
72 hours	WT	Control			0.15957552	0.24664611		
		5 µg/ml			0.186375913	0.32112955		
		10 µg/ml			0.178442483	0.304675367		
		20 µg/ml			0.173136517	0.156942757		
		50 µg/ml			0.137046777	0.152483243		
		100 µg/ml			0.14203723	0.152125413		
	Il1a/b KO	Control	0.707764547	0.6793479		0.6817239667		
		5 µg/ml	0.65800276	0.5369691		0.676743133		
		10 µg/ml	0.538719463	0.44437043		0.681650967		
		20 µg/ml	0.576743867	0.442215167		0.4368529033		
		50 µg/ml	0.320964193	0.354736333		0.158377833		
		100 µg/ml	0.3288314	0.2983965		0.143842433		

Table A5. 2 OD values following MWCNT-JP exposure

			OD 450 nm - 750 nm(mean value of 3 parallells)			
Exposure time	**Cell line**	**Concentration**	**Exp 1**	**Exp 2**	**Exp 3**	**Exp 4**
6 hours	**WT**	**Control**	0.233807713	0.261467943		0.25016028
		5 µg/ml	0.216100093	0.24247705		0.23542979
		10 µg/ml	0.185771683	0.2232724		0.192981083
		20 µg/ml	0.1865664567	0.2271985067		0.20512788
		50 µg/ml	0.16608816	0.2227849767		0.1877234
		100 µg/ml	0.152924353	0.186690667		0.171651767
	Il1a/b KO	**Control**	0.27053844	0.279249573	0.223946723	0.36739326
		5 µg/ml	0.281018143	0.266376543	0.22604135	0.392809967
		10 µg/ml	0.256467613	0.247767187	0.212529253	0.33026423
		20 µg/ml	0.2432897	0.239966633	0.204633717	0.279797933
		50 µg/ml	0.187238297	0.2251779	0.191478237	0.24211827
		100 µg/ml	0.1472713	0.206841967	0.185767777	0.228280533
24 hours	**WT**	**Control**	0.1997858	0.284818347		0.295190053
		5 µg/ml	0.17482886	0.21095198		0.293812327
		10 µg/ml	0.16370266	0.190400197		0.22447589
		20 µg/ml	0.17532165	0.191536073		0.210807713
		50 µg/ml	0.163002953	0.182897697		0.17419688
		100 µg/ml	0.15978979	0.172478413		0.1700532
	Il1a/b KO	**Control**	0.3451647	0.337874633		0.55256615
		5 µg/ml	0.2442160033	0.2152111433		0.38673935
		10 µg/ml	0.235948367	0.18555801		0.373485497
		20 µg/ml	0.19036059	0.1994972733		0.3690561
		50 µg/ml	0.168051467	0.2324777967		0.20727703
		100 µg/ml	0.1651988733	0.188616067		0.171910867
48 hours	**WT**	**Control**	0.219330347			
		5 µg/ml	0.15867453			
		10 µg/ml	0.157557407			
		20 µg/ml	0.155331433			
		50 µg/ml	0.152080747			
		100 µg/ml	0.155459277			
	Il1a/b KO	**Control**	0.487005347			
		5 µg/ml	0.223118333			
		10 µg/ml	0.233154767			
		20 µg/ml	0.158535257			
		50 µg/ml	0.154655183			
		100 µg/ml	0.154622387			
72 hours	**WT**	**Control**	0.2529906			
		5 µg/ml	0.162104767			
		10 µg/ml	0.163753253			
		20 µg/ml	0.160315837			
		50 µg/ml	0.15806858			
		100 µg/ml	0.164369433			
	Il1a/b KO	**Control**	0.621029657			
		5 µg/ml	0.278187093			
		10 µg/ml	0.23867299			
		20 µg/ml	0.159511167			
		50 µg/ml	0.165669473			
		100 µg/ml	0.161109033			

Table A5. 3 OD values following exposure to Crocidolite asbestos

			OD 450 nm - 750 nm(mean value of 3 parallells)		
Exposure time	**Cell line**	**Concentration**	**Exp 1**	**Exp 2**	**Exp 3**
6 hours	**WT**	**Control**	0.22019732	0.17793341	0.18904892
		5 µg/ml	0.19878179	0.16371993	0.1889122267
		10 µg/ml	0.19260971	0.156933593	0.175612643
		20 µg/ml	0.189064363	0.163679253	0.172171003
		50 µg/ml	0.175612443	0.163946473	0.16964807
		100 µg/ml	0.176819467	0.163416113	0.1764811
	Il1a/b KO	**Control**	0.191104357	0.164091303	0.24780594
		5 µg/ml	0.177296707	0.158203573	0.24902362
		10 µg/ml	0.183668707	0.1546312167	0.2463970967
		20 µg/ml	0.1876323	0.1605861267	0.257161575
		50 µg/ml	0.16842997	0.16354805	0.25068767
		100 µg/ml	0.178465433	0.1879743	0.248477933
24 hours	**WT**	**Control**	0.258332596	0.21654077	0.263635957
		5 µg/ml	0.2719631367	0.21932404	0.274592823
		10 µg/ml	0.245663593	0.19424304	0.283688835
		20 µg/ml	0.23211142	0.180423023	0.255887313
		50 µg/ml	0.1863611	0.172027853	0.275090157
		100 µg/ml	0.184120133	0.178807367	0.208805267
	Il1a/b KO	**Control**	0.305693553	0.301035647	0.376300963
		5 µg/ml	0.288349833	0.276765273	0.35644291
		10 µg/ml	0.283510817	0.25335178	0.3406053633
		20 µg/ml	0.27264	0.248838857	0.3629446967
		50 µg/ml	0.185826603	0.19220762	0.32450524
		100 µg/ml	0.165986533	0.191673533	0.34190104
48 hours	**WT**	**Control**	0.309595133	0.316762713	0.300654577
		5 µg/ml	0.393622543	0.29378571	0.33896834
		10 µg/ml	0.289325163	0.252780573	0.2961158733
		20 µg/ml	0.238691657	0.1846073667	0.258340577
		50 µg/ml	0.176071583	0.16503513	0.264594207
		100 µg/ml	0.1730272	0.187604467	0.187010793
	Il1a/b KO	**Control**	0.482310693	0.4389766567	0.481474927
		5 µg/ml	0.55791588	0.363526707	0.42780965
		10 µg/ml	0.493136243	0.417914843	0.40753328
		20 µg/ml	0.437642317	0.404515363	0.409213267
		50 µg/ml	0.182351887	0.199270243	0.391692513
		100 µg/ml	0.178435633	0.1874034	0.275470403
72 hours	**WT**	**Control**	0.26673263		0.262663633
		5 µg/ml	0.229554737		0.28238046
		10 µg/ml	0.18532647		0.266313635
		20 µg/ml	0.1736959867		0.2679420633
		50 µg/ml	0.1750832		0.212942433
		100 µg/ml	0.1842339		0.1420254367
	Il1a/b KO	**Control**	0.602669775		0.577670497
		5 µg/ml	0.5079488733		0.509043723
		10 µg/ml	0.3820284067		0.55321082
		20 µg/ml	0.399376077		0.518839423
		50 µg/ml	0.178168577		0.435089477
		100 µg/ml	0.1883719		0.320092033

Table A5. 4 OD values following exposure to H_2O_2.

			OD 450 nm - 750 nm(mean value of 3 parallells)		
Exposure time	**Cell line**	**Concentratio**	**Exp 1**	**Exp 2**	**Exp 3**
6 hours	**WT**	**Control**	0.3802971967	0.4207873933	0.2353612667
		1 µM	0.354055137	0.3603536367	0.2488423433
		2 µM	0.352011135	0.30100583	0.2666302533
		4 µM	0.30180679	0.36262686	0.1814894067
		5 µM	0.2703325267	0.3288270367	0.17469863
		10 µM	0.1781678833	0.1857049033	0.15654384
	Il1a/b KO	**Control**	0.5110509733	0.4273352733	0.2946156
		1 µM	0.3790627433	0.44721539	0.31724354
		2 µM	0.3678599833	0.3472947267	0.2812737133
		4 µM	0.374607867	0.329449467	0.2727695633
		5 µM	0.4239059833	0.3124588267	0.2336727633
		10 µM	0.1603216233	0.20722344	0.1495740833
24 hours	**WT**	**Control**	0.357313867	0.275900907	0.2322017367
		1 µM	0.34322221	0.2927663033	0.2130059733
		2 µM	0.34700955	0.2905489467	0.1861631367
		4 µM	0.354675893	0.2645427967	0.1559047333
		5 µM	0.313762747	0.2657741967	0.1386292833
		10 µM	0.1941376033	0.1773437233	0.1367636767
	Il1a/b KO	**Control**	0.4310474733	0.395822467	0.3609343133
		1 µM	0.38567212	0.3914078567	0.3558947167
		2 µM	0.3744508567	0.4191497067	0.3387171967
		4 µM	0.3925687833	0.3705978367	0.2825433233
		5 µM	0.36689136	0.31166848	0.21110113
		10 µM	0.2107194267	0.1843816967	0.1348262233
48 hours	**WT**	**Control**	0.35129865		0.16205881
		1 µM	0.441346165		0.15696686
		2 µM	0.3144196067		0.14928537
		4 µM	0.214846765		0.1195109
		5 µM	0.21002493		0.11790094
		10 µM	0.13164916		0.11377651
	Il1a/b KO	**Control**	0.5453515867	0.6417385967	0.35936789
		1 µM	0.669775033	0.71490325	0.37973242
		2 µM	0.5742728467	0.70960794	0.333320043
		4 µM	0.57954615	0.6000490433	0.170236767
		5 µM	0.2982590967	0.40528078	0.150873053
		10 µM	0.1467841633	0.1516537233	0.1258533867
72 hours	**WT**	**Control**	0.2974266433		0.175040115
		1 µM	0.3430201367		0.1902478133
		2 µM	0.3266709		0.1797117033
		4 µM	0.3676597267		0.14366308
		5 µM	0.2200195967		0.1448986167
		10 µM	0.1482985167		0.1500229833
	Il1a/b KO	**Control**	0.93409508	1.08107459	0.6740966267
		1 µM	0.94019497	1.00683437	0.7391728
		2 µM	1.051735677	1.091808123	0.6312731067
		4 µM	0.898755673	1.038355033	0.2888294233
		5 µM	0.33861874	0.68763828	0.18497451
		10 µM	0.14764738	0.25891227	0.1455815167

Fluorescence microscopy

Exposed cells and controls of the WT and *Il1a/b* KO cell line were counted as described in chapter 2.5. A minimum of 300 cells were counted per slide, 2 slides were counted per exposure, and a total of 3 experiments were performed. Table A5.5 shows the percentage of viable and dead cells, in addition to the percentage of apoptotic and necrotic cell death (percentage of total cell death).

Table A5.5: Percentage ± standard error cell viability, total cell death, apoptotic cell death and necrotic cell death in cells from the BalbC WT and *Il1a/b* KO cell lines exposed for 24 hours.

		Cell viability(%)		Total cell death(%)		Apoptosis (% of cell death)		Necrosis (% of cell death)		Cells counted per experiment
Cell line	**Sample**	**Mean**	**±SE**	**Mean**	**±SE**	**Mean**	**±SE**	**Mean**	**±SE**	**Mean**
BalbC WT	**Control**	**93.4**	0.8	**6.6**	0.8	**0.0**	0.0	**100.0**	0.0	669
	nTec 5 µg/ml	**84.9**	3.2	**15.1**	3.2	**0.6**	0.6	**99.4**	0.6	658
	nTec 10 µg/ml	**75.0**	5.9	**25.0**	5.9	**0.4**	0.2	**99.6**	0.2	660
	nTec 20 µg/ml	**56.7**	13.1	**43.3**	13.1	**0.5**	0.3	**99.5**	0.3	636
	Mitsui 5 µg/ml	**90.1**	3.3	**9.9**	3.3	**1.9**	0.7	**98.1**	0.7	631
	Crocidolite 20 µg/ml	**89.3**	3.4	**10.7**	3.4	**1.0**	0.5	**99.0**	0.5	654
	H2O2 4 µM	**86.8**	3.6	**13.2**	3.6	**2.2**	1.4	**97.8**	1.4	664
	Thapsigargin 100 nM	**60.7**	3.6	**39.3**	3.6	**16.9**	3.4	**83.1**	3.4	630
IL1α/β KO	**Control**	**90.0**	1.7	**10.0**	1.7	**0.6**	0.6	**99.4**	0.6	649
	nTec 5 µg/ml	**91.7**	2.2	**8.3**	2.2	**2.1**	1.7	**97.9**	1.7	650
	nTec 10 µg/ml	**76.5**	4.8	**23.5**	4.8	**0.8**	0.0	**99.2**	0.0	655
	nTec 20 µg/ml	**56.1**	9.6	**43.9**	9.6	**0.2**	0.2	**99.8**	0.2	641
	Mitsui 5 µg/ml	**78.8**	5.1	**21.2**	5.1	**2.1**	1.3	**97.9**	1.3	639
	Crocidolite 20 µg/ml	**85.6**	1.2	**14.4**	1.2	**0.9**	0.5	**99.1**	0.5	655
	H2O2 4 µM	**84.9**	5.2	**15.1**	5.2	**0.6**	0.6	**99.4**	0.6	648
	Thapsigargin 100 nM	**52.6**	4.3	**47.4**	4.3	**10.1**	1.7	**89.9**	1.6	650

qRT-PCR

The CT-values obtained from qRT-PCR from the WT cell line are shown in table A5.6 and A5.7, while the values for the *Il1a/b* KO cell line are shown in table A5.8 and A5.9. The given CT-values are the mean value of two parallels (from the same cDNA sample). For *Il1b*, *Tnfa* and *Il6* 50 ng cDNA template was used per sample. For *Ptgs2*, *Tp53* and *Actb*, 10, 5 and 2.5 ng cDNA template was used respectively.

Table A5. 6 CT values obtained from qRT-PCR of the genes *Il1b*, *Il6*, *Ptgs2* and *Actb* in the WT cell line.

Sample	Experiment	*Il1b*	*Il6*	*Ptgs2*	*Actb*
Control	1	36.878075	34.542557	30.314594	19.651894
		39.36492	33.475853	29.723906	19.400902
	2	38.05155	34.042526	28.831802	19.427017
		37.43442	33.98181	29.224548	19.68898
	3	37.1289745	34.33763	29.34467	19.420216
		37.1092245	34.55259	29.920818	20.142418
MWCNT-NO, 5 ug/ml	1	36.76297	33.810654	29.623283	19.360413
		38.087227	33.420723	29.46826	19.381275
	2	37.421803	33.802345	28.248627	19.088804
			35.779472	28.106762	19.194138
	3	38.26482	34.184227	29.51667	19.743534
		38.6347035	34.018906	29.5934	19.862427
MWCNT-NO, 10	1	37.415756	33.22491	29.09085	19.447811
		38.089035	34.022728	29.112001	19.36855
	2		33.481483	26.83374	19.239876
			33.452866	26.857187	19.244652
	3	39.805252	34.294724	28.243889	19.6738
			33.438248	28.174448	19.659645
MWCNT-JP, 5 ug/ml	1	35.85903	32.062683	26.903664	19.28952
		36.19031	32.28323	26.903664	19.181484
	2	38.31894	32.14131	27.010223	19.381775
		36.967907	32.81067	26.94833	19.379787
	3	39.545227	33.724888	27.044971	18.937979
		39.208145	34.02356	27.524055	19.399517
Crocidolite, 20 ug/ml	1	36.579617	33.472527	29.849274	18.961895
		37.665306	34.114395	29.849274	18.798489
	2	37.446617	34.290268	28.361916	19.207909
		37.623215	34.031967	28.161415	19.387169
	3	39.25969	34.552933	28.968353	18.975403
		38.00569	34.123703	28.9482	19.035313
H2O2 4 uM	1	37.072323	34.06766	29.734968	18.857586
		38.375557	35.170227	29.734968	19.475266
	2		34.061974	27.973099	19.07584
	3	39.169249	34.305164	28.289146	18.97579
		39.4663975	34.152996	29.034046	19.379055

Table A5.7 CT values obtained from qRT-PCR of the genes *Tp53*, *Tnfa* and *Actb* in the WT cell line.

Sample	Experiment	*Tp53*	*Tnfa*	*Actb*
Control	1	24.533875	29.333975	19.891193
		23.503666	28.850082	19.657309
	2	23.2091	29.194464	19.854939
		23.4921	29.454079	20.084892
	3	23.915714	29.450771	20.23163
		23.548107	29.75441	20.40524
MWCNT-NO, 5 ug/ml	1	23.33744	28.744656	19.404692
		23.0458	28.69152	19.547222
	2	23.440674	29.22525	19.871647
		23.295254	30.76294	19.477863
	3	23.447807	29.539547	19.991962
		23.235771	29.718748	20.629494
MWCNT-NO, 10	1	24.139542	29.02099	19.580004
		23.564571	28.995272	19.642872
	2	23.799994	28.488611	20.134508
		23.991478	28.677914	19.716759
	3	23.826775	29.51594	20.005486
		23.405884	29.416721	19.957134
MWCNT-JP, 5 ug/ml	1	22.98664	28.201565	19.715878
		23.444593	28.296024	19.583982
	2	22.27312	29.051064	19.806873
		22.960464	29.132908	19.766645
	3	23.47176	28.918076	19.200531
		23.972982	29.33498	19.703754
Crocidolite, 20 ug/ml	1	22.746616	29.394695	19.334259
		23.172005	29.026806	19.099201
	2	23.084084	29.319695	19.16824
		22.800608	29.288643	19.570612
	3	23.684776	29.405605	19.255554
		23.120684	29.560314	19.324238
H2O2 4 uM	1	23.112822	28.670204	19.156542
		24.744503	29.492176	19.701183
	2	22.769924	28.705273	19.454485
	3	23.248161	28.764431	19.404224
		23.04668	28.937832	19.766582

Table A5.8 CT values obtained from qRT-PCR of the genes *Il1b*, *Il6*, *Ptgs2* and *Actb* in the *Il1a/b* KO cell line

Sample	Experiment	*Il1b*	*Il6*	*Ptgs2*	*Actb*
Control	1		27.219025	23.606487	19.472248
			27.515985	23.868917	19.664665
	2		26.494507	23.27513	19.82814
			26.687317	23.471937	19.862371
	3		26.71368	23.82877	19.814362
			26.999992	24.14245	20.416653
MWCNT-NO, 5 ug/ml	1		29.179747	22.972973	19.747425
			29.553665	23.181477	19.776249
	2		27.714506	22.718277	19.75773
			28.335983	22.633835	19.45631
	3		28.04367	23.300083	19.709942
			28.092028	23.586403	19.884071
MWCNT-NO, 10	1		29.284245	22.791843	19.473103
			29.354538	22.760212	19.549522
	2				
			27.763565	21.889362	18.912119
	3		28.708824	23.420162	20.285881
			28.550665	23.270271	20.14954
MWCNT-JP, 5 ug/ml	1		25.749186	21.23241	20.142857
			25.63424		20.532917
	2		26.501749	22.733212	20.134083
			26.61484	22.835274	20.00959
	3		27.47308	22.268188	19.609337
			27.509003	22.366283	19.49092
Crocidolite, 20 ug/ml	1		28.565834	23.110315	19.324005
			28.644005	23.110315	19.531837
	2		28.12317	22.813137	19.634045
			28.210972	22.88607	19.399353
	3		28.23959	22.894032	19.430618
			27.992676	22.62843	19.442753
H2O2 4 uM	1		27.200325	23.260105	19.440937
			27.172829	23.260105	19.599451
	2		26.47263	22.938213	19.481174
	3		26.905752	23.610783	19.84064
			26.691078	23.455154	19.66492

Table A5.9 CT values obtained from qRT-PCR of the genes *Tp53*, *Tnfa* and *Actb* in the *Il1a/b* KO cell line.

Sample	Experiment	*Tp53*	*Tnfa*	*Actb*
Control	1	23.815252	33.102417	19.940573
		24.26728	33.048424	19.995014
	2	23.933163	32.4243	20.316095
		23.965391	32.859886	20.102654
	3	23.247063	33.09233	20.08117
		23.463367	33.580986	20.511002
MWCNT-NO, 5 ug/ml	1	23.438559	37.09587	19.627253
		23.958557	36.9378	19.64812
	2	23.099758	35.743454	20.262627
		23.954323	35.47274	19.666975
	3	23.48954	36.243706	19.892647
		23.283531	36.100883	20.125443
MWCNT-NO, 10	1	23.951078	37.58086	19.845434
		24.160507	37.079803	19.867844
	2			
		23.461805	36.404995	19.440636
	3	23.897179	37.16093	20.46455
		23.782513	35.692772	20.362728
MWCNT-JP, 5 ug/ml	1	23.00061	31.495968	20.779547
		22.897242	31.77754	20.994226
	2	23.035225	32.909668	20.862366
		23.260647	32.866447	20.147236
	3	23.305443	37.06971	19.668123
		23.55775	37.89265	19.618458
Crocidolite, 20 ug/ml	1	23.249714	34.393692	19.744228
		23.545364	34.52546	19.960844
	2	23.133223	35.57187	19.663094
		23.006155	35.24981	20.14648
	3	23.296806	36.92176	19.836138
		23.171608	36.084	19.774197
H2O2 4 uM	1	23.561195	32.704536	19.560863
		23.064632	32.913574	19.648579
	2	22.955132	31.922615	19.927025
		23.676912	32.45511	20.065765
	3	23.13012	33.63288	20.282948
		23.297428	33.312454	20.264229